INFORMATION TO USERS

This dissertation was produced from a microfilm copy of the original document. While the most advanced technological means to photograph and reproduce this document have been used, the quality is heavily dependent upon the quality of the original submitted.

The following explanation of techniques is provided to help you understand markings or patterns which may appear on this reproduction.

1. The sign or "target" for pages apparently lacking from the document photographed is "Missing Page(s)". If it was possible to obtain the missing page(s) or section, they are spliced into the film along with adjacent pages. This may have necessitated cutting thru an image and duplicating adjacent pages to insure you complete continuity.

2. When an image on the film is obliterated with a large round black mark, it is an indication that the photographer suspected that the copy may have moved during exposure and thus cause a blurred image. You will find a good image of the page in the adjacent frame.

3. When a map, drawing or chart, etc., was part of the material being photographed the photographer followed a definite method in "sectioning" the material. It is customary to begin photoing at the upper left hand corner of a large sheet and to continue photoing from left to right in equal sections with a small overlap. If necessary, sectioning is continued again — beginning below the first row and continuing on until complete.

4. The majority of users indicate that the textual content is of greatest value, however, a somewhat higher quality reproduction could be made from "photographs" if essential to the understanding of the dissertation. Silver prints of "photographs" may be ordered at additional charge by writing the Order Department, giving the catalog number, title, author and specific pages you wish reproduced.

University Microfilms

300 North Zeeb Road
Ann Arbor, Michigan 48106

A Xerox Education Company

Reproduced with permission of the copyright owner. Further reproduction prohibited without permission.

72-22,612

OWYOUNG, Adelbert, 1945-
THE ORIGINS OF THE NONLINEAR REFRACTIVE INDICES OF LIQUIDS AND GLASSES.

California Institute of Technology, Ph.D., 1972
Engineering, electrical

University Microfilms, A XEROX Company, Ann Arbor, Michigan

Reproduced with permission of the copyright owner. Further reproduction prohibited without permission.

THE ORIGINS OF THE NONLINEAR REFRACTIVE INDICES OF LIQUIDS AND GLASSES

Thesis by

Adelbert Owyoung

In Partial Fulfillment of the Requirements

for the Degree of

Doctor of Philosophy

California Institute of Technology

Pasadena, California

1972

(Submitted December 9, 1971)

Reproduced with permission of the copyright owner. Further reproduction prohibited without permission.

PLEASE NOTE:

Some pages may have

indistinct print.

Filmed as received.

University Microfilms, A Xerox Education Company

Reproduced with permission of the copyright owner. Further reproduction prohibited without permission.

ACKNOWLEDGMENTS

My sincere thanks go to Professor Nicholas George for his excellent advice and constant personal encouragement during the course of this research. His fundamental approach to the understanding of physical phenomena was most refreshing and his understanding and personal interest in each student were especially valuable.

My thanks are extended also to Professor Robert W. Hellwarth for his most valuable advice in the theoretical aspects of this research. His interest and faithful correspondence during a leave of absence provided a wealth of stimulation and encouragement.

I wish to express my appreciation to Professor John H. Marburger for a number of stimulating and interesting discussions during the course of this work.

A special note of thanks goes to Mrs. Ruth Stratton for a masterful typing of the manuscript.

Finally, thanks go to my wife Helen for her abiding love and support.

The financial assistance of the California Institute of Technology, the Ford Foundation, the Fairchild Camera and Instrument Corporation and the Air Force Office of Scientific Research is gratefully acknowledged.

Reproduced with permission of the copyright owner. Further reproduction prohibited without permission.

ABSTRACT

Nonlinear refractive index changes in isotropic media are a consequence of two distinct types of mechanisms. An "electronic" mechanism arises from the nonlinear distortion of the electron orbits about the nuclei and a "nuclear" mechanism arises from an electric-field-induced change in the motions of nuclei.

A general treatment of nonlinear optical phenomena involving a polarization cubic in the electric field strength is given with the topic of nonlinear index changes treated as a special case. A central result of this theory is the following expression for the nonlinear polarization $\underline{P}_3(t)$ in terms of the electric field $\underline{E}(t)$, the "electronic" parameter σ and the "nuclear response functions" $a(t)$ and $b(t)$:

$$\underline{P}_3(t) = \frac{\sigma}{2}\underline{E}(t)\cdot\underline{E}(t)\underline{E}(t) + \int a(t-\tau)\underline{E}(\tau)\cdot\underline{E}(\tau)d\tau\ \underline{E}(t) + \int b(t-\tau)\underline{E}(\tau)\cdot\underline{E}(t)\underline{E}(\tau)d\tau$$

In the theory the relationship between these parameters and the nonlinear susceptibility tensor $\underline{\underline{\chi}}_3$ is established. Several experiments in nonlinear optics are analyzed; in particular, it is shown that Kerr effect measurements lead to a determination of the quantity $\sigma + \beta$ (where $\beta = \int b(t)dt$) whereas measurements of the intensity dependent rotation of the polarization ellipse of a monochromatic optical beam yield the quantity $\sigma + 2\beta$. Hence together these two techniques offer a means of uniquely determining both the "electronic" parameter σ and the "nuclear" parameter β in any isotropic medium.

Reproduced with permission of the copyright owner. Further reproduction prohibited without permission.

The nonlinear susceptibility element $\chi_3^{1221}(-\omega,\omega,\omega,-\omega) = \frac{\sigma+2\beta}{24}$ is calculated from ellipse rotation measurements in fused quartz, BK-7 borosilicate crown glass, and SF-7 dense flint glass giving values of 1.5, 2.3, and 9.9 x 10^{-15} esu at $\lambda = 6943\text{Å}$, respectively. These measurements constitute the first observations of ellipse rotation in any solid and (with an absolute accuracy of 11%) are the most accurately known of any nonlinear optical parameter in glasses.

Although the interpretation of these results along with Kerr, three-wave mixing, and third harmonic generation data nominally indicate that $\sigma >> \beta$ for glasses, we hesitate to conclude that the nonlinear refractive indices in glasses are purely "electronic" in origin until the uncertainties in the latter measurements are reduced. If it is assumed however that electronic contributions are dominant, these experimental data would indicate that the nonlinear refractive index n_2 for a linearly polarized beam in fused quartz, BK-7 glass, and SF-7 glass is 1.2, 1.7, and 6.9 x 10^{-13} esu respectively.

Parallel investigations of "ellipse rotation" in the symmetric molecule liquid CCl_4 show that $\chi_3^{1221}(-\omega,\omega,\omega,-\omega) = 6.1 \times 10^{-15}$ esu. This value when interpreted along with very accurate Kerr measurements indicate that the fractional electronic contribution to the Kerr constant of CCl_4 is given by $\frac{\sigma}{\sigma+\beta} = 0.54 \pm 0.17$. Hence both electronic and nuclear contributions are significant to nonlinear refractive index changes in CCl_4.

Reproduced with permission of the copyright owner. Further reproduction prohibited without permission.

TABLE OF CONTENTS

		Page
I.	INTRODUCTION	
	1.0 Introduction	1
	1.1 Summary of Research	5
II.	THE FORMAL DESCRIPTION OF NONLINEAR OPTICAL PHENOMENA	
	2.0 Introduction	10
	2.1 Macroscopic Linear Susceptibility	11
	2.2 Nonlinear Optical Susceptibilities	13
	2.3 Nonlinear Optical Response to a Discrete Spectral Input	18
	References	21
III.	THE DETERMINATION OF THE THIRD ORDER NONLINEAR SUSCEPTIBILITY TENSOR IN ISOTROPIC MEDIA	
	3.0 Introduction	23
	3.1 The Nonlinear Wave Equation in Isotropic Media	24
	3.2 Harmonic Generation	26
	3.3 Optical Mixing	28
	3.4 Induced Kerr Birefringence	30
	3.5 Self-Induced Changes in Refractive Index	32
	References	41
IV.	MECHANISMS FOR THE THIRD ORDER NONLINEAR POLARIZATION IN ISOTROPIC MEDIA	
	4.0 Introduction	43
	4.1 Direct Electronic Distortion	44
	4.2 Nuclear Nonlinearities	49

Reproduced with permission of the copyright owner. Further reproduction prohibited without permission.

		Page
4.2.1	Molecular Reorientation	50
4.2.2	Raman Type Nonlinearities	59
4.2.3	Molecular Librations	64
4.2.4	Molecular Redistribution	69
4.2.5	Electrostrictive Effects	76
4.3	Summary of Nonlinear Polarization Mechanisms	81
	References	82
V.	INTERPRETATION OF THE NONLINEAR POLARIZATION	
5.0	Interpreting the Model for $\tilde{P}_3(t)$	87
5.1	Interpretation of the Nonlinear Susceptibility	89
	References	95
VI.	EXPERIMENTAL IMPLEMENTATION OF THE ELLIPSE ROTATION STUDY	
6.0	Introduction	96
6.1	The Experimental Arrangement	98
6.2	Sample Selection and Preparation	105
6.3	Ellipse Rotation Using Focused Gaussian Beams	108
6.4	Interpretation of the Ellipse Rotation Signal	119
6.5	Experimental Procedure and Data Reduction	123
6.6	Calibration Standard for Ellipse Rotation	130
6.7	Results of Ellipse Rotation Measurements	132
	References	135
VII.	INTERPRETATION OF THE NONLINEAR SUSCEPTIBILITY MEASUREMENTS IN ISOTROPIC MEDIA	
7.0	The Accuracy of Experimental Determinations of $\chi_3^{ijk\ell}$	137

Reproduced with permission of the copyright owner. Further reproduction prohibited without permission.

		Page
7.1	Conclusions Concerning Optical Glasses	145
7.2	Conclusions Concerning CCl_4	149
7.3	Summary	154
	References	157

APPENDICES

A	Electron Oscillator Model for $\tilde{P}_2(t)$	159
B	Expanded Form for $P_3(\omega)$	161
C	The Ellipse Rotation Angle	163
D	Local Field Corrections for $\chi_3^{ijk\ell}$	165
E	Dispersion Corrections for Electronic Nonlinearities	168
F	The Polarizability Tensor $\underline{\underline{\alpha}}(\theta,\phi)$	172
G	The Distribution Function for Molecular Reorientation	175
H	Stimulated Scattering of Light and the Polarization Properties of $\tilde{P}_3(t)$	182
I	Relating the Scattering Cross Section to the Nonlinear Polarization	191
J	Focusing Optics in the Ellipse Rotation Study	208
K	The Hyperpolarizability of CS_2	212
	References for Appendices A-K	215
L	Intensity-Induced Changes in Optical Polarization in Glasses (Preprint)	218
M	Origin of the Nonlinear Refractive Index of Liquid CCl_4 (Preprint)	240

Reproduced with permission of the copyright owner. Further reproduction prohibited without permission.

CHAPTER I

INTRODUCTION

1.0 Introduction

The origins of the nonlinear refractive indices of optically dense media have for many years been uncertain due to the large number of plausible mechanisms which may be responsible for these index effects in any given medium. Lacking were both a consistent theoretical formulation and a group of suitable experiments which would enable one to effectively separate out the various possible contributions. To be sure it is generally agreed that nonlinear refractive index changes in liquids of highly anisotropic molecules arise primarily from the reorientation of these molecules by the applied field.[1] However the role of other mechanisms which are dominant in symmetric molecule liquids and amorphous solids where the reorientation mechanism is small or nonexistent has been somewhat uncertain.

The scope of this thesis is to present a unified approach to this problem by considering the nonlinear refractive indices in isotropic media as very special cases of a more general class of nonlinear optical effects. A formulation of the nonlinear polarization will be presented based upon the mechanisms which have been proposed as being responsible for nonlinear index changes. The various nonlinear optical effects which arise as a consequence of this nonlinear polarization are examined in the light of this formulation and an experimental investigation is conducted to demonstrate the feasibility of a technique which shows particular promise in providing a quantitative statement

Reproduced with permission of the copyright owner. Further reproduction prohibited without permission.

concerning the contributions to the nonlinear refractive index which arise from an electronic distortion mechanism.[2]

As with many topics in physics, the area of nonlinear optics has both an early and a recent history. In this case these two periods of time are rather sharply delineated by the first successful achievement of optical maser action in ruby by Maiman in 1960[3] followed shortly thereafter by the development of Q-spoiling by Hellwarth.[4]

The first observation of a nonlinear phenomenon involving a change in the optical susceptibility which is proportional to the square of the applied field strength is the observation of field induced birefringence by John Kerr in 1875.[5,6] This phenomenon which has been termed the d.c. Kerr effect occurs with the application of a strong static electric field to the medium to produce an optical birefringence which is detected by monitoring the polarization of a weak optical beam as it propagates through the medium. Since its discovery a wealth of experimental data has become available reporting the size of this "electro-optic" effect in various liquids.[7] Attempts have also been made to account for the physical mechanisms which produce Kerr birefringence. In particular Voight has suggested the possibility of an induced change in refractive index due to a deformation of the electron orbits of the medium by the strong field[8] and Langevin[9] and Havelock[10] have considered the field induced changes in the arrangement of nuclei whose electrons then respond linearly to the applied field.

With the invention of the Q-spoiled laser a host of new nonlinear optical effects which involve nonlinear polarizations which are

Reproduced with permission of the copyright owner. Further reproduction prohibited without permission.

cubic in the electric field strength have been observed[11] and measurements of the d.c. Kerr effect have been made with greatly improved accuracy.[12] In particular the generation of optical harmonics and optical frequency mixing have been observed by Maker, Terhune and Savage,[13,14] intensity dependent changes in refractive index resulting in self-focusing of the optical beam were reported by Chiao, Garmire, and Townes[15] and a variety of stimulated light scattering processes have been reported by various authors.[16-18] Also Maker, Terhune and Savage have observed birefringence effects induced by an optical beam which produce a change in the polarization characteristics of the beam itself[19] and Mayer and Gires have observed an a.c. Kerr effect in which the strong field producing the birefringence is supplied by an optical beam.[20]

Since all of the effects which were outlined above are a consequence of a nonlinear polarization cubic in the electric field strength which we denote by $\tilde{P}_3(t)$,* we would expect that a phenomenological expression for this nonlinear polarization would provide a basis for relating the various nonlinear phenomena. These relationships will serve as a basis whereby we shall extract quantitative information concerning the various contributing mechanisms to the nonlinear polarization.

More specifically, the experimental investigation which we report in this work involves the study of the intensity dependent

*Here and throughout this text, the tilde (~) will be used to denote all functions of time to distinguish them from frequency domain functions.

Reproduced with permission of the copyright owner. Further reproduction prohibited without permission.

change in the state of polarization of an elliptically polarized beam as it propagates through an isotropic medium. Maker et al.[19] first predicted and observed this "ellipse rotation" phenomenon by monitoring the state of polarization of an elliptically polarized ruby laser giant pulse after it had traversed a liquid filled absorption cell. Although this ellipse rotation phenomenon is seemingly only a special case of the Kerr effect in which the strong Kerr field is provided by the beam which itself sees the induced birefringence, it will be shown that ellipse rotation measures a quantity different from that of the Kerr effect. In fact it will be seen that together the Kerr effect and ellipse rotation experiments provide a practical means of separating direct electronic from nuclear rearrangement type contributions to the nonlinear refractive index in any isotropic medium.

The specific isotropic materials which have been examined in this work are the symmetric molecule liquid CCl_4 and several optical glasses of varying density including fused quartz. By making several modifications to overcome difficulties which were encountered in previous ellipse rotation studies, we obtain the first experimental determinations of the ellipse rotation parameter in any solid. With an approximate absolute accuracy of 11%, these measurements constitute the most accurate determinations of any nonlinear optical constant in glass. Additionally the measurements in liquid CCl_4 provide the most accurate determination of the electronic distortion contribution to the nonlinear refractive index and the Kerr constant of CCl_4 currently available.

Reproduced with permission of the copyright owner. Further reproduction prohibited without permission.

1.1 Summary of Research

The description of this research is divided into seven separate chapters including this chapter of introduction.

A review of the formalism of "nonlinear optical susceptibilities" which are employed in the formal description of nonlinear optical processes is given in Chapter II. Particular attention is devoted to the nonlinear susceptibility tensor $\underset{\sim}{\chi}_3$ which is employed to describe induced refractive index changes and other processes which involve a nonlinear polarization $\tilde{\underset{\sim}{P}}_3(t)$ which is cubic in the electric field strength.

Having laid the foundation for the description of nonlinear optical processes, Chapter III provides a review of four experimental techniques which have been employed to measure elements of the nonlinear susceptibility tensor $\underset{\sim}{\chi}_3$ in isotropic media. These are (1) the generation of radiation at the third harmonic of an optical monochromatic wave, (2) the optical mixing of three monochromatic waves, (3) the Kerr effect, and (4) effects involving index changes governing the propagation of an optical beam which are induced by the beam itself, such as ellipse rotation.

In Chapter IV a phenomenological model is developed for the nonlinear polarization $\tilde{\underset{\sim}{P}}_3(t)$ which is cubic in the electric field strength. This model is based upon the various mechanisms which have been proposed as sources of nonlinear refractive index changes in isotropic media and the resulting expression for $\tilde{\underset{\sim}{P}}_3(t)$ will provide a basis for the physical interpretation of the various results of the experimental determinations which were described in Chapter III. This

Reproduced with permission of the copyright owner. Further reproduction prohibited without permission.

interpretation of the various measurements of the nonlinear susceptibility elements will be presented in Chapter V. The results of this analysis show that the Kerr effect and ellipse rotation measurements enable us to separate electronic distortion and nuclear rearrangement contributions to the nonlinear refractive index in any isotropic medium.

In Chapter VI a complete description and analysis of our experimental investigation of ellipse rotation is presented. Finally in Chapter VII of this work the results of the ellipse rotation study are compared with and interpreted in the light of the other measurements of the nonlinear susceptibility. The merits and weaknesses of each experimental measurement are discussed and the data are interpreted to show that the electronic contributions tend to dominate the nonlinear refractive index in glasses whereas both nuclear rearrangement and direct electronic contributions are significant in CCl_4.

Several appendices have been added to provide supplementary material which was felt to be inappropriate for inclusion into the main text. Particularly important are Appendices H and I which are addressed to considering the polarization properties of nonlinear processes involving $\tilde{\underline{P}}_3(t)$ and to the relationship between the spontaneous scattering of light and the nonlinear susceptibility. This latter appendix could possibly give several insights into the possibility of determining the sources of nuclear contributions to the nonlinear polarization of isotropic media through the use of light scattering studies.

As a final note Appendices L and M include preprints of two articles which provide a concise summary of the essence of the work

Reproduced with permission of the copyright owner. Further reproduction prohibited without permission.

reported in this thesis. These articles have been accepted for publication in Physical Review B (Jan. 1972) and Physical Review A (Dec. 1971) respectively.

Reproduced with permission of the copyright owner. Further reproduction prohibited without permission.

REFERENCES - CHAPTER I

1. P. Debye, Marx's Handbuch der Radiologie VI, Chap. V, Akademische Verlagsgesellschaft, Leipzig, 1925.

2. A. D. Buckingham and B. J. Orr, "Molecular Hyperpolarizabilities", Quart. Rev. (London) 21, 195 (1967).

3. T. H. Maiman, "Stimulated Optical Radiation in Ruby Masers," Nature 187, 493 (1960).

4. R. W. Hellwarth, "Control of Fluorescent Pulsations," in Advances in Quantum Electronics, ed. by J. R. Singer (Columbia Univ. Press, New York, 1961) pp. 334-341.

5. J. Kerr, "A New Relation between Electricity and Light: Dielectrified Media Birefringent," Phil. Mag. 50 [4], 337, 446 (1875).

6. J. Kerr, "Electro-Optic Observations on Various Liquids," Phil. Mag. 8 [8], 85,229 (1879).

7. Landolt-Borstein Zahlenwerte und Funktionen II/8 (Springer-Verlag Berlin 1962) pp. 849-860.

8. W. Voight, Ann. der Physik 4, 197 (1901) and Magneto und Electro-Optik, Lehb Teubner, 1907, p. 161.

9. P. Langevin, Ann. Chim. Phys. 5, 70 (1907) and Le Radium 7, 249 (1910).

10. T. H. Havelock, Proc. Roy. Soc. A80, 28 (1908).

11. R. W. Terhune and P. D. Maker, "Nonlinear Optics" in Lasers, Vol.2, ed. by A. K. Levine (M. Dekker Inc., 1968) p. 295.

12. N. George, R. W. Hellwarth and C. R. Cooke, "Kerr Constant Measurements Using a Laser Polarimeter," Electron Technology (Poland) 2, 229 (1969).

13. P. D. Maker, R. W. Terhune, and C. M. Savage, "Optical Third Harmonic Generation," in Quantum Electronics III, ed. by P. Grivet and N. Bloembergen (Columbia Univ. Press, 1964), p. 1559.

Reproduced with permission of the copyright owner. Further reproduction prohibited without permission.

14. P. D. Maker and R. W. Terhune, "Study of Optical Effects Due to an Induced Polarization Third Order in the Electric Field Strength," Phys. Rev. 137, A801 (1965).

15. R. Y. Chiao, E. Garmire, and C. H. Townes, "Self Trapping of Optical Beams," Phys. Rev. Lett. 13, 479 (1964)

16. G. Eckhardt, R. W. Hellwarth, F. J. McClung, S. E. Schwarz, and D. Weiner, "Stimulated Raman Scattering from Organic Liquids," Phys. Rev. Lett. 9, 455 (1962).

17. R. Y. Chiao, C. H. Townes, and B. P. Stoicheff, "Stimulated Brillouin Scattering and Coherent Generation of Intense Hypersonic Waves," Phys. Rev. Lett. 12, 892 (1964).

18. N. Bloembergen and P. Lallemand, "Complex Intensity-Dependent Index of Refraction, Frequency Broadening of Stimulated Raman Lines, and Stimulated Rayleigh Scattering," Phys. Rev. Lett. 16, 81 (1966).

19. P. D. Maker, R. W. Terhune, and C. M. Savage, "Intensity Dependent Changes in the Refractive Index of Liquids," Phys. Rev. Lett. 12, 507 (1964).

20. G. Mayer and F. Gires, "Action d'une onde Lumineuse Intense Sur l'indice de Refraction des Liquides," Comptes Rendus 258, 4 (1964).

Reproduced with permission of the copyright owner. Further reproduction prohibited without permission.

CHAPTER II

THE FORMAL DESCRIPTION OF NONLINEAR OPTICAL PHENOMENA

2.0 Introduction

The problem of the interaction of a classical electromagnetic field with an atomic system was given early consideration in the development of perturbation theory in modern quantum mechanics.[1,2] In recent years the development of the laser has renewed interest in processes involving the interaction of optical radiation and dielectric media which involve an induced polarization which is nonlinear in the electric field strength. In particular Armstrong et al. have employed perturbation theory to derive a set of "nonlinear susceptibilities" which characterize the interaction of a superposition of monochromatic waves with a dielectric medium assuming an interaction Hamiltonian of the form $\tilde{H}' = -\underline{\mu} \cdot \tilde{E}(t)$ where $\underline{\mu}$ is the dipole moment operator.[3,4] Other workers have also considered the contributions arising from the inclusion of magnetic dipole and electric quadrupole type terms in the Hamiltonian and shown them to be negligible at optical frequencies.[5]

In this chapter our aim will be to review the formalism which has been established for the description of nonlinear optical interactions. Our intent will be to establish a means of describing such interactions rather than to be concerned about the explicit quantum mechanical forms taken on by the parameters in this formalism. In Section 2.1 a brief review of the standard macroscopic linear susceptibility relations is given. Section 2.2 contains a generalization

Reproduced with permission of the copyright owner. Further reproduction prohibited without permission.

of the linear theory to all orders in the electric field based upon Butcher's formulation of nonlinear optical interactions which gives both time and frequency domain expressions for the nonlinear polarization.[6] The "nonlinear susceptibility" which describes the nonlinear polarization in the frequency domain is defined and related to the temporal response characteristics of the nonlinear polarization. Finally, in Section 2.3, the definition of the nonlinear susceptibility is particularized to consider the case where the incident field consists of a discrete number of monochromatic components.

2.1 Macroscopic Linear Susceptibility

The response of a dielectric medium to an electric field $\tilde{\underline{E}}(t)$ in the linear theory of dielectrics may be characterized by writing polarization $\tilde{\underline{P}}(t)$ in the form

$$\tilde{\underline{P}}_i(t) = \int_{-\infty}^{\infty} \tilde{\chi}^{ij}(t-\tau)\, \tilde{E}_j(\tau)\, d\tau \qquad (2.1)$$

Here a sum is assumed to be taken over the repeated indices of a Cartesian coordinate system and $\tilde{\chi}^{ij}(t)$ is the ij^{th} element of the second rank "linear response tensor". This expression gives the polarization $\tilde{\underline{P}}(t)$ in the form of a linear response to a forcing function $\tilde{\underline{E}}(t)$ for a time invariant system. Since causality requires that $\tilde{\underline{P}}(t)$ only depend on $\tilde{\underline{E}}(\tau)$ for $t > \tau$, the response tensor $\tilde{\chi}^{ij}(t-\tau)$ must be zero for $t-\tau < 0$.

Problems involving the interaction of an electromagnetic field with a dielectric are most commonly considered in the frequency domain where the relationship between the field and the polarization is

Reproduced with permission of the copyright owner. Further reproduction prohibited without permission.

considerably simplified. In order to transform Equation (2.1) into the frequency domain, the Fourier transform pair will be defined by the convention[7]

$$f(\omega) = \frac{1}{2\pi} \int_{-\infty}^{\infty} \tilde{f}(\tau)\, e^{i\omega\tau}\, d\tau \equiv F(\tilde{f}(t)) \tag{2.2a}$$

$$\tilde{f}(t) = \int_{-\infty}^{\infty} f(\omega)\, e^{-i\omega t}\, d\omega \equiv F^{-1}(f(\omega)) \tag{2.2b}$$

where the tilde ($\tilde{}$) will be employed over all functions of time to distinguish them from frequency domain functions. Now by taking the Fourier transform of Equation (2.1) and applying the Fourier convolution theorem[7]

$$2\pi f(\omega)\, g(\omega) = F\Big(\int_{-\infty}^{\infty} \tilde{f}(t-\tau)\, \tilde{g}(\tau)\, d\tau \Big) \tag{2.3}$$

one arrives at the frequency domain equivalent of Equation (2.1) given by

$$P_i(\omega) = \chi^{ij}(\omega)\, E_j(\omega) \tag{2.4}$$

Here $P_i(\omega)$ and $E_j(\omega)$ are the Fourier transforms of $\tilde{P}_i(t)$ and $\tilde{E}_j(t)$ respectively and $\chi^{ij}(\omega)$ is the ij^{th} element of the linear susceptibility tensor defined by the convention $\chi^{ij}(\omega) = \int_{-\infty}^{\infty} \tilde{\chi}^{ij}(t)\, e^{i\omega t} dt$.[8] We note that since $\tilde{\underline{P}}(t)$ and $\tilde{\underline{E}}(t)$ are both real valued functions of time, $\tilde{\chi}^{ij}(t)$ must also be real. Hence

$$\chi^{ij*}(\omega) = \chi^{ij}(-\omega^*) \tag{2.5}$$

where the asterisk denotes the complex conjugate.

Reproduced with permission of the copyright owner. Further reproduction prohibited without permission.

In summary, it is seen that in the linear macroscopic theory, Equation (2.1) adequately describes the response of a dielectric medium to an applied field $\tilde{\underline{E}}(t)$. The specific form of the linear response function and linear susceptibility may be arrived at on the basis of a classical[9] or a quantum mechanical[10] microscopic model of the dielectric assuming a dipolar interaction between the atomic system and the electromagnetic field.

2.2 Nonlinear Optical Susceptibilities

The linear response of a dielectric medium which is described by Equation (2.1) gives an adequate description of the interaction process between the field and dielectric for cases in which the applied field is small compared to the fields which bind the charged particles of which the dielectric medium consists. At high field strengths however, the same dipole-field interaction Hamiltonian $\tilde{H}' = -\mu \cdot \tilde{\underline{E}}(t)$ which is used to obtain the linear susceptibility will also yield significant contributions to the polarization which arise from higher order perturbation theory and which are nonlinear in the applied field strengths.[4]

Butcher[6] has considered the nonlinear response of a dielectric medium to an applied field $\tilde{\underline{E}}(t)$ and shown that the polarization may be written in the time domain in the form,

Reproduced with permission of the copyright owner. Further reproduction prohibited without permission.

$$\tilde{P}_i(t) = \tilde{P}_{1i}(t) + \tilde{P}_{2i}(t) + \tilde{P}_{3i}(t) + \cdots$$

$$= \int_{-\infty}^{\infty} \tilde{\chi}^{ij}(t-\tau)E_j(\tau)d\tau + \int_{-\infty}^{\infty}\int_{-\infty}^{\infty} \tilde{\chi}_2^{ijk}(t-\tau_1,t-\tau_2)\tilde{E}_j(\tau_1)\tilde{E}_k(\tau_2)d\tau_1 d\tau_2$$

$$+ \int_{-\infty}^{\infty}\int_{-\infty}^{\infty}\int_{-\infty}^{\infty} \tilde{\chi}_3^{ijk\ell}(t-\tau_1,t-\tau_2,t-\tau_3)\tilde{E}_j(\tau_1)\tilde{E}_k(\tau_2)\tilde{E}_\ell(\tau_3)d\tau_1 d\tau_2 d\tau_3 + \cdots \tag{2.6}$$

which includes contributions to the polarization from quadratic, cubic, and higher order terms in the field $\tilde{E}(t)$. It should be noted that a sum is to be taken over all repeated indices in Equation (2.6) and that $\tilde{P}_m(t)$, the nonlinear polarization m^{th} order in the electric field strength, is characterized by a "nonlinear response tensor" of rank m+1 whose elements are denoted by $\tilde{\chi}_m^{ij\cdots}(\tau_1,\tau_2,\cdots,\tau_m)$. These "nonlinear response functions" collectively serve as the basis for the description of nonlinear optical phenomena.*

In this work the primary concern is with isotropic media which possess inversion symmetry. Hence a spatial inversion of $\tilde{E}(t)$ must result in a spatial inversion of the polarization $\tilde{P}(t)$. The nonlinear response $\tilde{\chi}_2^{ijk}(t_1,t_2)$ is consequently ruled out in such materials.[11] This requirement explains the absence of generation[12] and optical rectification[13] in media possessing inversion symmetry.

*The fact that Equation (2.6) gives the proper form for the nonlinear polarization terms is illustrated in Appendix A for the case of a nonlinear polarization quadratic in the field, $\tilde{P}_2(t)$. The assertion that the cubic term $\tilde{P}_3(t)$ is also appropriate is borne out by the models for the cubic nonlinearities which are given in Chapter 4.

Reproduced with permission of the copyright owner. Further reproduction prohibited without permission.

Primary consideration will thus be given to the nonlinear response tensor $\tilde{\chi}_3^{ijk\ell}(\tau_1,\tau_2,\tau_3)$ which characterizes a nonlinear polarization cubic in the electric field strength.*

Just as it is often convenient to work in the frequency domain in considering a linear medium, an equivalent approach may be taken in characterizing the nonlinear response. This is implemented by substituting

$$\tilde{\underline{E}}(t) = \int_{-\infty}^{\infty} \underline{E}(\omega)\, e^{-i\omega t}\, d\omega \tag{2.7}$$

into the third order term of Equation (2.6) and interchanging the order of integration. This operation yields

$$\tilde{P}_{3i}(t) = \iiint_{-\infty}^{\infty} \tilde{\chi}_3'^{ijk\ell}(\omega_1,\omega_2,\omega_3)E_j(\omega_1)E_k(\omega_2)E_\ell(\omega_3)e^{-j(\omega_1+\omega_2+\omega_3)t}\, d\omega_1 d\omega_2 d\omega_3 \tag{2.8}$$

where

$$\tilde{\chi}_3'^{ijk\ell}(\omega_1,\omega_2,\omega_3) \equiv \iiint_{-\infty}^{\infty} \tilde{\chi}_3^{ijk\ell}(t_1,t_2,t_3)e^{i\omega_1 t_1}\, e^{i\omega_2 t_2}\, e^{i\omega_3 t_3}\, dt_1 dt_2 dt_3 \tag{2.9}$$

is the fourth rank nonlinear susceptibility tensor. By taking the Fourier transform of Equation (2.8) and using the definition of the Dirac delta function $\delta(\omega-\omega_o) = \frac{1}{2\pi}\int_{-\infty}^{\infty} e^{i(\omega-\omega_o)t}\, dt$, it becomes clear

*Since our interest in this work is only in effects involving a nonlinear polarization cubic in the electric field strength, it should be understood that the term nonlinear response tensor will apply to the fourth rank tensor $\tilde{\chi}_3^{ijk\ell}(\tau_1,\tau_2,\tau_3)$ unless specifically noted otherwise.

Reproduced with permission of the copyright owner. Further reproduction prohibited without permission.

that Equations (2.8-2.9) describe the nonlinear mixing of three frequency components of the field to produce a polarization at their sum frequency. Thus we find

$$P_{3i}(\omega) = \iiint_{-\infty}^{\infty} \tilde{\chi}_3^{ijk\ell}(\omega_1,\omega_2,\omega_3) E_j(\omega_1) E_k(\omega_2) E_\ell(\omega_3) \delta(\omega-\omega_1-\omega_2-\omega_3)\, d\omega_1 d\omega_2 d\omega_3 \tag{2.10}$$

The nonlinear susceptibility $\tilde{\chi}_3^{ijk\ell}(\omega_1,\omega_2,\omega_3)$ and the nonlinear response function $\tilde{\chi}_3^{ijk\ell}(t_1,t_2,t_3)$ have several qualities analogous to their linear counterparts. In particular the reality condition on $\tilde{\chi}_3^{ijk\ell}(\tau_1,\tau_2,\tau_3)$ must hold and hence

$$\{\chi_3^{ijk\ell}(\omega_1,\omega_2,\omega_3)\}^* = \chi_3^{ijk\ell}(-\omega_1^*,-\omega_2^*,-\omega_3^*). \tag{2.11}$$

the causality condition must also apply so that

$$\tilde{\chi}_3^{ijk\ell}(\tau_1,\tau_2,\tau_3) = 0 \tag{2.12}$$

if any of the arguments τ_1, τ_2, or τ_3 are negative.

In examining the nonlinear response tensor, two symmetry restrictions are of particular interest. Firstly, it is to be recognized that $\tilde{\chi}_3^{ijk\ell}(\tau_1,\tau_2,\tau_3)$ has not been uniquely specified with respect to the interchange of the pairs j,τ_1, k,τ_2, and ℓ,τ_3. Since it is evident from the integral expression for $\underset{\sim}{P}_3(t)$ given in Equation (2.6) that the ordering of the electric field components is of no consequence, a natural choice is to symmetrize $\tilde{\chi}_3^{ijk\ell}(\tau_1,\tau_2,\tau_3)$ with respect to the interchange of pairs j,τ_1, k,τ_2, and ℓ,τ_3. Thus we write

Reproduced with permission of the copyright owner. Further reproduction prohibited without permission.

$$\tilde{\chi}_3^{ijk\ell}(\tau_1,\tau_2,\tau_3) \equiv \frac{1}{6}[\tilde{\chi}_3^{ijk\ell}(\tau_1,\tau_2,\tau_3) + \tilde{\chi}_3^{i\ell jk}(\tau_3,\tau_1,\tau_2)$$

$$+ \tilde{\chi}_3^{ik\ell j}(\tau_2,\tau_3,\tau_1) + \tilde{\chi}_3^{ij\ell k}(\tau_1,\tau_3,\tau_2)$$

$$+ \tilde{\chi}_3^{ikj\ell}(\tau_2,\tau_1,\tau_3) + \tilde{\chi}_3^{i\ell kj}(\tau_3,\tau_2,\tau_1)] \quad (2.13)$$

In like manner it is evident from applying Equation (2.9) to Equation (2.13) that the nonlinear susceptibility $\chi_3^{ijk\ell}(-\omega,\omega_1,\omega_2,\omega_3)$ is invariant with respect to the interchange of pairs j,ω_1, k,ω_2, and ℓ,ω_3. Thus we may write

$$\chi_3^{ijk\ell}(\omega_1,\omega_2,\omega_3) = \frac{1}{6}[\chi_3^{ijk\ell}(\omega_1,\omega_2,\omega_3) + \chi_3^{i\ell jk}(\omega_3,\omega_1,\omega_2)$$

$$+ \chi_3^{ik\ell j}(\omega_2,\omega_3,\omega_1) + \chi_3^{ij\ell k}(\omega_1,\omega_3,\omega_2)$$

$$+ \chi_3^{ikj\ell}(\omega_2,\omega_1,\omega_3) + \chi^{i\ell kj}(\omega_3,\omega_2,\omega_1)]$$

(2.14)

Secondly it will be noted that materials belonging to each crystallographic group will have certain symmetry restrictions imposed

Reproduced with permission of the copyright owner. Further reproduction prohibited without permission.

upon them.[11] These restrictions will in general reduce the number of independent non-vanishing tensor elements and help to make the experimental determination of the nonlinear susceptibility a more readily realizable task. The symmetry properties of $\chi_3^{ijk\ell}(\omega_1,\omega_2,\omega_3)$ have been tabulated by Birss[14] and by Maker and Terhune.[15] The symmetry relations for isotropic media are particularly simple; in this case the 81 elements of the fourth rank nonlinear susceptibility (or nonlinear response tensor) are reduced to a set of three independent elements.[16]

2.3 Nonlinear Optical Response to a Discrete Spectral Input

Since the fields which are employed in the experimental investigations of nonlinear optical phenomena are most often monochromatic or the superposition of several monochromatic waves, it is of value to specialize the formulation of Section 2.2 to the case where the spectrum of the input field consists of a discrete set of frequencies. This approach was adopted by Bloembergen[3] and by Maker and Terhune[16] to obtain the nonlinear polarization resulting from the mixing of three monochromatic waves; we shall also adopt this approach in the present work.

Consider an applied field of the form

$$\tilde{\underline{E}}(t) = \mathrm{Re}\left\{\sum_{i=1}^{n} \underline{E}_{\omega_i}(\underline{r})\, e^{-i\omega_i t}\right\} \tag{2.15}$$

which may be written in the frequency domain in the form

$$\underline{E}(\omega) = \frac{1}{2}\sum_{i=1}^{n} \underline{E}_{\omega_i}\left(\delta(\omega-\omega_i) + \delta(\omega+\omega_i)\right) \tag{2.16}$$

Reproduced with permission of the copyright owner. Further reproduction prohibited without permission.

Substituting this field into Equation (2.10) and considering the component of the nonlinear polarization $P_{3i}(\omega)$ at the frequency $\omega_s = \omega_a + \omega_b + \omega_c$ where ω_a, ω_b, and ω_c are three frequency components of $\underline{E}(\omega)$, we find that

$$P_{3i}(\omega_s) = \frac{D\chi_3'^{ijk\ell}(\omega_a,\omega_b,\omega_c)}{8} (E_{\omega_a})_j (E_{\omega_b})_k (E_{\omega_c})_\ell \, \delta(\omega_s - \omega_a - \omega_b - \omega_c) \tag{2.17}$$

Here the degeneracy factor $D = 6$, 3, or 1 depending on whether none, two, or all of the frequencies ω_a, ω_b, or ω_c are degenerate; see Appendix B.

Since the field of Equation (2.15) will invariably result in a nonlinear polarization which also possesses a discrete frequency spectrum as in Equations (2.17) and (B.3), it is convenient to write $P_{3i}(\omega_s)$ in the form

$$P_{3i}(\omega_s) = 1/2(P_{3,\omega_s})_i \, \delta(\omega_s - \omega_a - \omega_b - \omega_c) \tag{2.18}$$

and to redefine the nonlinear susceptibility in the form

$$\chi_3^{ijk\ell}(-\omega_s,\omega_a,\omega_b,\omega_c) = \frac{1}{4}\chi_3'^{ijk\ell}(\omega_a,\omega_b,\omega_c) \tag{2.19}$$

so as to eliminate the factor of 1/8 in Equation (2.17).

Here the additional argument ω_s has been adopted to conform to convention[16] and it serves as a reminder that we are considering the nonlinear polarization at the frequency $\omega_s = \omega_a + \omega_b + \omega_c$. Using this convention it is seen that Equation (2.17) may be written in the form

Reproduced with permission of the copyright owner. Further reproduction prohibited without permission.

$$(P_{3,\omega_s})_i = D\chi_3^{ijk\ell}(-\omega_s,\omega_a,\omega_b,\omega_c)(E_{\omega_a})_j(E_{\omega_b})_k(E_{\omega_c})_\ell \qquad (2.20)$$

Although we shall use the convention of Equation (2.20) in this work, the reader is cautioned that both definitions of the nonlinear susceptibilities which are related by Equation (2.19) are to be found in the literature, sometimes with a slightly different notation. Hence care should be taken to avoid confusion regarding the factor of 4 difference in the two definitions of the nonlinear susceptibility.[3,16]

Reproduced with permission of the copyright owner. Further reproduction prohibited without permission.

REFERENCES - CHAPTER II

1. P. A. M. Dirac, "The Quantum Theory of Dispersion," Proc. Roy. Soc. (London) A114, 710 (1927).

2. M. Geoppert-Mayer, "Uber Elementarakte mit zwei Quantensprungen," Ann. Physik 9, 273 (1931).

3. N. Bloembergen, Nonlinear Optics (W. A. Benjamin, Inc., New York, 1965).

4. J. A. Armstrong, N. Bloembergen, J. Ducuing, and P. S. Pershan, "Interaction between Light Waves in a Nonlinear Dielectric," Phys. Rev. 127, 1918 (1962).

5. P. S. Pershan, "Nonlinear Optical Properties of Solids: Energy Considerations," Phys. Rev. 130, 919 (1963).

6. P. N. Butcher in Nonlinear Optical Phenomena, Bull. 200, Engineering Experiment Station, Ohio State Univ., Columbus (1965).

7. This convention for the Fourier transform pair is commonly used in quantum mechanical calculations. See for example H. Margenau and G. M. Murphy, The Mathematics of Physics and Chemistry, Vol. I, pp. 246-263, (D. Van Nostrand Company, Inc., Princeton, 1956).

8. It is to be noted here that this is not the Fourier transform defined in Equation (2.2).

9. C. J. F. Bottcher, Theory of Electric Polarisation (Elsevier Publ. Co., Amsterdam, 1952).

10. R. H. Pantell and H. E. Puthoff, Fundamentals of Quantum Electronics Chap. 3, pp. 55-97 (John Wiley and Sons, New York, 1969).

11. See for example J. F. Nye, Physical Properties of Crystals (Univ. Press, Oxford, 1957).

12. P. A. Franken, A. E. Hill, C. W. Peters, G. Weinreich, "Generation of Optical Harmonics," Phys. Rev. Lett. 7, 118 (1961).

Reproduced with permission of the copyright owner. Further reproduction prohibited without permission.

13. M. Bass, P. A. Franken, J. F. Ward, "Optical Rectification," Phys. Rev. 138, A534 (1965).

14. R. R. Birss, "Property Tensors in Magnetic Crystal Classes," Proc. Phys. Soc. (London) 79, 946 (1962).

15. P. D. Maker, R. W. Terhune, and C. M. Savage, "Optical Third Harmonic Generation," Quantum Electronics III, Vol. 2, (Columbia Univ. Press, New York, 1964), p. 1559.

16. P. D. Maker and R. W. Terhune, "Study of Effects Due to an Induced Polarization Third Order in the Electric Field Strength," Phys. Rev. 137, A801 (1965).

Reproduced with permission of the copyright owner. Further reproduction prohibited without permission.

CHAPTER III

THE DETERMINATION OF THE THIRD ORDER NONLINEAR SUSCEPTIBILITY TENSOR IN ISOTROPIC MEDIA

3.0 Introduction

In Chapter II the formalism of the nonlinear susceptibility coefficients $\chi_3^{ijk\ell}$ was reviewed.[1,2] The convention proposed by Maker and Terhune[3] has been adopted to characterize $\chi_3^{ijk\ell}$ in the present work.

Research in the experimental determination of the nonlinear susceptibility tensor elements in dielectric media has progressed along several directions. The variety of experiments which have been performed involve a wide range of frequencies and thus provide information on the spectral dependence of $\chi_3^{ijk\ell}$ as well as its spatial dependence.

In this chapter we present a review of several techniques which have been employed to determine the size of $\chi_3^{ijk\ell}$ in isotropic media. Our intent shall be firstly to recognize the particular element of $\chi_3^{ijk\ell}$ which is determined by each of the techniques so as to provide a framework for their later comparison and interpretation and secondly to review the interaction process which is involved in each of these experiments thus laying the basis for understanding the strengths and weaknesses of each of the experimental techniques.

The discussion of the techniques of determining $\chi_3^{ijk\ell}$ may be divided into four distinct groups of experiments. Firstly we shall examine the third harmonic generation technique which was first employed by Maker et al. to study the nonlinear susceptibility of calcite.[4]

Reproduced with permission of the copyright owner. Further reproduction prohibited without permission.

Secondly, we shall review the three-wave mixing process of Maker and Terhune[3] which is a generalization of the third harmonic generation process and involves the optical mixing of three monochromatic waves to produce radiation at their sum frequency. Thirdly, we direct our attention to field induced birefringence effects in which strong optical or low frequency fields at a given frequency induce refractive index changes within the medium which are experienced by an optical wave at another frequency. Such effects are exemplified by the d.c. Kerr effect discovered by John Kerr in 1875[5] and the optical a.c. Kerr effect which was observed more recently by Mayer and Gires.[6] Finally, we shall review induced refractive index changes which are experienced by a monochromatic optical beam which itself induced the change. Examples of these "self-induced effects" are the self-focusing of optical beams observed by Chiao, Garmire, and Townes[7] and the self-induced rotation of an elliptically polarized beam which was first proposed and observed by Maker et al.[8]

3.1 The Nonlinear Wave Equation in Isotropic Media

Since our interest in this work will be restricted to the consideration of isotropic media, the nonlinear susceptibility $\chi_3^{ijk\ell}$ must be invariant under all spatial symmetry transformations. The 81 elements of this fourth rank tensor are consequently reduced to a set of three independent elements which will be denoted by χ_3^{1221}, χ_3^{1212}, and χ_3^{1122}.[3] Here the superscripts 1 and 2 denote x, y, or z. In the spatially degenerate case where $i=j=k=\ell$ it is observed

Reproduced with permission of the copyright owner. Further reproduction prohibited without permission.

that $\chi_3^{1111} = \chi_3^{1221} + \chi_3^{1212} + \chi_3^{1122}$.

Recognizing the form which is taken by $\chi_3^{ijk\ell}$ in an isotropic medium, let us consider Maxwell's equations in a region free of currents and charges at the frequency ω_s which was defined in Equation (2.17) as being a frequency at which the nonlinear polarization exhibited a nonzero component, i.e., $\omega_s = \omega_a + \omega_b + \omega_c$. Hence we write

$$\nabla \times \underline{H}_{\omega_s}(\underline{r}) = -\frac{i\omega\varepsilon(\omega_s)}{c}\underline{E}_{\omega_s}(\underline{r}) - i\frac{4\pi\omega_s}{c}\underline{P}_{3,\omega_s}(\underline{r}) \tag{3.1}$$

$$\nabla \times \underline{E}_{\omega_s}(\underline{r}) = \frac{i\omega_s}{c}\underline{H}_{\omega_s}(\underline{r}) \tag{3.2}$$

where $\varepsilon(\omega_s)$ is the linear dielectric constant which is a scalar in isotropic media and the permeability of the medium is assumed to be that of free space. Combining Equations (3.1-3.2) we find the wave equation which takes the form

$$\nabla^2\underline{E}'_{\omega_s}(\underline{r}) + \frac{\omega_s^2 n^2}{c^2}\underline{E}'_{\omega_s}(\underline{r}) = -\frac{4\pi\omega_s^2}{c^2}\underline{P}'_{3,\omega_s}(\underline{r}) \tag{3.3}$$

for the wave at frequency ω_s . Here the linear refractive index n is defined by $n^2 = \varepsilon(\omega_s)$ and the primes have been added to avoid confusion between these fields and those which will be defined directly below.

It is evident that one solution of Equation (3.3) is that in which the field $\underline{E}'_{\omega_s}$ is assumed to take the form of a wave traveling in some direction in space; hence it is convenient to pick the propagation direction along the z axis and to separate out the rapidly

Reproduced with permission of the copyright owner. Further reproduction prohibited without permission.

oscillating optical component by writing

$$E'_{\omega_s}(\underline{r}) = E_{\omega_s}(\underline{r})\, e^{ik(\omega_s)z} \tag{3.4a}$$

$$P'_{3,\omega_s}(\underline{r}) = P_{3,\omega_s}(\underline{r})\, e^{ik(\omega_s)z} \tag{3.4b}$$

where $k(\omega_s) = n(\omega_s)\omega_s/c$ and the "complex amplitudes" $\underline{E}_{\omega_s}$ and $\underline{P}_{3,\omega_s}$ now vary slowly in space and are constant over dimensions of the order of a wavelength. Substituting Equation (3.4) into Equation (3.3) we find the form

$$2ik(\omega_s)\frac{\partial \underline{E}_{\omega_s}}{\partial z} = -\frac{4\pi(k^2(\omega_s)}{n^2}\underline{P}_{3,\omega_s}(\underline{r}) \tag{3.5}$$

where it is assumed that $\left|\nabla^2 \underline{E}_{\omega_s}\right| << \left|k(\omega_s)\frac{\partial \underline{E}_{\omega_s}}{\partial z}\right|$. From Equation (3.5) it is clearly seen that the spatial variations in $\underline{E}_{\omega_s}$ are driven by the nonlinear polarization $\underline{P}_{3,\omega_s}$. In the sections to follow this relationship will serve as a basis for reviewing the various elements of $\chi_3^{ijk\ell}$ which have been experimentally determined through four types of experimental techniques.

3.2 Harmonic Generation

Perhaps one of the most striking examples of the nonlinear optical processes predicted by Equation (3.5) is that of the generation of radiation at the third harmonic 3ω of a monochromatic input wave of frequency ω. Third harmonic generation (THG) was first experimentally observed by Terhune et al. in calcite using a Q-switched ruby

Reproduced with permission of the copyright owner. Further reproduction prohibited without permission.

laser.[4]

Assuming an input wave of the form

$$\tilde{\underline{E}}(t) = \mathrm{Re}\ \{\underline{E}_\omega\ e^{i(kz-\omega t)}\} \tag{3.6}$$

the nonlinear polarization takes the form

$$\underline{P}'_{3,3\omega}(\underline{r}) = 3\chi_3^{1122}(-3\omega,\omega,\omega,\omega)\underline{E}_{\omega}\underline{E}_{\omega}\cdot\underline{E}_{\omega}\ e^{i3\underline{k}(\omega)z} \tag{3.7}$$

where the completely degenerate frequency arguments reduce $\chi_3^{ijk\ell}$ to a scalar by the relation[3]

$$\chi_3^{1111} = 3\chi_3^{1122} = 3\chi_3^{1221} = 3\chi_3^{1212} \tag{3.8}$$

(see Equation (2.13)). Using Equation (3.7) in Equation (3.5) it is found that

$$2ik(3\omega)\frac{\partial \underline{E}_{3\omega}}{\partial z} = -\frac{3k^2(3\omega)}{n^2(3\omega)}\chi^{1122}(-3\omega,\omega,\omega,\omega)\underline{E}_{\omega}\cdot\underline{E}_{\omega}\underline{E}_{\omega}\ e^{i\Delta kz} \tag{3.9}$$

where $\Delta k = 3k(\omega) - k(3\omega) = (3\omega/c)\ [n(\omega) - n(3\omega)]$. This expression may be integrated along z to yield

$$\underline{E}_{3\omega} = \frac{3k(3\omega)}{2\Delta kn^2(3\omega)}\chi_3^{1122}(-3\omega,\omega,\omega,\omega)\underline{E}_{\omega}\cdot\underline{E}_{\omega}\underline{E}_{\omega}(e^{i\Delta k\ell} - 1) \tag{3.10}$$

where P is the length of the sample. From Equation (3.10) it is seen that the amount of third harmonic power is limited by the coherence length $\ell_c \equiv \pi/\Delta k$ which is the path length over which the radiating nonlinear dipoles $\underline{P}_{3\omega}$ can interfere constructively.[9] Typical

Reproduced with permission of the copyright owner. Further reproduction prohibited without permission.

values for ℓ_c in glass with the fundamental input at $\lambda = 1.06\mu$ are of the order $\ell_c \simeq 1\text{-}5\mu$. As the length of the sample ℓ varies over two coherence lengths the third harmonic power oscillates through a cycle.

It is clear that THG gives a measure of $\chi_3^{1111}(-3\omega,\omega,\omega,\omega)$; however the extremely short coherence lengths make accurate direct measurements virtually impossible. Since the medium is isotropic ℓ_c cannot be extended by index matching as would be possible in anisotropic media.[10] This experimental difficulty has been overcome in part by measuring the THG emitted upon reflection of the fundamental wave from the sample surface.[11,12]

3.3 Optical Mixing

A generalization of the THG mixing process is three-wave mixing (TWM), the creation of a wave at the sum frequency of three other waves. In this case the input wave may be written in the form

$$\tilde{\underline{E}}(t) = \mathrm{Re}\{\underline{E}_{\omega_1} e^{i(k_1 z - \omega_1 t)} + \underline{E}_{\omega_2} e^{i(k_2 z - \omega_2 t)} + \underline{E}_{\omega_3} e^{i(k_3 z - \omega_3 t)}\} \tag{3.11}$$

where $k_i = \omega_i n(\omega_i)/c$ and the waves $\underline{E}_{\omega_1}$, $\underline{E}_{\omega_2}$, and $\underline{E}_{\omega_3}$ are assumed to be parallel and linearly polarized for simplicity. The resultant $\underline{P}'_{3,\Omega}$ is consequently given by Equation (2.20) to be

$$P'_{3,\Omega} = 6\chi_3^{1111}(-\Omega,\omega_1,\omega_2,\omega_3) E_{\omega_1} E_{\omega_2} E_{\omega_3} e^{i\{(k_1 + k_2 + k_3)z\}} \tag{3.12}$$

where $\Omega = \omega_1 + \omega_2 + \omega_3$.

Reproduced with permission of the copyright owner. Further reproduction prohibited without permission.

In the partially degenerate case $\omega_1 = \omega_2 = \omega$, $\omega_3 = -(\omega - \Delta)$ which was considered experimentally by Maker and Terhune[3]

$$P'_{3,\omega+\Delta} = 3\chi_3^{1111}(-(\omega+\Delta),\omega,\omega,-(\omega-\Delta))E_\omega^2 E^*_{\omega-\Delta} e^{ik'z} \qquad (3.13)$$

where $k' = 2k(\omega) - k(\omega-\Delta)$.

Again Equation (3.5) may be integrated using Equation (3.13) as a source term to yield

$$E_{\omega+\Delta} = \frac{3k(\omega+\Delta)}{2\Delta k' n^2(\omega+\Delta)} \chi_3^{1111}(-(\omega+\Delta),\omega,\omega,-(\omega-\Delta))\ E_\omega^2 E^*_{\omega-\Delta}(e^{i\Delta k'z} - 1) \qquad (3.14)$$

where $\Delta k' = k(\omega+\Delta) - k' = k(\omega+\Delta) + k(\omega-\Delta) - 2k(\omega)$

$$= [n(\omega+\Delta) + n(\omega-\Delta) - 2n(\omega)]\ \frac{\omega}{c}$$

It is clear from this development that the special case of partially degenerate three-wave mixing will determine one of two independent elements of $\chi_3^{ijk\ell}(-(\omega+\Delta),\omega,\omega,-(\omega-\Delta))$. The other element χ_3^{1221} may be obtained by polarizing E_ω perpendicular to $E_{\omega-\Delta}$.

In contrast to the case of third harmonic generation the experimental determination of χ_3^{1111} may be implemented by direct application of Equation (3.14) since the coherence length ℓ_c is now generally three orders of magnitude larger than in the case of THG. In this case $\Delta << 2\omega$ and dispersive effects are consequently much smaller. Hence ℓ_c may be adjusted to yield maximum generated power at $\omega+\Delta$.[3]

Reproduced with permission of the copyright owner. Further reproduction prohibited without permission.

3.4 Induced Kerr Birefringence

In an isotropic medium, a test beam of frequency ω will exhibit birefringence in the presence of a strong linearly polarized beam of frequency Ω. This "electric-field-induced birefringence" is known as the Kerr effect after John Kerr[5] who first observed this phenomenon in 1875. Generally the "d.c. Kerr effect"[5] in which the frequency Ω is a d.c. or radio frequency is distinguished from the more recently observed "a.c. Kerr effect"[6,13,14] in which Ω is an optical frequency. Both cases however are described in terms of a Kerr constant B_o defined by the expression

$$B_o = \frac{\omega(\delta n_{\parallel} - \delta n_{\perp})}{2\pi c \langle \tilde{E}^2 \rangle_{av}} \tag{3.15}$$

where $\delta n_{\parallel} - \delta n_{\perp}$ is the difference in refractive indices parallel and perpendicular to the direction of polarization of the strong beam and $\langle \tilde{E}^2 \rangle_{av}$ is the mean square value in time of the strong field.

Consider a wave $\tilde{\underline{E}}(t)$ consisting of two linearly polarized components traveling in the z direction

$$\tilde{\underline{E}}(t) = \text{Re}\left\{\underline{E}_{\Omega}\, e^{i(Kz-\Omega t)} + \underline{E}_{\omega}\, e^{i(kz-\omega t)}\right\} \tag{3.16}$$

where $|E_{\Omega}| >> |E_{\omega}|$. The nonlinear polarization responsible for the index change seen by $\underline{E}(\omega)$ may be deduced from Equation (2.20) to be of the form

Reproduced with permission of the copyright owner. Further reproduction prohibited without permission.

$$(P'_{3,\omega})_i = 6\chi^{1221}_3(-\omega,\omega,\Omega,-\Omega)E_{\omega,j}E_{\Omega,j}E^*_{\Omega,i}\, e^{ikz}$$

$$+ 6\chi^{1212}_3(-\omega,\omega,\Omega,-\Omega)E_{\omega,j}E^*_{\Omega,j}E_{\Omega,i}\, e^{ikz}$$

$$+ 6\chi^{1122}_3(-\omega,\omega,\Omega,-\Omega)\ |\underline{E}_\Omega|^2\, E_{\omega,i}\, e^{ikz} \qquad (3.17)$$

Clearly the strong field $\underline{E}_\Omega$ serves to produce a constant change in the polarizability of the medium which is seen by the weak field $\underline{E}_\omega$. In terms of the induced change in the linear susceptibility $\delta\chi^{ij}$ one may write

$$\delta\chi^{ij}(\omega) = 6\chi^{1221}_3(-\omega,\omega,\Omega,-\Omega)\ E^*_{\Omega,i}E_{\Omega,j}$$

$$+ 6\chi^{1212}_3(-\omega,\omega,\Omega,-\Omega)\ E^*_{\Omega,j}E_{\Omega,i}$$

$$+ 6\chi^{1122}_3(-\omega,\omega,\Omega,-\Omega)\ E_{\Omega,k}E^*_{\Omega,k}\,\delta^{ij} \qquad (3.18)$$

where $\delta\chi^{ij}$ is defined by $P_{3i} = \delta\chi^{ij}(\omega)\ E_{\omega,j}$. The change in the index of refraction corresponding to such a change in the susceptibility may be obtained by differentiating the expression $n = \sqrt{\epsilon} = \sqrt{1 + 4\pi\chi}$ to obtain

$$\delta n = \frac{1}{2}\frac{4\pi\,\delta\chi}{\sqrt{1+4\pi\chi}} = \frac{2\pi\delta\chi}{n} \qquad (3.19)$$

Thus using Equation (3.18) in Equation (3.19) one finds that the induced index changes parallel and perpendicular to the direction of polarization of the intense beam $\underline{E}_\Omega$ are given by

Reproduced with permission of the copyright owner. Further reproduction prohibited without permission.

$$\delta n_{\parallel} = \frac{2\pi}{n} 6[\chi_3^{1221}(-\omega,\omega,\Omega,-\Omega) + \chi_3^{1212}(-\omega,\omega,\Omega,-\Omega) + \chi_3^{1122}(-\omega,\omega,\Omega,-\Omega)]|\underline{E}_\Omega|^2 \qquad (3.20)$$

and

$$\delta n_{\perp} = \frac{2\pi}{n} 6[\chi_3^{1122}(-\omega,\omega,\Omega,-\Omega)]|\underline{E}_\Omega|^2$$

The Kerr constant of Equation (3.15) may thus be expressed in the form

$$B_o = \frac{24\pi}{\lambda n(\omega)} [\chi_3^{1221}(-\omega,\omega,\Omega,-\Omega) + \chi_3^{1212}(-\omega,\omega,\Omega,-\Omega)] \qquad (3.21)$$

Here we note that $|E_\Omega|^2 \langle\cos^2\Omega t\rangle_{av} = \frac{1}{2}|E_\Omega|^2$. The experimental measurement of Kerr birefringence consequently enables us to determine a linear combination of two of the three independent elements of $\chi_3^{ijk\ell}(-\omega,\omega,\Omega,-\Omega)$ in isotropic media.

3.5 Self-Induced Changes in Refractive Index

A particularly interesting case of intensity induced changes in the refractive index is that in which the high intensity beam induces the changes which in turn govern its own propagation characteristics. These self-induced changes in refractive index are seen to be responsible for the self-focusing of spatially limited beams.[7] Indeed it is this fact which is a motivating factor for the study of intensity dependent refractive index changes.

In order to see the refractive index changes which are induced by a plane wave in an isotropic medium, we substitute the monochromatic wave of Equation (3.6) into Equation (2.20) to obtain in vector form

Reproduced with permission of the copyright owner. Further reproduction prohibited without permission.

$$\underline{P}'_{3,\omega} = \{6\chi_3^{1212}(-\omega,\omega,\omega,-\omega)\}\,|\underline{E}_\omega|^2\underline{E}_\omega\, e^{ikz}$$

$$+\ 3\chi_3^{1221}(-\omega,\omega,\omega,-\omega)\underline{E}_\omega^2\,\underline{E}_\omega^*\, e^{ikz} \qquad (3.22)$$

where we have used the relation $\chi_3^{1212}(-\omega,\omega,\omega,-\omega) = \chi_3^{1122}(-\omega,\omega,\omega,-\omega)$ from Equation (2.13). This expression may be substituted directly into the wave equation (3.3), to solve exactly for the induced refractive index change δn. Alternately by applying Equation (3.19) to estimate δn we find that for a linearly polarized plane wave

$$\delta n_\ell = \frac{6\pi}{n}\chi_3^{1111}(-\omega,\omega,\omega,-\omega)\,|\underline{E}_\omega|^2 \qquad (3.23)$$

where it is recalled that $\chi_3^{1111} = \chi_3^{1212} + \chi_3^{1122} + \chi_3^{1221}$. In contrast we find for a circularly polarized wave that

$$\delta n_c = \frac{12\pi}{n}\chi_3^{1122}(-\omega,\omega,\omega,-\omega)\ |E_\omega|^2 \qquad (3.24)$$

where $|E_\omega|^2$ is specified by the convention $|\underline{E}_\omega|^2 = 2\langle\tilde{\underline{E}}^2(t)\rangle_{av}$.

If the optical beam is spatially limited, the spatial gradient in the intensity profile of the beam will produce a corresponding gradient in the index of refraction of the medium. Hence a net "self-focusing" effect occurs when the resultant lensing effect of the induced index change becomes large enough to overcome diffraction spreading of the beam.[15] It is thus seen that Equations (3.23) and (3.24) offer in principle a means of determining several nonlinear susceptibility tensor elements by direct measurement of the power thresholds required for self focusing to occur.[7,15]

Reproduced with permission of the copyright owner. Further reproduction prohibited without permission.

Practically speaking, the accurate direct determination of nonlinear refractive index changes is an extremely difficult task to perform. Both the theoretical complexities of the nonlinear diffraction process and the experimental difficulty of specifying and reproducing the spatial and temporal output from a high power solid state laser serve to put a practical limit on the accuracy with which such self-focusing measurements may be made. Perhaps the most accurate determinations of nonlinear index changes via self-focusing measurements are the studies performed by McAllister, DeShazer, and others[16, 17] where the change in the spatial profile of the laser beam is monitored as the self-trapping process takes place. Notwithstanding, self focusing is necessarily associated with rather large index changes and high intensities (compared to the Kerr effect, for example). Hence the measurements performed are more likely to be influenced by instabilities in the trapping process or other nonlinear effects such as multiphoton absorption and stimulated scattering.[18] This is particularly true in solid media where the nonlinear index of refraction is small and self focusing is often accompanied by damage.

In addition to self focusing, the index changes induced by a monochromatic beam may also be reflected in a change in the polarization properties of the beam as it propagates through the medium. In contrast to self focusing, such effects may be observed in spatially uniform optical beams and may be detected when phase shifts of only a few degrees have been produced; thus much lower intensities may be used to observe this effect. Maker et al. were the first to predict and observe this phenomenon when they monitored the intensity dependent

Reproduced with permission of the copyright owner. Further reproduction prohibited without permission.

rotation of an elliptically polarized ruby laser giant pulse after it had traversed a liquid filled absorption cell.[8] Additionally, this effect which we term "induced ellipse rotation" may be measured over a large range of powers which are well below the thresholds for self focusing. Thus ellipse rotation offers a possibly effective and accurate means of characterizing and determining the self-induced refractive index changes in an isotropic medium.

Since ellipse rotation involves the same self-induced refractive index changes which govern self-focusing effects, the nonlinear polarization of Equation (3.22) may be employed directly in the consideration of this phenomenon. Here it is interesting to note that this relation is simply a degenerate case of the a.c. Kerr effect expressed by Equation (3.17). The "probe field" itself now acts as its own "Kerr field".

Clearly the nonlinear polarization given by Equation (3.22) may be specified in terms of two independent parameters since χ_3^{1122} cannot be differentiated from χ_3^{1212} in this relation. Hence Maker et al. have chosen to write the nonlinear polarization in the form[3]

$$\underline{P}'_{3,\omega} = \{A\, \underline{E}_\omega \underline{E}_\omega \cdot \underline{E}^*_\omega + \frac{1}{2} B\, \underline{E}^*_\omega\, \underline{E}_\omega \cdot \underline{E}_\omega\} e^{ikz} \tag{3.25}$$

where

$$A = 3\{\chi_3^{1122}(-\omega,\omega,\omega,-\omega) + \chi_3^{1212}(-\omega,\omega,\omega,-\omega)\}$$

and (3.26)

$$B = 6\chi_3^{1221}(-\omega,\omega,\omega,-\omega)$$

Reproduced with permission of the copyright owner. Further reproduction prohibited without permission.

The first term is noted to be parallel to $\underline{E}_\omega$ whereas the second term can in general manifest a birefringent component. Substituting Equation (3.25) into the nonlinear wave equation, Equation (3.5) yields

$$\frac{\partial \underline{E}_\omega(z)}{\partial z} = \frac{2\pi i k}{n^2(\omega)} \{A\, \underline{E}_\omega \cdot \underline{E}^*_\omega\, \underline{E}_\omega + \frac{1}{2} B\, \underline{E}_\omega \cdot \underline{E}_\omega\, \underline{E}^*_\omega\} \tag{3.27}$$

Let us consider the case of Equation (3.27) in which $\underline{\tilde{E}}(t)$ is an elliptically polarized wave and it is assumed that A and B are real. In this case $\underline{\tilde{E}}(t)$ may be characterized as the sum of a right and a left circularly polarized component.[3] Hence

$$\underline{E}_\omega = \underline{E}_{+\omega} + \underline{E}_{-\omega}$$

where

$$\underline{E}_{+\omega} = \frac{E_{+\omega}}{\sqrt{2}} (\hat{e}_x + i\hat{e}_y) = E_{+\omega}\, \hat{e}_+$$

and

$$\underline{E}_{-\omega} = \frac{E_{-\omega}}{\sqrt{2}} (\hat{e}_x - i\hat{e}_y) = E_{-\omega}\, \hat{e}_- \tag{3.28}$$

$\hat{e}_x$ and $\hat{e}_y$ being unit vectors in the x and y direction respectively. Substituting Equation (3.28) into Equation (3.27) one finds

$$\frac{\partial(\underline{E}_{+\omega} + \underline{E}_{-\omega})}{\partial z} = \frac{2\pi i k(\omega)}{n^2(\omega)} \{A[\underline{E}_{+\omega} + \underline{E}_{-\omega}] \cdot [\underline{E}_{+\omega} + \underline{E}_{-\omega}]^* [\underline{E}_{+\omega} + \underline{E}_{-\omega}]$$

$$+ \frac{B}{2}[\underline{E}_{+\omega} + \underline{E}_{-\omega}] \cdot [\underline{E}_{+\omega} + \underline{E}_{-\omega}][\underline{E}_{+\omega} + \underline{E}_{-\omega}]^* \} \tag{3.29}$$

Noting that

$$\hat{e}_+ \cdot \hat{e}_+ = 0 \qquad \hat{e}_- \cdot \hat{e}_- = 0$$

$$\hat{e}_+ \cdot \hat{e}_- = 1 \qquad \hat{e}^*_+ = \hat{e}_- \tag{3.30}$$

Reproduced with permission of the copyright owner. Further reproduction prohibited without permission.

Equation (3.29) reduces to

$$\frac{\partial [\underline{E}_{+\omega} + \underline{E}_{-\omega}]}{\partial z} = \frac{2\pi i k}{n^2(\omega)} \{A|E_{+\omega}|^2 + (A+B)|E_{-\omega}|^2\}\underline{E}_{+\omega}$$

$$+ \frac{2\pi i k}{n^2(\omega)} \{A|E_{-\omega}|^2 + (A+B)|E_{+\omega}|^2\}\ \underline{E}_{-\omega} \qquad (3.31)$$

It is seen from Equation (3.27) that since A and B are assumed to be real

$$\frac{\partial(|\underline{E}_{\omega}|^2)}{\partial z} = \underline{E}_{\omega} \cdot \frac{\underline{E}^*_{\omega}}{\partial z} + \text{c.c.} = 0 \qquad (3.32)$$

Also, from Equations (3.30) and (3.31),

$$\frac{\partial(|E_{+\omega}|^2}{\partial z} = \frac{\partial(|E_{-\omega}|^2)}{\partial z} = 0 \qquad (3.33)$$

Thus in the case where A and B are real, one finds that Equation (3.31) may be separated into the forms

$$\frac{\partial \underline{E}_{+\omega}}{\partial z} = \frac{2\pi i k}{n^2(\omega)} \{A|E_{+\omega}|^2 + (A+B)|E_{-\omega}|^2\}\underline{E}_{+\omega} \qquad (3.34)$$

$$\frac{\partial \underline{E}_{-\omega}}{\partial z} = \frac{2\pi i k}{n^2(\omega)} \{A|E_{-\omega}|^2 + (A+B)|E_{+\omega}|^2\}\underline{E}_{-\omega} \qquad (3.35)$$

Applying the definition of the induced refractive index change given in Equation (3.19) to Equations (3.34) and (3.35) it is seen that the induced index changes δn_+ and δn_- for right and left circularly polarized components are given by

Reproduced with permission of the copyright owner. Further reproduction prohibited without permission.

$$\delta n_{\pm} = \frac{2\pi}{n(\omega)} \{A|E_{\pm\omega}|^2 + (A+B)|E_{\mp\omega}|^2\} \tag{3.36}$$

Since the solution to Equations (3.34) and (3.35) are of the form

$$E_{\pm\omega}(z) = E_{\pm\omega}(0)\, e^{jk\frac{\delta n_{\pm}}{n(\omega)}z} = E_{\pm\omega}(0)\, e^{i\phi_{\pm}(z)}, \tag{3.37}$$

it is seen that the difference in the phase shift $\phi(z)$ between the left and right circular components of the wave is given by

$$\phi(z) = \phi_+(z) - \phi_-(z) = \frac{\omega}{c}(\delta n_+ - \delta n_-)z \tag{3.38}$$

This phase shift results in a rotation of the major axis of the polarization ellipse by an angle $\theta = \frac{\phi(z)}{2}$ (see Appendix C). Thus an elliptically polarized plane wave $\underline{E}_{\omega} = \underline{E}_{+\omega} + \underline{E}_{-\omega}$ experiences a rotation of its major axis of polarization by an amount

$$\theta = \frac{\omega}{2c}(\delta n_+ - \delta n_-)z$$

$$= \frac{\pi\omega B}{nc}\{|E_{-\omega}|^2 - |E_{+\omega}|^2\}z \tag{3.39}$$

in propagating a distance z through an isotropic medium. Measurement of this rotation angle thus gives a direct measurement of $B = 6\chi^{1221}_{3}(-\omega,\omega,\omega,-\omega)$.[8]

The various elements of the nonlinear susceptibility tensor which are measured by the techniques described in this chapter are tabulated in Table 3.1 for convenient reference. As we proceed in the following

Reproduced with permission of the copyright owner. Further reproduction prohibited without permission.

chapters to develop physical models to characterize the nonlinear susceptibility, it will become evident that the tensor elements which are displayed in Table 3.1 bear a definite relationship to one another and that their determination will provide information on physical constants which will serve to specify the nature of the nonlinear polarization.

Reproduced with permission of the copyright owner. Further reproduction prohibited without permission.

TABLE 3.1

Experimental Technique	Input Field	Measured Nonlinear Susceptibility Element
Third Harmonic Generation (THG)	$\uparrow \underline{E}_{\omega}$	$\chi_3^{1111}(-3\omega,\omega,\omega,\omega)$
Three Wave Mixing (TWM) (Degenerate Case)	$\uparrow \underline{E}_{\omega} + \uparrow \underline{E}_{\omega-\Delta}$	$\chi_3^{1111}(-(\omega+\Delta),\omega,\omega,-(\omega-\Delta))$
	$\uparrow \underline{E}_{\omega} + \overrightarrow{\underline{E}}_{\omega-\Delta}$	$\chi_3^{1221}(-(\omega+\Delta),\omega,\omega,-(\omega-\Delta))$
Kerr Effect	$\uparrow \underline{E}_{\Omega} + \nearrow \underline{E}_{\omega}$	$\chi_3^{1221}(-\omega,\omega,\Omega,-\Omega) + \chi_3^{1212}(-\omega,\omega,\Omega,-\Omega)$
Self Focusing Linear Polarization	$\uparrow \underline{E}_{\omega}$	$\chi_3^{1111}(-\omega,\omega,\omega,-\omega)$
Self Focusing Circular Polarization	$\circlearrowleft \underline{E}_{\omega}$	$\chi_3^{1122}(-\omega,\omega,\omega,-\omega) = \chi_3^{1212}(-\omega,\omega,\omega,-\omega)$
Ellipse Rotation (ER)	$\circlearrowright \underline{E}_{\omega}$	$\chi_3^{1221}(-\omega,\omega,\omega,-\omega)$

Reproduced with permission of the copyright owner. Further reproduction prohibited without permission.

REFERENCES - CHAPTER III

1. J. A. Armstrong, N. Bloembergen, J. Ducuing, and P. S. Pershan, "Interaction between Light Waves in a Nonlinear Dielectric," Phys. Rev. 127, 1918 (1962).

2. P. N. Butcher and T. P. McLean, "The Nonlinear Constitutive Relations in Solids at Optical Frequencies I-II," Proc. Phys. Soc. 81, 219 (1963) and 83, 579 (1964).

3. P. D. Maker and R. W. Terhune, "Study of Optical Effects Due to an Induced Polarization Third Order in the Electric Field Strength," Phys. Rev. 137, A801 (1965).

4. R. W. Terhune, P. D. Maker, and C. M. Savage, "Optical Harmonic Generation in Calcite," Phys. Rev. Lett. 8, 404 (1962).

5. J. Kerr, "A New Relation between Electricity and Light: Dielectrified Media Birefringent," Phil. Mag. 50 [4], 337 (1875).

6. G. Mayer and F. Gires, "Action d'une onde lumineuse intense sur l'indice de refraction des liquides," Compt. Rend. 258, 2039 (1964).

7. R. Y. Chiao, E. Garmire, and C. H. Townes, "Self-Trapping of Optical Beams," Phys. Rev. Lett. 13, 479 (1964).

8. P. D. Maker, R. W. Terhune, and C. M. Savage, "Intensity Dependent Changes in the Refractive Index of Liquids," Phys. Rev. Lett. 12, 507 (1964).

9. D. A. Kleinman, "Theory of Second Harmonic Generation of Light," Phys. Rev. 128, 1761 (1962).

10. J. A. Giordmaine, "Mixing of Light Beams in Crystals," Phys. Rev. Lett. 8, 19 (1962).

11. N. Bloembergen and P. S. Pershan, "Light Waves at the Boundary of Nonlinear Media," Phys. Rev. 128, 606 (1962).

12. C. C. Wang and E. L. Baardsen, "Study of Third-Harmonic Generation in Reflection," Phys. Rev. 185, 1079 (1969). Errata Phys. Rev. B 1, 2827 (1970).

Reproduced with permission of the copyright owner. Further reproduction prohibited without permission.

13. M. Paillette, "Mesures de l'effet Kerr induit par une onde lunineuse intense," Compt. Rend. 262, 264 (1966)

14. M. A. Duguay and J. W. Hansen, "Measurement of the Nonlinear Index n_2 of Glass Using Picosecond Laser Pulses," Symposium on Damage in Laser Materials, Boulder, Colorado, June 24-25, 1970, NBS Spec. Publ. 341, pp. 45-50.

15. P. L. Kelley, "Self-Focusing of Optical Beams," Phys. Rev. Lett. 15, 1005 (1965).

16. G. L. McAllister, J. H. Marburger, and L. G. DeShazer, "Observation of Optical Pulse Shaping by the Self-Focusing Effects," Phys. Rev. Lett. 21, 1648 (1968).

17. L. G. DeShazer and B. R. Newman (private communication).

18. N. Bloembergen, "The Stimulated Raman Effect", Am. J. Phys. 35, 989 (1967).

Reproduced with permission of the copyright owner. Further reproduction prohibited without permission.

CHAPTER IV

MECHANISMS FOR THE THIRD ORDER NONLINEAR POLARIZATION IN ISOTROPIC MEDIA

4.0 Introduction

The nonlinear susceptibility tensor $\chi_3^{ijk\ell}$ which we employ to characterize nonlinear optical processes in isotropic media was defined in Chapter II. In Chapter III the various experimental techniques which have been employed to measure elements of this tensor in isotropic media have been reviewed. The results of this discussion are summarized in Table 3.1. Recognizing that the nonlinear susceptibility elements are functions of their four frequency arguments as well as their spatial indices, we see that the comparison of the various experimental determinations of this tensor will require the development of some phenomenological model which will relate the various tensor elements and aid in specifying their dispersion characteristics.

In this chapter we shall give consideration to the various mechanisms which contribute to the nonlinear polarization in isotropic media. We shall review phenomenological models for each of the contributing mechanisms and demonstrate that each of these mechanisms produces a nonlinear polarization which conforms to a unique functional form which we shall propose for $\tilde{P}_3(t)$. This form for $\tilde{P}_3(t)$ will serve as a basis for the comparison and interpretation of the experimental determinations of $\chi_3^{ijk\ell}$ which will be considered in subsequent chapters.

More specifically, it will be shown in this chapter that the nonlinear polarization arising from each physical mechanism may be

Reproduced with permission of the copyright owner. Further reproduction prohibited without permission.

written in the form

$$\tilde{P}_3(t) = \frac{\sigma}{2}\tilde{E}(t)\cdot\tilde{E}(t)\tilde{E}(t) + \int \tilde{a}(t-\tau)\tilde{E}(\tau)\cdot\tilde{E}(\tau)d\tau\ \tilde{E}(t)$$

$$+ \int \tilde{b}(t-\tau)\tilde{E}(\tau)\cdot\tilde{E}(t)\tilde{E}(\tau)d\tau \qquad (4.1)$$

Here the first term gives the "fast responding" electronic contribution to the nonlinear polarization which arises as a result of a direct distortion of the electronic orbits from their region of linear response and the latter two terms model the slower nuclear nonlinearities which are a consequence of electric field induced changes in the motions of nuclei whose electrons then respond linearly to the applied fields.[1,2]

Our consideration of the mechanisms of nonlinear polarization will be divided into two major sections. In Section 4.1 the electronic distortion mechanism will be considered by employing a simple classical model for the nonlinear response. The nuclear rearrangement type mechanisms will be given consideration in the various subsections of Section 4.2.

4.1 Direct Electronic Distortion

The idea that the electronic structure of any atom or molecule may be distorted by the application of an electric field to produce a net dipole moment which is linearly proportional to that field is a well known empirical postulate of the theory of dielectrics. This assumption of a linear electronic polarizability is well established in both the classical[3] and quantum mechanical[4] theory of dielectric media.

Reproduced with permission of the copyright owner. Further reproduction prohibited without permission.

In the classical theory, the electron oscillator model or "Lorentz model"[5] of the atom is employed to predict the response of the system to an applied field $\underline{\tilde{E}}(t)$ *. The equation of motion of the electron is then written as

$$\frac{d^2\underline{\tilde{r}}(t)}{dt^2} + \gamma \frac{d\underline{\tilde{r}}(t)}{dt} + \omega_o^2 \underline{\tilde{r}}(t) = \frac{-e\underline{\tilde{E}}(t)}{m} \qquad (4.2a)$$

where $-e$ is the electron charge, $\underline{\tilde{r}}(t)$ the displacement of the electron from its zero field equilibrium position, m the electron mass, ω_o the transition (absorption) frequency of the atom, and γ the linewidth of the transition which phenomenologically models the damping of the electron oscillator. Although the oscillator model generally presents quite an adequate description of the electronic response arising from a particular electric dipole transition of the system, it is to be recognized that each electron in the system is in actuality bound by the many charges which surround it. Hence the harmonic potential would be expected to be a valid approximation of the binding potential for small values of $\underline{\tilde{r}}(t)$ only. For high electric fields $\underline{\tilde{E}}(t)$ one would expect that anharmonic terms would enter into the power series expansion of the binding potential and that $\tilde{r}(t)$ would consequently exhibit a nonlinear response to the applied field.[1]

Bloembergen has used the electron oscillator of Equation (4.1) to model the nonlinear response by adding an anharmonic forcing term to this relation which is proportional to $\tilde{r}^2(t)$.[6] Since our concern in this work is primarily with isotropic media, the model which we consider should be invariant with respect to all symmetry

*See Appendix D for local field corrections.

Reproduced with permission of the copyright owner. Further reproduction prohibited without permission.

transformations. Hence we choose to modify Equation (4.2a) by considering the form

$$\frac{d^2\tilde{\underline{r}}(t)}{dt^2} + \gamma \frac{d\tilde{\underline{r}}(t)}{dt} + \omega_o^2 \tilde{\underline{r}}(t) + d\tilde{\underline{r}}(t) \cdot \tilde{\underline{r}}(t)\, \tilde{\underline{r}}(t) = -\frac{e\tilde{\underline{E}}(t)}{m} \quad (4.2b)$$

which is a vector form of Duffing's equation[7,8] where d is assumed to be small so as to produce only a perturbation of $\tilde{\underline{r}}(t)$ from its linear solution. Armstrong et al.[9] and Wang[10] have both considered the scalar form of Equation (4.2) as a model for direct electronic nonlinearities in the polarization.

Although the model of Equation (4.2b) is for an isotropic oscillator, it is to be recognized that it is applicable to media consisting of randomly oriented anisotropic molecular units. In this case the linear and nonlinear responses would represent the orientationally averaged responses which characterize the macroscopic behavior of the system.[1,11]

An approximate solution of Equation (4.2b) may be obtained by employing a perturbation series in powers of d which would take the form[8]

$$\tilde{\underline{r}}(t) = \tilde{\underline{r}}_o(t) + d\tilde{\underline{r}}_1(t) + d^2\tilde{\underline{r}}_2(t) + \cdots \quad (4.3)$$

Here $\tilde{\underline{r}}_o(t)$ gives the solution which is linear in the field $\tilde{\underline{E}}(t)$ and the succeeding terms represent small corrections to the linear solution. This trial solution is quite a reasonable one to assume since the frequency of the incident field is well below the oscillator absorption frequency and is known to produce a linear response for sufficiently small

Reproduced with permission of the copyright owner. Further reproduction prohibited without permission.

field strengths. Substituting Equation (4.3) into Equation (4.2b) and solving iteratively for $\tilde{\underline{r}}_i(t)$, one obtains for the first two terms

$$\tilde{\underline{r}}_o(t) = -\int_{-\infty}^{\infty} \tilde{Z}(t-\tau)\,\frac{e\tilde{\underline{E}}(\tau)}{2\pi m}\,d\tau \tag{4.4}$$

$$d\tilde{\underline{r}}_1(t) = -\frac{d}{2\pi}\int_{-\infty}^{\infty} \tilde{Z}(t-\tau)\tilde{\underline{r}}_o(\tau)\cdot\tilde{\underline{r}}_o(\tau)\tilde{\underline{r}}_o(\tau)\,d\tau \tag{4.5}$$

where $\tilde{Z}(t)$ is the inverse Fourier transform of the oscillator response function $Z(\omega) = [\omega_o^2 - \omega^2 - i\omega\gamma]^{-1}$.

Since the classical polarization is defined by $\tilde{\underline{P}}(t) = -Ne\,\tilde{\underline{r}}(t)$ where N is the number density of oscillating electrons in the dielectric, the polarization due to the transiton of interest may be written in the form

$$\begin{aligned}\tilde{\underline{P}}(t) &= \tilde{\underline{P}}_1(t) + \tilde{\underline{P}}_3(t) + \cdots \\ &= \int_{-\infty}^{\infty} \tilde{\chi}(t-\tau)\tilde{\underline{E}}(\tau)d\tau - \frac{dm}{N^3e^4}\int\!\!\int\!\!\int_{-\infty}^{\infty} \tilde{\chi}(\tau)\tilde{\chi}(t-\tau_1-\tau)\tilde{\chi}(t-\tau_2-\tau)\tilde{\chi}(t-\tau_3-\tau)d\tau \\ &\qquad \times\ \tilde{\underline{E}}(\tau_1)\tilde{\underline{E}}(\tau_2)\tilde{\underline{E}}(\tau_3)d\tau_1 d\tau_2 d\tau_3\end{aligned} \tag{4.6}$$

where $\tilde{\underline{P}}_1(t)$ and $\tilde{\underline{P}}_3(t)$ are the linear and third order nonlinear polarizations respectively and the linear response function is given by $\tilde{\chi}(t) = \frac{Ne^2}{2\pi m}\tilde{Z}(t)$. Comparing Equation (4.6) with Equation (2.6) it is

Reproduced with permission of the copyright owner. Further reproduction prohibited without permission.

seen that the third order nonlinear response tensor takes the form

$$\tilde{\chi}_3^{ijk\ell}(t_1,t_2,t_3) = \frac{-dm}{3N^3e^4} \int_{-\infty}^{\infty} \tilde{\chi}(\tau)\tilde{\chi}(t_1-\tau)\tilde{\chi}(t_2-\tau)\tilde{\chi}(t_3-\tau)\, d\tau$$

$$\times \{\delta_{ij}\delta_{k\ell} + \delta_{i\ell}\delta_{jk} + \delta_{ik}\delta_{j\ell}\} \qquad (4.7)$$

Using Equation (2.9) to transform this response tensor into the frequency domain, it is clear that the nonlinear susceptibility tensor takes the form

$$D\chi_3^{ijk\ell}(-\omega,\omega_1,\omega_2,\omega_3) = -\frac{Ddm}{3N^3e^4}\chi(\omega)\chi(\omega_1)\chi(\omega_2)\chi(\omega_3)$$

$$\times \{\delta_{ij}\delta_{k\ell} + \delta_{i\ell}\delta_{jk} + \delta_{ik}\delta_{j\ell}\} \qquad (4.8)$$

Here the linear susceptibility is given by $\chi(\omega) = \frac{Ne^2}{m} Z(\omega)$, D is the degeneracy factor which is 6, 3, or 1 depending on whether the frequency arguments $\omega_1,\omega_2,\omega_3$ are nondegenerate, partially degenerate, or totally degenerate, and the result has been divided by a factor of 4 in accordance with the convention adopted in Equation (2.19).

In the experimental situations which we shall consider the medium is transparent at all frequencies which are involved in the nonlinear interaction and the resonant frequency of the electronic transition ω_o is assumed to be well above any of the interacting frequencies $\omega_i = \omega,\omega_1,\omega_2,\omega_3$ so that $\omega_o^2 - \omega_i^2 >> \omega\gamma$. Under this condition it is easy to see that $\chi(\omega)$ is real valued and that $\partial\chi/\partial\omega$ is small so that dispersion is negligible. Thus Equation (4.8)

Reproduced with permission of the copyright owner. Further reproduction prohibited without permission.

may be approximated by the form

$$\chi_3^{ijk\ell}(-\omega,\omega_1,\omega_2,\omega_3) = \frac{\sigma}{24}\left(\delta_{ij}\delta_{k\ell} + \delta_{i\ell}\delta_{jk} + \delta_{ik}\delta_{j\ell}\right) \qquad (4.9)$$

where $\sigma = \frac{-2dm}{N^3 e^4}\chi^4(\bar{\omega})$; the $\bar{\omega}$ denoting a mean value of the frequencies involved in the interaction.

Equation (4.9) is readily transformed into the time domain again where it is seen to yield a nonlinear polarization of the form

$$\tilde{\underline{P}}_3(t) = \frac{\sigma}{2}\,\tilde{\underline{E}}(t)\cdot\tilde{\underline{E}}(t)\,\tilde{\underline{E}}(t) \qquad (4.10)$$

in conformity with our proposed form of Equation (4.1). In essence Equation (4.10) relays the fact that in the low frequency limit, the anharmonic oscillators are lossless and the polarization responds instantaneously to the field.

Since the materials to be examined in this work are highly transparent in the visible, the dispersionless estimates given by Equations (4.9) and (4.10) will prove to be quite adequate in approximating the electronic nonlinear response of these materials; see Appendix E.

4.2 Nuclear Nonlinearities

In this section (which we have divided into five parts) we consider contributions to the nonlinear polarization which arise as a consequence of a rearrangement in the positions of nuclei in the medium. These "slow" responding nonlinearities which we shall term "nuclear" nonlinearities or "nuclear rearrangement type" nonlinearities

Reproduced with permission of the copyright owner. Further reproduction prohibited without permission.

are many in number and it is often difficult to attribute the nuclear contribution to a nonlinear optical phenomenon to any one nuclear mechanism. Our intent in this section will be to review some simple classical models for the most commonly proposed nuclear mechanisms and to show that these yield contributions to the nonlinear polarization $\underset{\sim}{P}_3(t)$ which conform to the last two terms of Equation (4.1) thus building a phenomenological basis for asserting the general applicability of this relation. Specifically, the five nuclear mechanisms which we shall consider are (1) molecular reorientation, (2) Raman type nonlinearities, (3) molecular librations, (4) molecular redistribution, and (5) electrostriction. With the exception of electrostriction, these mechanisms do not involve macroscopic density changes in the medium, but rather local electric field induced changes in the arrangement of nuclei which are reflected in changes in the electronic polarizability of the molecular system as a whole.

4.2.1 Molecular Reorientation

Perhaps the most common nonlinear optical effect resulting in an induced refractive index change is the d.c. Kerr effect which is a special case of the a.c. Kerr effect discussed in Section 3.3. In liquids of nonpolar anisotropic molecules such as CS_2 it is well known that the alignment or "reorientation" of the molecules by the applied electric field yields a major contribution to the induced birefringence of the medium.[2,12,13]

Although molecular reorientation effects are generally associated with liquid media in which the relaxation times for reorientation may be as short as a few picoseconds,[14] reorientation phenomena

Reproduced with permission of the copyright owner. Further reproduction prohibited without permission.

are also known to occur in solids. Generally speaking the reorientation times associated with molecular solids are long enough to exclude them from being considered as a possible mechanism for the induced refractive index changes seen under high power (nanosecond or picosecond) laser excitation.[15] However it should be noted that the freedom of rotation which is exhibited by a molecule is highly dependent upon its symmetry and hence such symmetric molecules as CH_4 and CCl_4 possess a rather large degree of rotational freedom in the crystalline state.[16,17] Recently, investigations of the "plastic crystal" succinonitrile demonstrate that cases do exist in which anisotropic molecules in the solid state may exhibit quite rapid reorientation times ($\sim$50 psec).[18,19] Hence although reorientation effects are unlikely to be of great importance in the determination of induced refractive index changes in solids, they cannot be ruled out completely.

The general problem of the reorientation of polar molecules in a static electric field was considered by Debye in 1912.[20] It is a well known result that the average orientation of these molecules will take on a Maxwell-Boltzmann energy distribution

$$f(U) = \frac{e^{-U/kT}}{\int e^{-U/kT}\, d\Theta} \qquad (4.11a)$$

where the integral is taken over the entire sphere and U is the energy of the molecule in the presence of the applied field. Hence the average moment of a system of polar molecules each with a permanent dipole moment μ may be written in the form

Reproduced with permission of the copyright owner. Further reproduction prohibited without permission.

$$\bar{\mu} = \int \mu \cos\theta \, f(-\mu E \cos\theta) \, d\Theta \qquad (4.11b)$$

where θ is the angle between the permanent moment μ and the d.c. field E, the "bar" denotes an orientational average over the sphere, and the energy of each dipole in the field is given by $U = -\mu E \cos\theta$.

When the orienting field $\underline{E}$ is varying in time, the equilibrium distribution function f is no longer applicable to this problem. Debye was the first to address himself to the problem of polar molecules in an a.c. electric field.[20,21] Using Einstein's theory of Brownian motion to model the damped rotation of the molecules, Debye found that the system may be characterized in terms of a time varying distribution function $\tilde{f}(\theta,t)$ which obeys the relationship[21]

$$\zeta \frac{\partial \tilde{f}}{\partial t} = \frac{1}{\sin\theta} \frac{\partial}{\partial \theta} \left[\sin\theta \left(kT \frac{\partial \tilde{f}}{\partial \theta} - M\tilde{f}\right)\right] \qquad (4.12)$$

Here θ is again the angle between the polar axis of the molecule and the electric field, $M = \mu E \sin\theta$ is the torque on the molecule due to the applied field, and ζ is the damping constant of inner friction which specifies a "damping torque" by the relation $M_{damp} = \zeta \frac{d\theta}{dt}$. This coefficient has been estimated by Stokes to be given by $\zeta = 8\pi\eta a^3$ for a liquid with a viscosity coefficient η consisting of spherical molecules of radius "a".[21,22]

Since the torque on a permanent dipole is seen to reverse its sign as the direction of the applied field is reversed, it is clear that such a permanent dipole will play no part in contributing to

Reproduced with permission of the copyright owner. Further reproduction prohibited without permission.

nonlinear index changes which are induced by optical fields (i.e., the orientation of the molecules will not be able to follow the rapid oscillations of the optical field). It will be shown however that the torque experienced by a molecule with an anisotropic polarizability tensor under optical excitation will possess a component which varies slowly in time. Hence the molecules will exhibit a reorientation by the impressed field which will result in an induced birefringence due to the inherent anisotropy in the polarizability of the individual molecules.

The problem of the reorientation of anisotropic polarizable molecules in a time varying field has recently been considered in connection with stimulated Rayleigh wing scattering of light in liquids.[23-25] In particular it has been noted by Bloembergen and Lallemand that the description of such a system of molecules in an a.c. field will be adequately accomplished by the distribution function of Equation (4.12) provided that the correct expression is substituted for the torque $\tilde{M}(t)$ in this relationship.[25]

In order to see the effects of reorientation on the induced refractive index changes of a medium, let us consider a system of "cigar shaped symmetric top molecules" each of which has a polarizability tensor of the form

$$\underline{\alpha} = \begin{pmatrix} \alpha_1 & 0 & 0 \\ 0 & \alpha_1 & 0 \\ 0 & 0 & \alpha_2 \end{pmatrix} \tag{4.13}$$

in its principal coordinate system and which may be re-expressed in the more general form

Reproduced with permission of the copyright owner. Further reproduction prohibited without permission.

$$\underline{\alpha}(\theta,\phi) = \underline{A}^{t} \cdot \underline{\alpha} \cdot \underline{A} =$$

$$\begin{pmatrix} \alpha_1+(\alpha_2-\alpha_1)\sin^2\theta\cos^2\phi & (\alpha_2-\alpha_1)\sin^2\theta\sin\phi\cos\phi & (\alpha_2-\alpha_1)\cos\theta\sin\theta\cos\phi \\ (\alpha_2-\alpha_1)\sin^2\theta\sin\phi\cos\phi & \alpha_1+(\alpha_2-\alpha_1)\sin^2\theta\sin^2\phi & (\alpha_2-\alpha_1)\cos\theta\sin\theta\sin\phi \\ (\alpha_2-\alpha_1)\sin\theta\cos\theta\cos\phi & (\alpha_2-\alpha_1)\sin\theta\cos\theta\sin\phi & \alpha_1+(\alpha_2-\alpha_1)\cos^2\theta \end{pmatrix} \tag{4.14}$$

for an arbitrary orientation (θ,ϕ) of the α_2 principal axis with respect to the fixed spatial axes x, y, and z as shown in Figure 4.1.; see Appendix F.

If the molecule is assumed to react instantaneously to the applied field (no dispersion) then the dipole moment $\underline{p}$ may be written in the form

$$\tilde{\underline{p}}(t) = \underline{\alpha}(\theta,\phi) \cdot \tilde{\underline{E}}(t) \tag{4.15}$$

and the energy of the molecule in the field $\tilde{\underline{E}}(t)$ may be written[26,27]

$$\tilde{U}(t) = -\frac{1}{2}\,\underline{\alpha}(\theta,\phi) : \tilde{\underline{E}}(t)\,\tilde{\underline{E}}(t) \tag{4.16}$$

Assuming $\tilde{E}(t)$ to be linearly polarized along the z axis in Figure 4.1, the torque $\tilde{M}$ experienced by the molecule is given by

$$\tilde{M} = -\frac{\partial U}{\partial \theta} = \frac{\partial(\alpha_{zz})}{\partial\theta}\tilde{E}^2(t) = (\alpha_2-\alpha_1)\,\tilde{E}^2(t)\sin(2\theta) \tag{4.17}$$

which is clearly seen to be symmetric about $E = 0$.

Substituting this expression into Equation (4.12) we find

$$\frac{\zeta}{kT}\frac{\partial \tilde{f}}{\partial t} = \frac{1}{\sin\theta}\frac{\partial}{\partial\theta}\left\{\sin\theta\frac{\partial \tilde{f}}{\partial\theta} + \tilde{f}\,\frac{(\alpha_2-\alpha_1)\tilde{E}^2(t)\sin 2\theta}{2kT}\right\} \tag{4.18}$$

Reproduced with permission of the copyright owner. Further reproduction prohibited without permission.

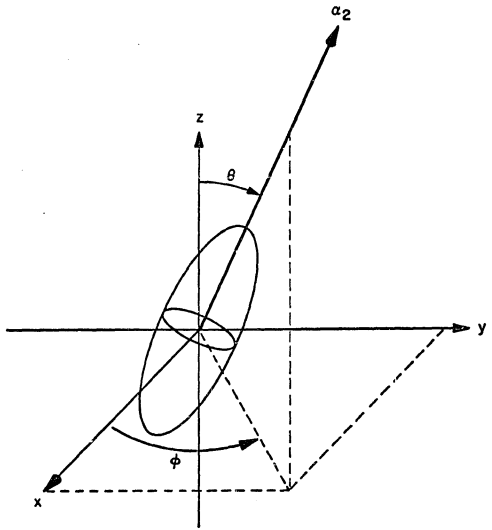

Figure 4.1

Reproduced with permission of the copyright owner. Further reproduction prohibited without permission.

for a field polarized along the z axis. Here the torque has been written as a negative quantity since it is directed in the direction of decreasing θ .

The solution of Equation (4.18) may be obtained in two steps the details of which are outlined in Appendix G. A special case is first considered in which $\tilde{\underline{E}}(t)$ is a d.c. field which is turned off at $t = 0$. The solution for this case yields a general form for a trial solution for the general case of arbitrary $\tilde{\underline{E}}(t)$. The outcome of these calculations show that retaining terms up to second order in the field, the solution of Equation (4.18) for a field $\tilde{\underline{E}}(t)$ of any polarization is given by

$$\tilde{f}(\Theta,t) = \frac{1}{4\pi}\left\{1+\frac{1}{2kT}(\alpha_{ij}(\Theta)-\overline{\alpha_{ij}(\Theta)})\int_{-\infty}^{t}\tilde{\rho}(t-\tau)\tilde{E}_i(\tau)\tilde{E}_j(\tau)\,d\tau\right\} \quad (4.19)$$

where Θ specifies the angular orientation of the molecule, $\alpha_{ij}(\Theta)$ is the ij^{th} component of the molecular polarizability tensor, $\overline{\alpha_{ij}(\Theta)} = (1/4\pi)\int\alpha_{ij}(\Theta)d\Theta = ((\alpha_2+2\alpha_1)/3)\delta_{ij} = \alpha\delta_{ij}$ is the average polarizability, and $\tilde{\rho}(t) = e^{-t/\tau_R}/\tau_R$ is the orientational response function. Here the relaxation time τ_R is given by $\tau_R = \tau_D/3 = \frac{\zeta}{6kT}$ where τ_D is the Debye relaxation time.[21]

Clearly the solution given by Equation (4.19) reduces to the Maxwell-Boltzmann distribution to second order in $\underline{E}$ when the applied field is constant. It is also noteworthy that for a monochromatic optical field, the finite response time τ_R , which is at least a few picoseconds in liquids, will cause an averaging over all optical components of $\tilde{E}^2(t)$ and consequently $\tilde{f}(\Theta,t)$ will only depend on the

Reproduced with permission of the copyright owner. Further reproduction prohibited without permission.

time averaged value of $\tilde{E}^2(t)$. This is physically reasonable since one would expect that rapid oscillations would be damped out by the orientational system response and that the molecules would only see the "d.c." component of the torque expressed in Equation (4.17).

The distribution function given by Equation (4.19) may be applied to find the orientationally averaged polarizability tensor of each molecule in the medium. This average polarizability is given by

$$\overline{\tilde{\alpha}_{ij}(t)} = \int \alpha_{ij}(\Theta)\, \tilde{f}(\Theta, t)\, d\Theta \qquad (4.20)$$

which upon substitution of Equation (4.19) yields

$$\overline{\tilde{\alpha}_{ij}(t)} = \alpha\delta_{ij} + \frac{1}{2kT}\left(\overline{\alpha_{ij}\alpha_{k\ell}} - \alpha^2\delta_{ij}\delta_{k\ell}\right) \int_{-\infty}^{t} \tilde{\rho}(t-\tau)\tilde{E}_k(\tau)\tilde{E}_\ell(\tau)dt \qquad (4.21)$$

where α is the average linear polarizability $(\alpha_2 + 2\alpha_1)/3$. By neglecting dispersion and comparing Equation (2.6) to Equation (4.21) it is easy to see that the latter is a special case of the former where the triple integral over three time variables in the nonlinear term is reduced to a single integral over two of the fields. The single integral expresses the fact that the polarizability is modulated by low frequency components in $\tilde{E}^2(t)$ whereas high frequency optical terms are "averaged out" by the response function $\tilde{\rho}(t)$.

The explicit evaluation of Equation (4.21) is simplified considerably by recalling that for isotropic media, the 81 independent terms of $\chi_3^{ijk\ell}$ reduce to three terms corresponding to the three permutations of $\tilde{E}_i(t)\tilde{E}_i(t)\tilde{E}_j(t)$.[28] Furthermore, since Equation (4.21)

Reproduced with permission of the copyright owner. Further reproduction prohibited without permission.

is symmetric with respect to the fields $\tilde{E}_k$ and $\tilde{E}_\ell$, there are only two independent elements and $\overline{\tilde{\alpha}_{ij}(t)}$ may be cast in the form

$$N\overline{\tilde{\alpha}_{ij}(t)} = N\alpha\delta_{ij} + \int \tilde{a}_1(t-\tau)\,\tilde{E}_k(\tau)\tilde{E}_\ell(\tau)\,d\tau\,\delta_{ij}\delta_{k\ell}$$

$$+ \frac{1}{2}\int \tilde{b}_1(t-\tau)\tilde{E}_k(\tau)\tilde{E}_\ell(\tau)d\tau\,\{\delta_{ik}\delta_{j\ell} + \delta_{i\ell}\delta_{jk}\} \qquad (4.22)$$

where N is the number density of molecules and Equations (4.21) and (F.6) yield the relationship

$$\tilde{b}_1(t) = -3\tilde{a}_1(t) = N\frac{(\alpha_2-\alpha_1)^2}{15kT}\tilde{\rho}(t) \qquad (4.23)$$

Thus the nonlinear polarization $\tilde{\underline{P}}_3(t)$ may be written in the form

$$\tilde{\underline{P}}_3(t) = \int \tilde{a}_1(t-\tau)\tilde{\underline{E}}(\tau)\cdot\tilde{\underline{E}}(\tau)d\tau\,\tilde{\underline{E}}(t)$$

$$+ \int \tilde{b}_1(t-\tau)\tilde{\underline{E}}(\tau)\cdot\tilde{\underline{E}}(t)\underline{E}(\tau)d\tau \qquad (4.24)$$

This relationship clearly establishes the fact that the molecular reorientation mechanism yields a form for $\tilde{\underline{P}}_3(t)$ which is in agreement with the form proposed in Equation (4.1). Moreover it is seen from Equation (4.23) that the anisotropy parameter $(\alpha_2-\alpha_1)^2$ is the one molecular parameter on which this effect depends.

Although our primary concern in this work is with the refractive changes which are predicted by $\tilde{\underline{P}}_3(t)$, it is to be noted that the reorientation mechanism is also partially responsible for the Rayleigh wing scattering of light[25] to which we will give further

Reproduced with permission of the copyright owner. Further reproduction prohibited without permission.

consideration in Appendices H and I. Since Equations (4.23) and (4.24) completely specify the properties of the reorientational nonlinear polarization, they will determine the polarization properties of all nonlinear processes arising from this mechanism. We shall however defer any further discussion of these properties to Appendices H and I.

4.2.2 Raman Type Nonlinearities

In addition to molecular reorientation, any medium may exhibit a nonlinear polarization as a result of the modulation of its polarizability by the (Raman) vibrational modes which are driven by an incident field. Raman scattering processes are well understood both in liquid and in crystalline solid media. In the former the interaction is on the localized level of intra-molecular vibrations[29] whereas collective vibrational (optical phonon) modes are responsible for the light scattering processes in the latter case.[30] In the case of amorphous materials, however, an incomplete understanding of the material structure has limited the understanding of the basic excitations involved in the scattering process.[31]

A fundamental understanding of the Raman process may be obtained by expanding the electronic polarizability α_{ij} of the medium in a Taylor series in one of its vibrational coordinates Q_k as suggested by Placzek.[32] We then obtain

$$\alpha_{ij} = (\alpha_{ij})_o + \frac{\partial \alpha_{ij}}{\partial Q_k} Q_k + \cdots \qquad (4.25)$$

This relationship conveys the fact that the polarizability of the

Reproduced with permission of the copyright owner. Further reproduction prohibited without permission.

fundamental unit of scattering is modulated by the vibration of some nuclear coordinate. In liquids this polarizability would be characterized by the individual molecules whereas the unit cell would be the characteristic unit in the case of crystalline solids.

Assuming that the Fourier spectrum of $\tilde{\underline{E}}(t)$ lies well below the fundamental electronic absorption in α_{ij} and neglecting dispersion it is easily shown that the energy of interaction between α_{ij} and the electric field $\tilde{\underline{E}}(t)$ takes the form[26,27]

$$\tilde{U}(t) = -\frac{1}{2}\,\alpha_{ij}\,\tilde{E}_i(t)\,\tilde{E}_j(t)$$

where a sum is taken over the repeated indices. Hence the force driving the vibrational oscillations is given by

$$\tilde{F}(t) = -\frac{\partial \tilde{U}}{\partial Q_k} = \frac{1}{2}\left(\frac{\partial \alpha_{ij}}{\partial Q_k}\right)\tilde{E}_i(t)\,\tilde{E}_j(t) \qquad (4.26)$$

If it is assumed that the vibrations are harmonic, the equation of motion for Q_k may be written in the form

$$\frac{d^2\tilde{Q}_k}{dt^2} + \Gamma\frac{d\tilde{Q}_k}{dt} + \Omega_o^2\,\tilde{Q}_k = \frac{1}{2\mu}\left(\frac{\partial \alpha_{ij}}{\partial Q_k}\right)\tilde{E}_i(t)\tilde{E}_j(t) \qquad (4.27)$$

where Ω_o is the resonant frequency of the vibration, μ is the reduced mass of the system and Γ is a loss which is phenomenologically added.

Since Equation (4.27) is linear, the solution may be expressed in terms of an impulse response $\tilde{\phi}(t)$ convoluted over the forcing function. Thus we may write

Reproduced with permission of the copyright owner. Further reproduction prohibited without permission.

$$\tilde{Q}_k(t) = \frac{1}{2\mu} \frac{\partial \alpha_{ij}}{\partial Q_k} \int \frac{\tilde{\phi}(t-\tau)}{2\pi} \tilde{E}_i(\tau)\, \tilde{E}_j(\tau)\, d\tau \qquad (4.28)$$

Here $\tilde{\phi}(t)$ is given by the inverse Fourier transform of the frequency response $\phi(\omega) = (\Omega_o^2 - \omega^2 - i\omega\Gamma)^{-1}$.

Using Equations (4.25) and (4.28) the nonlinear polarization is found to be given by

$$\tilde{P}_{3i}(t) = \frac{\partial \alpha_{ij}}{\partial Q_k} \tilde{Q}_k \tilde{E}_j = \frac{1}{2\mu} \frac{\partial \alpha_{ij}}{\partial Q_k} \frac{\partial \alpha_{\ell m}}{\partial Q_k} \int \frac{\tilde{\phi}(t-\tau)}{2\pi} \tilde{E}_\ell(\tau) \tilde{E}_m(\tau) d\tau\, \tilde{E}_j(t) \qquad (4.29)$$

The time integral of Equation (4.29) is quite similar to Equation (4.21) which describes the case of reorientation. Again the response of $\tilde{P}_3(t)$ is determined by a single integral over time. The Raman response function $\tilde{\phi}(t)$ however differs from the reorientation response $\tilde{\rho}(t)$ in that it possesses a resonance at some frequency Ω_o in the <u>infrared</u> region rather than exhibiting a simple relaxational response. The response drops off rapidly for frequencies $\omega > \Omega_o$ so that the Raman nonlinearities will also "average out" optical components of $\tilde{E}^2(t)$ while responding most strongly to frequency components near Ω_o . In essence the vibrational modes of the medium are seen to slowly modulate α_{ij} in time as they are driven by the components of $\tilde{E}^2(t)$ near the resonance frequency Ω_o .

Since the interest in this work is in isotropic media, it is again necessary to average Equation (4.29) over all possible orientations of the scattering units. The specific form of $\tilde{P}_3(t)$ will depend on the symmetry properties of $\partial \alpha_{ij}/\partial \tilde{Q}_k$ for the individual scatterers, however, it has already been noted in connection with

Reproduced with permission of the copyright owner. Further reproduction prohibited without permission.

Equation (4.22) that an orientational average of Equation (4.29) will result in a nonlinear polarization of the form

$$\underline{\tilde{P}}_3(t) = \int \tilde{a}_2(t-\tau)\underline{\tilde{E}}(\tau)\cdot\underline{\tilde{E}}(\tau)d\tau\ \underline{\tilde{E}}(t) + \int \tilde{b}_2(t-\tau)\underline{\tilde{E}}(\tau)\cdot\underline{\tilde{E}}(t)\underline{\tilde{E}}(\tau)d\tau \qquad (4.30)$$

where Equation (4.29) now gives

$$\tilde{a}_2(t) = \frac{1}{2\mu}\overline{\frac{\partial\alpha_{11}}{\partial Q_k}\frac{\partial\alpha_{22}}{\partial Q_k}}\frac{\tilde{\phi}(t)}{2\pi} \quad \text{and} \quad \tilde{b}_2(t) = \frac{1}{\mu}\overline{\frac{\partial\alpha_{12}}{\partial Q_k}\frac{\partial\alpha_{12}}{\partial Q_k}}\frac{\tilde{\phi}(t)}{2\pi}$$

the "bar" denoting an average over all directions and the indices 1 and 2 representing x, y, or z .

For the special case of "cigar shaped" molecules, the averages to be performed here are identical to those employed evaluating Equation (4.22); see Appendix F. Equation (F.6) clearly shows that $\tilde{a}_2(t)$ and $\tilde{b}_2(t)$ may no longer be characterized by one parameter as was done for $\tilde{a}_1(t)$ and $\tilde{b}_1(t)$ in the previous subsection. Rather, it is found that in the more general case where the scattering unit has polarizabilities α_1, α_2 and α_3 along its three principal axes $\tilde{a}_2(t)$ and $\tilde{b}_2(t)$ are dependent upon two parameters.[29] Hence we find

$$\tilde{a}_2(t) = \frac{1}{90\mu}(45\xi^2 - 2\psi^2)\frac{\tilde{\phi}(t)}{2\pi} \qquad (4.31)$$

$$\tilde{b}_2(t) = \frac{3}{45\mu}\psi^2\frac{\tilde{\phi}(t)}{2\pi} \qquad (4.32)$$

where

$$\xi = \frac{1}{3}\left(\frac{\partial\alpha_1}{\partial Q_k} + \frac{\partial\alpha_2}{\partial Q_k} + \frac{\partial\alpha_3}{\partial Q_k}\right) \qquad (4.33)$$

Reproduced with permission of the copyright owner. Further reproduction prohibited without permission.

and

$$\psi^2 = \frac{1}{2}\left\{\left(\frac{\partial\alpha_1}{\partial Q_k} - \frac{\partial\alpha_2}{\partial Q_k}\right)^2 + \left(\frac{\partial\alpha_2}{\partial Q_k} - \frac{\partial\alpha_3}{\partial Q_k}\right)^2 + \left(\frac{\partial\alpha_3}{\partial Q_k} - \frac{\partial\alpha_1}{\partial Q_k}\right)^2\right\} \tag{4.34}$$

It is clear from the preceding development that Raman type nonlinearities also conform to Equation (4.1). Several factors, however, distinguish this mechanism from reorientation. Firstly, the polarization properties of $\tilde{\underline{P}}_3(t)$ are specified by <u>two</u> independent parameters ξ and ψ which depend on the symmetry of the fundamental scattering unit. We note that this is equivalent to saying that all elements of $\overline{(\partial\alpha_{ij}/\partial Q_k)(\partial\alpha_{\ell m}/\partial Q_k)}$ are completely determined by ξ and ψ ; see Appendix F. Secondly, the response functions in the Raman process exhibit resonances at some frequency Ω_o which is characteristic of the molecular vibration. Generally speaking this resonance may lie anywhere in the region of 100 cm^{-1} out to several thousand cm^{-1}, however it is worthwhile to note that a Raman vibration may contribute to $\tilde{\underline{P}}_3(t)$ even if it is being driven at a frequency which is over a hundred linewidths off resonance.[33,34] This will be discussed further in connection with the interpretation of specific experimental results in Chapter 7. Finally we note that $\tilde{b}_2(t) \neq -3\tilde{a}_2(t)$ unless $\xi = 0$. This last property is reflected in the polarization characteristics of the Raman process[35] which will be discussed further in Chapter 8.

The Raman model presented above may be straightforwardly employed to consider Raman processes arising from molecular vibrations in liquids. Consideration of similar processes in glasses and other

Reproduced with permission of the copyright owner. Further reproduction prohibited without permission.

amorphous solids have been hindered by a lack of knowledge concerning the fundamental excitations involved in the scattering process.[31] Also, although Raman scattering studies have been conducted in glasses since the early days of its discovery, it is only recently that data worthy of interpretation have become available.[36] Attempts have been made to consider the structure of fused quartz in terms of SiO_4 tetrahedral units or $(SiO_2)_n$ units with limited success.[37,38] Very recently Shuker and Gammon[39] have attempted to describe the Raman scattering in fused quartz with the aid of the random network model of SiO_4 tetrahedra proposed by Bell et al.[40,41] This treatment of the problem is based upon the same displacement dependence of the electronic polarizability which is expressed by Equation (4.25); however rather than assuming an almost infinite coherence length for the optical phonons as in a true crystal, the coherence is assumed to extend over only a few hundred angstroms, which is small compared to an optical wavelength. Hence the scattering is determined by the modes of excitation of structural units containing several hundred atoms. In contrast to crystals, the momentum matching restrictions are superseded since the coherence length of the interaction is much shorter than an optical wavelength. Yet in contrast to a liquid, the SiO_4 tetrahedra which make up the network model are still strongly coupled on a local level and this coupling determines the modes of excitation of the medium.

4.2.3 Molecular Librations

In our consideration of molecular librations in Subsection 4.2.1 it was found that a system of molecules which are assumed to undergo

Reproduced with permission of the copyright owner. Further reproduction prohibited without permission.

continuous rotational motion damped by a Brownian type collisional relaxation may be described by a generalization of the Maxwell-Boltzmann distribution in a time varying electric field. Debye, however, in attempting to determine the permanent dipole moments of various molecules by measuring the dielectric constant, found that this theory exhibited large discrepancies between liquid and gaseous phases. Even larger discrepancies (over three orders of magnitude) were exhibited in predicting the saturation behavior of liquids from the measured dipole moments. This led to the first postulation of the possibility of elastic rotational oscillations of molecules in liquid media.[22,42] These oscillations would be the result of the local fields of surrounding molecules which form a "potential well" in which the molecule rests.

Although the relaxational reorientation and elastic rotational oscillations may appear to be mutually exclusive in any given system of molecules, we may see that this is not necessarily the case by viewing the rotational oscillations or "librations" as having a finite lifetime τ_ℓ after which the molecule makes a small "jump" to a new equilibrium orientation about which it again exhibits librations. Assuming that τ_ℓ is much smaller than the rotational relaxation time τ_R, these elementary "jumps" may be viewed as incremental changes in position which sum up to produce the reorientational relaxation effects.

Recently librational oscillations have been proposed by Staranov to model the lineshape of light scattering from liquids.[43] Shapiro and Broida have suggested them as a possible explanation for the deviation of the lineshape of reorientational Rayleigh wing scattering in

Reproduced with permission of the copyright owner. Further reproduction prohibited without permission.

CS_2 from the predicted Lorentzian shape;[14] and Cubeddu et al. suggest that these librations contribute significantly to the intensity dependent refractive index of CS_2 under picosecond pulse excitation.[44, 45] It is worthwhile noting that stimulated librational scattering has also been observed in liquids of polar molecules in which one would expect the dipole-dipole interactions to be large.[46]

The simplest model of the small orientational displacements $\delta\theta$ experienced by librating molecules is obtained by assuming oscillation in a harmonic potential.[43] Assuming the same system of cigar shaped symmetric top molecules characterized by Equation (4.13), one may write the equation of motion

$$I\frac{d^2\delta\tilde{\theta}}{dt^2} + \Lambda\frac{d\delta\tilde{\theta}}{dt} + G\delta\tilde{\theta} = -\frac{1}{2}(\alpha_2-\alpha_1)\tilde{E}^2(t)\sin 2\theta \qquad (4.35)$$

where I is the moment of inertia of the molecule, Λ the coefficient of internal friction, G the elastic force constant, and the torque resulting from the applied field $\tilde{\underline{E}}(t)$ along the z direction was derived in Equation (4.17).

Equation (4.35) is clearly linear and thus the solution may be written directly to give

$$\delta\tilde{\theta} = -\frac{1}{2}(\alpha_2-\alpha_1)\sin(2\theta)\int \frac{\tilde{H}(t-\tau)}{2\pi}\tilde{E}^2(\tau)\,d\tau \qquad (4.36)$$

where the response function $\tilde{H}(t)$ is given by the Fourier transform relation $\tilde{H}(t) = F^{-1}\{(G - I\omega^2 - i\omega\Lambda)^{-1}\}$.

Equation (4.36) again expresses a response which involves a convolution of the square of the field over the oscillator response

Reproduced with permission of the copyright owner. Further reproduction prohibited without permission.

function. The change in the susceptibility of the medium along the field direction may be calculated by noting that the polarizability change along the applied field may be shown from Equation (4.14) to be $\delta\tilde{\alpha}_{zz} = \frac{\partial \alpha_{zz}}{\partial \theta}\,\delta\tilde{\theta} = -2(\alpha_2-\alpha_1)\sin\theta\cos\theta\,\delta\tilde{\theta}$. Averaging over a random distribution of N molecules per unit volume, one finds that the change in susceptibility along the direction of the applied field is given by

$$\delta\tilde{\chi}_{zz} = \frac{N}{4\pi}\int \delta\alpha_{zz}(t)\,d\theta$$

$$= \frac{4}{15}N(\alpha_2-\alpha_1)^2\int \frac{\tilde{H}(t-\tau)}{2\pi}E^2(\tau)\,d\tau \qquad (4.37)$$

Here we have used the average $\overline{\sin^2(2\theta)} = 8/15$ for a uniform distribution. Likewise in a direction perpendicular to the applied field the change in the susceptibility is

$$\delta\tilde{\chi}_{xx} = \frac{N}{4\pi}\int \delta\alpha_{xx}(t)\,d\theta$$

$$= -\frac{2}{15}N(\alpha_2-\alpha_1)^2\int \frac{\tilde{H}(t-\tau)}{2\pi}E^2(\tau)d\tau \qquad (4.38)$$

where again Equation (4.14) gives $\delta\alpha_{xx} = 2(\alpha_2-\alpha_1)\sin\theta\cos\theta\sin^2\phi\,\delta\theta$ and $\overline{\sin^2(2\theta)\sin^2\phi} = \frac{4}{15}$

Comparison of Equations (4.37) and (4.38) with Equation (4.22) which exhibits the most general form of induced polarizability involving a convolution over $\tilde{E}^2(t)$ for isotropic media, clearly shows that the induced librational susceptibility may be written in the form

Reproduced with permission of the copyright owner. Further reproduction prohibited without permission.

$$\delta\tilde{X}_{ij} = \int \tilde{a}_3(t-\tau)\tilde{E}_k(\tau)\tilde{E}_\ell(\tau)d\tau\ \delta_{ij}\delta_{k\ell}$$

$$+ \frac{1}{2}\int \tilde{b}_3(t-\tau)\tilde{E}_k(\tau)\tilde{E}_\ell(\tau)d\tau\ (\delta_{i\ell}\delta_{jk} + \delta_{ik}\delta_{j\ell}) \qquad (4.39)$$

where $\tilde{b}_3(t) = -3\tilde{a}_3(t) = \frac{2}{5}N(\alpha_2-\alpha_1)^2\frac{\tilde{H}(t)}{2}$. Thus the nonlinear polarization is again seen to take the form given by Equation (4.1)

$$\underline{\tilde{P}}_3(t) = \int \tilde{a}_3(t-\tau)\underline{\tilde{E}}(\tau)\cdot\underline{\tilde{E}}(\tau)d\tau\ \underline{\tilde{E}}(t)$$

$$+ \int \tilde{b}_3(t-\tau)\underline{E}(\tau)\cdot\underline{E}(t)\underline{E}(\tau)d\tau \qquad (4.40)$$

It is evident from the foregoing discussion that librational scattering exhibits the same polarization characteristics as scattering which arises from molecular reorientation (Rayleigh wing scattering) since $\tilde{b}_3(t) = -3\tilde{a}_3(t)$. Librations however would exhibit resonances in the range of approximately 20 cm^{-1} to several hundred wave numbers with response times of the order of 0.1 psec or greater.[45] One would expect that since the librational motions involve small perturbations in the orientation of molecules, these orientational modes of vibration would be much more likely to contribute to the nonlinear polarization in solids where the relaxational reorientation times would be expected to be extremely long.

Reproduced with permission of the copyright owner. Further reproduction prohibited without permission.

4.2.4 Molecular Redistribution

In a dense polarizable medium the application of a strong electric field causes a mutual interaction to occur between each of the induced dipoles in the medium. The induced anisotropic dipole-dipole forces experienced by the molecules are proportional to the time average of the square of the field strength and are naturally a function of the dipole separation and hence the density of the medium. Consequently the impressed field will cause the system of molecules to be "redistributed" from its zero field distribution in establishing a new equilibrium. This mechanism termed "molecular redistribution" was first proposed by Hellwarth[47] in 1965. Since it involves field dependent changes in the short range order of the system (short compared to an optical wavelength) a resultant induced change in the refractive index of the medium is observed.

In considering the nonlinear mechanisms presented thus far the approach has been to present the most straightforward models by largely ignoring local field effects and only taking them into consideration as a correction after calculating the nonlinear susceptibility; see Appendix D. For example in the case of molecular reorientation, each molecule was treated as an independent entity and the distribution function was calculated for that molecule without regard for how the orientation of the molecule itself or the distribution of the surrounding molecules might affect the local fields used in the calculation.

Since the redistribution mechanism is by its very nature a collective mechanism which is a consequence of the dipole-dipole

Reproduced with permission of the copyright owner. Further reproduction prohibited without permission.

interaction forces, it is naturally impossible to consider this problem in terms of independent molecules. Perhaps the simplest example of redistribution would be the artificial situation where we consider only two molecules of polarizability α and separated by the vector $\underline{r}$ which interact solely through their induced dipolar fields. Their mutual energy of interaction U_{int} in a field $\underline{E}$ would simply be the energy necessary to bring one dipole into the field of the other. Thus,

$$U_{int} = -\alpha\underline{E} \cdot (-\underline{D} \cdot \alpha\underline{E}) = \alpha^2 \underline{\underline{D}} : \underline{E}\,\underline{E} \qquad (4.41)$$

where $\underline{\underline{D}} = \dfrac{(\underline{\underline{I}} - 3\underline{r}\underline{r})}{r^5}$ is the dipole field tensor. Clearly U_{int} is maximized when $\underline{r}$ is perpendicular to $\underline{E}$ and minimized when $\underline{r}$ is parallel to $\underline{E}$ (assuming $|r|$ to be constant). Hence the latter situation would be the more probable in equilibrium.

The form of the nonlinear susceptibility arising from molecular redistribution in a d.c. or monochromatic optical field was derived by Hellwarth[33] for the special case of the d.c. or optical Kerr effects where a strong linearly polarized field produced an optical birefringence which was probed by a weak field; see Section 3.3. The assumption of d.c. or high frequency optical fields permitted the derivation to be carried out without giving consideration to transient effects as the molecular motions are unable to follow the rapid optical oscillations. Hence the system could be assumed to be in a state of statistical mechanical equilibrium in the presence of an electric field whose mean square value helps to determine the statistical state of the system.

Reproduced with permission of the copyright owner. Further reproduction prohibited without permission.

Although there is no simple model yet available to characterize the transient time response of the redistribution mechanism, we will argue that a response of the form given by Equation (4.1) is to be expected on a phenomenological basis. For the sake of completeness we give the derivation of the steady state susceptibility change arising from redistribution to show that it does indeed exhibit the expected E^2 dependence, possesses the proper symmetry, and is in fact a special case of Equation (4.1).[33]

The calculation of the effect of molecular redistribution on the polarizability of a medium involves a statistical mechanical average over all possible ways of arranging N molecules of polarizability $\alpha(\omega)$ in a volume $V << \lambda^3$ in the presence of an applied field $\tilde{\underline{E}}(t) = Re\{\underline{E}_\omega e^{i(\underline{k}\cdot\underline{r} - \omega t)}\}$.

A molecule at a point $\underline{r}$ in the volume V will exhibit a dipole moment

$$\underline{m}^\phi = \alpha(\omega)\, \underline{E}^\phi_{\mathscr{L}} \tag{4.42}$$

in the presence of the local electric field $\underline{E}^\phi_{\mathscr{L}}$ at the point $\underline{r}^\phi$. Since the local field is simply that which results from the impressed field plus the dipolar field of the surrounding N-1 molecules in the volume V , we may write

$$\underline{m}^\phi = \alpha(\omega)\{\underline{E}_\omega \exp\{i\underline{k}\cdot\underline{r}^\phi\} - \underline{\underline{D}}^{\phi\theta}\cdot \underline{m}^\theta\} \tag{4.43}$$

where $\underline{\underline{D}}^{\phi\theta}$ is the dipole field tensor defined in Equation (4.41) with $\underline{r}$ now taken to be $\underline{r}^\phi - \underline{r}^\theta$. It is assumed that a sum is taken over all repeated indices. Equation (4.43) may easily be solved for $\underline{m}^\phi$

Reproduced with permission of the copyright owner. Further reproduction prohibited without permission.

giving

$$\underline{m}^{\phi} = \alpha(\omega)\ \underline{\underline{X}}^{\phi\theta} \cdot \underline{E}_{\omega} \exp\{i\underline{k}\cdot\underline{r}^{\theta}\} \tag{4.44}$$

where $\underline{\underline{X}}^{\phi\theta} = [\delta^{\phi\theta}\underline{\underline{I}} + \alpha(\omega)\underline{\underline{D}}^{\phi\theta}]^{-1}$. Thus we have expressed the dipole moment of any molecule at the point $\underline{r}^{\phi}$ in terms of the applied field assuming the other N-1 molecules are in a certain configuration which we denote by $\{\underline{r}^{\phi}\}$. The average polarization of the medium may then be obtained by summing over the N molecules and averaging over all possible configurations. This gives

$$\underline{P}_{\omega} = \left\langle \frac{1}{V}\, \underline{m}^{\phi} \exp(-i\underline{k}\cdot\underline{r}^{\phi}) \right\rangle \tag{4.45}$$

where the brackets $\langle\rangle$ denote an average over all possible configurations $\{r^{\phi}\}$ of the N molecules and $\tilde{P}(t) = \mathrm{Re}\{\underline{P}_{\omega}\, e^{i(\underline{k}\cdot\underline{r}-\omega t)}\}$. Substituting Equation (4.44) into Equation (4.45) one finds that $\underline{P}_{\omega}$ may be expressed in the familiar form

$$\underline{P}_{\omega} = \underline{\underline{X}}(\omega) \cdot \underline{E}_{\omega} \tag{4.46}$$

where the linear susceptibility

$$\underline{\underline{X}}(\omega) \equiv \langle \underline{\underline{T}}_{\omega}(\{\underline{r}^{\phi}\}) \rangle = \left\langle \frac{\alpha_{\omega}}{V}\, \underline{\underline{X}}^{\phi\theta} \exp(i\underline{k}\cdot(\underline{r}^{\theta}-\underline{r}^{\phi})) \right\rangle$$

Now if the field $\underline{E}_{\omega}$ in Equation (4.46) is considered to be a weak "probe" field and another strong field denoted by $\mathrm{Re}\{\underline{E}_{\Omega} e^{i(\underline{k}\cdot\underline{r}-\Omega t)}\}$ is applied to the medium, it will in general affect the average over $\{r^{\phi}\}$ which was taken to obtain $\underline{\underline{X}}(\omega)$. Again we note that this is a consequence of the redistribution which takes place to lower the dipole-dipole interaction energy of the system.

Reproduced with permission of the copyright owner. Further reproduction prohibited without permission.

More specifically the average may be expressed in the form of the classical average

$$\underline{\underline{\chi}}(\omega) = \langle \underline{\underline{T}}_\omega(\{r^\phi\}) \rangle = \frac{\int dr_1 \cdots dr_N \, \underline{\underline{T}}_\omega(\{r^\phi\}) \exp\left(-\frac{v+v_o}{kT}\right)}{\int dr_1 \cdots dr_N \exp\left(-\frac{v+v_o}{kT}\right)} \tag{4.47}$$

where the integration is taken over the volume V for each of the N particles in that volume; v is the zero field intermolecular potential and the dipole-dipole interaction energy v is given by

$$v = -\frac{1}{4} V \, \underline{\underline{T}}_\Omega(\{r^\phi\}) : \underline{E}_\Omega \, \underline{E}^*_\Omega \tag{4.48}$$

which is simply Equation (4.41) summed over all of the $\frac{1}{2} N(N-1)$ possible pairs of particles in the volume V with the local fields expressed in terms of the applied field $\underline{E}_\Omega$.

Rewriting Equation (4.47) with the integrand expanded in a power series, it is seen that

$$\underline{\underline{\chi}}(\omega) = \frac{\int dr_1 \cdots dr_N \, \underline{\underline{T}}_\omega(\{r^\phi\})(1 - \frac{v}{kT} - \cdots) \exp(-\frac{v_o}{kT})}{\int dr_1 \cdots dr_N (1 - \frac{v}{kT} - \cdots) \exp(-\frac{v_o}{kT})} \tag{4.49}$$

$$\simeq \langle \underline{\underline{T}}_\omega \rangle_o + \frac{V}{4kT} \{ \langle \underline{\underline{T}}_\omega \, \underline{\underline{T}}_\Omega \rangle_o - \langle \underline{\underline{T}}_\omega \rangle_o \langle \underline{\underline{T}}_\Omega \rangle_o \} : \underline{E}_\Omega \, \underline{E}^*_\Omega$$

where the average $\langle \rangle_o$ is taken with $v = 0$ (i.e., $\underline{E}_\Omega = 0$).

It is clear that Equation (4.49) exhibits a nonlinear susceptibility of the form

Reproduced with permission of the copyright owner. Further reproduction prohibited without permission.

$$\delta\chi_{\omega}^{ij} = \chi_3^{ijk\ell}(-\omega,\omega,\Omega,-\Omega)\ E_{\Omega,k}\ E_{\Omega,\ell}^{*} \qquad (4.50)$$

Moreover it is to be noted that $\chi_3^{ijk\ell}$ is independent of k for long wavelengths where $k^{-3} >> V$. In this limit $\chi_3^{ijk\ell}$ must take on the rotational symmetry of an isotropic medium. Hence from Equations (4.46) and (4.49) we see that $\delta\chi^{ij}$ may be written in the form

$$\delta\chi_{\omega}^{ij} = A' E_{\Omega,k}\ E_{\Omega,k}^{*}\ \delta_{ij} + \frac{1}{2}B'\{(E_{\Omega,i}E_{\Omega,j}^{*} + E_{\Omega,i}^{*}E_{\Omega,j}\} \qquad (4.51)$$

where A' and B' are constants. Equation (4.51) exhibits the same form derived for the Kerr tensor of an isotropic medium as shown in Equation (3.18). Moreover one sees that $\frac{1}{2}B' = 6\chi_3^{1221}(-\omega,\omega,\Omega,-\Omega) = 6\chi_3^{1212}(-\omega,\omega,\Omega,-\Omega)$. Hellwarth has demonstrated by an expansion of Equation (4.49) that $B' = -3A'$.[33] Thus the symmetry of $\chi_3^{ijk\ell}$ for the redistribution process is identical to that which is obtained for reorientation and librations.

Equation (4.51) suggests that the equilibrium distribution which is attained with the medium subject to the strong field $\underline{E}_{\Omega}$ involves a change in the linear susceptibility which is proportional to the mean square value of that strong field. Since the processes which are involved in establishing this equilibrium involve the physical redistribution of nuclei as they respond to the change in dipole-dipole interaction forces induced by the field, one would expect that a response function could also be defined to characterize the transient behavior of this process. Indeed, it is reasonable to expect (at least in fluids) that the intermolecular collision times would be

Reproduced with permission of the copyright owner. Further reproduction prohibited without permission.

characteristic of these response functions since it is the dipole-dipole forces experienced in these collision processes which produce the redistribution effects.[48] Hence a general form for the time response of the susceptibility change in the redistribution process would be given by

$$\delta\tilde{\chi}^{ij}_{\omega}(t) = \int \tilde{a}_4(t-\tau)\tilde{E}_k(\tau)\tilde{E}_\ell(\tau)\, d\tau\, \delta_{ij}\delta_{k\ell} + \frac{1}{2}\int \tilde{b}_4(t-\tau)\tilde{E}_k(\tau)\,\tilde{E}_\ell(\tau)\, d\tau\, (\delta_{ik}\delta_{j\ell} + \delta_{i\ell}\delta_{jk}) \qquad (4.52)$$

where $\tilde{b}_4(t) = -3\tilde{a}_4(t)$ and $\tilde{a}_4(t)$ and $\tilde{b}_4(t)$ vanish as $t \to \infty$. Again this is of the same form as that derived for molecular reorientation although the time response functions will now most probably not be a simple exponential relaxation. Thus again Equation (4.1) should adequately describe redistribution and the contribution to the nonlinear polarization would be written as

$$\underline{\tilde{P}}_3(t) = \int \tilde{a}_4(t-\tau)\underline{\tilde{E}}(\tau)\cdot\underline{\tilde{E}}(\tau)\, d\tau\, \underline{\tilde{E}}(t) + \int \tilde{b}_4(t-\tau)\tilde{E}(\tau)\cdot\tilde{E}(t)E(\tau)d\tau \qquad (4.53)$$

Although the precise character of the response functions for molecular redistribution are not presently known, one would expect that information regarding the spectral character of these functions could be obtained by light scattering measurements; see Appendix I. Several investigations have been conducted to measure the Raman†

†Here the word "Raman" is used in its more general sense to denote any light scattering process in which a frequency shift is observed.

Reproduced with permission of the copyright owner. Further reproduction prohibited without permission.

spectra of such symmetric molecule liquids as CCl_4,[17] argon,[49-50] and xenon[48] in which the low frequency scattering spectrum (involving Stokes shifts of less than 200 cm^{-1}) can only result from the intermolecular processes which are responsible for molecular redistribution. Although many anomalies still exist with respect to the specific lineshapes obtained and the dependence of the scattered spectra on temperature, density, and other parameters, it is found in all of the cases investigated that (1) the decay of the scattered intensity in the wings of the spectrum (greater than approximately 20 cm^{-1} Stokes shift) exhibit an exponential falloff with frequency; (2) the linewidths of the scattering indicate that the response times involved are of the order of tenths of picoseconds; and (3) the scattering is depolarized† indicating that $\tilde{b}_4(t) = -3\tilde{a}_4(t)$.

At present further work is being pursued to obtain a better understanding of the microscopic processes which are involved in intermolecular light scattering.[51] It is hoped that these studies will provide further insight into the character of the response functions involved in the redistribution process.

4.2.5 Electrostrictive Effects

Our treatment of the major mechanisms which are responsible for a nonlinear polarization which is cubic in the electric field

† A depolarized scattering process is defined to be one in which the ratio of intensities between the scattered light with its plane of polarization parallel and perpendicular to the input polarization respectively takes on a value of 4/3 . It is shown in Appendix I that this requirement is equivalent to having $\tilde{b}(t) = -3\tilde{a}(t)$.

Reproduced with permission of the copyright owner. Further reproduction prohibited without permission.

strength would not be complete without a consideration of electrostriction. In contrast to all of the other mechanisms which have been considered thus far, electrostrictive changes in the refractive index of a medium are a direct consequence of induced changes in the macroscopic density rather than changes in the local arrangement of molecules.[52]

In essence electrostriction arises as a result of internal forces which are produced in any dielectric medium as a consequence of a nonuniform electric field. Since the dipoles which are induced by the field are proportional to the field strength and the net force which is experienced by each of these dipoles is proportional to the gradient of the electric field strength, it is seen that the net force on each molecule must be proportional to the gradient of the square of the field, that is, to the gradient of the intensity.[52]

The role of electrostriction in producing self focusing of optical beams was first proposed by Chiao, Garmire, and Townes in their original investigation of self-trapping.[53] Shen[54,55] and others[56,57] have made subsequent studies of the relative importance of electrostriction in the self-focusing process in liquid media. Recently, Kerr[58-60] gave extensive consideration to this mechanism in his theoretical investigations of electrostrictive self focusing in glasses. In the present work we shall not give extensive consideration to this particular mechanism since, as we will show, it is the one contribution to the nonlinear polarization which does not enter directly into the parameters which are determined by our experimental investigations. Hence we intend only to summarize several important

Reproduced with permission of the copyright owner. Further reproduction prohibited without permission.

characteristics of the electrostrictive mechanism referring the reader to the literature for further details.[52-60]

Kerr in his consideration of electrostrictive self focusing has demonstrated that the refractive index change arising from the induced electrostrictive density variations in the medium is determined by the relation[59]

$$v_s^2 \nabla^2 \tilde{n} - \frac{\partial^2 \tilde{n}}{\partial t^2} = \frac{1}{c\rho_o} \left(\rho_o \frac{\partial n}{\partial \rho}\right)^2 \nabla^2 I \qquad (4.54)$$

where ρ_o is the equilibrium density of the medium in the absence of the strong field, $I = \langle E^2 \rangle_{av}$ is the average intensity of the strong beam, v_s is the velocity of sound in the medium, and n is the refractive index. Here it is worthwhile to note that the refractive index change which is produced by the strong field is independent of the polarization of the strong beam (i.e., only dependent on its intensity). This suggests that electrostrictive effects cannot induce birefringence in isotropic media. Consequently $\tilde{b}(t)$ in Equation (4.1) must be zero for electrostriction.

Since electrostriction produces an isotropic refractive index change it will not yield any direct contribution to induced birefringence effects such as the Kerr measurements and the study of ellipse rotation. It may be shown however that since Equation (4.54) is linear in n, the expression for an electrostrictively produced nonlinear polarization may be characterized in terms of a phenomenological $\tilde{a}(t)$ found in Equation (4.1). In this case however the interpretation of $\tilde{a}(t)$ must be generalized to include spatial operators

Reproduced with permission of the copyright owner. Further reproduction prohibited without permission.

which act upon $\tilde{E}^2(\underline{r},t)$ since the induced changes in refractive index are not directly coupled to the intensity of the applied beam but rather through the relationship given by Equation (4.54). The details of this development have been reported by Kerr.[60]

Since electrostrictive contributions to the nonlinear polarization involve macroscopic density changes, it may be argued that they will also play no role in optical mixing experiments such as third harmonic generation and three-wave mixing. These processes involve rapid changes in the polarizability to which the density variations will not respond. It should be noted however that electrostrictively produced density changes may affect the results of these studies as well as the induced birefringence studies by changing the intensity profiles of the input beams employed in the experiments through electrostrictive self focusing.

Generally speaking electrostrictive self-focusing effects may be neglected unless the duration of the incident laser pulse is longer than a characteristic time t_c which is defined as the period required for an acoustic wave to propagate across the radius of the incident beam a_o. Physically we see that this is the time required for the density wave which is generated by the electrostrictive force (which is maximum at the edge of the beam where the gradient is large) to propagate to the center of the beam where it will have a maximal effect in the self-focusing process. In order to obtain an estimate of some typical pulse times and power thresholds which are required for electrostrictive self-focusing effects, let us calculate

Reproduced with permission of the copyright owner. Further reproduction prohibited without permission.

$t_c = a_o/v_s$ and the parameter

$$K = \frac{c\lambda^2 \rho_o v_s^2}{8\pi n_o (\rho_o \frac{\partial n}{\partial \rho})^2} \tag{4.55}$$

which was shown by Kerr[59] to be the critical power for electrostrictive self focusing of a Gaussian (intensity profile) beam in the steady state (long pulse duration) approximation. For the case where we have a focused beam with $a_o = 75\mu$ and $\lambda = 694$ nm we find for CCl_4 that $t_c = 100$ nsec and $K = 13$ kW whereas for fused quartz $t_c = 12.5$ nsec and $K = 1.1$ MW or 3.7 MW depending on whether theoretical or experimental values are used for $\rho_o \frac{\partial n}{\partial \rho}$ in the calculation.[59] These estimates provide some guidelines as to the experimental parameters which must be chosen to avoid electrostrictive self-focusing effects in the experimental investigations.

As we consider the experimental determination of the nonlinear susceptibilities in the chapters to follow, the possibility of electrostrictive self focusing will be kept in mind to prevent any misinterpretation of the results. The experimental parameters will be picked so that either the pulse duration is shorter than t_c or the pulse power is well below the critical power for the material under investigation. In our particular experimental investigation of ellipse rotation, we will see that the proportionality of the ellipse rotation angle to the input power of the beam as expressed in Equation (3.39) will give an additional means of verifying the fact that electrostrictive self focusing is not affecting the results.

Reproduced with permission of the copyright owner. Further reproduction prohibited without permission.

4.3 Summary of Nonlinear Polarization Mechanisms

It has been demonstrated in this chapter that each of the mechanisms which contribute to a nonlinear polarization cubic in the electric field strength may be shown to produce a contribution which conforms to Equation (4.1). Using this fact we will show in subsequent chapters how this expression may be employed to experimentally distinguish the nuclear contributions to $\tilde{P}_3(t)$ from those which are purely electronic in nature.

The problem of experimentally resolving the various nuclear contributions to the nonlinear polarization is a more complex issue to which we shall not give extensive consideration in this work. In Appendices H and I it will be shown how light scattering measurements may be employed to supplement the nonlinear optical measurements of the nuclear response functions $\tilde{a}(t)$ and $\tilde{b}(t)$, however it is to be recognized that even a knowledge of these functions would not assure the ability to separate uniquely the various nuclear mechanisms.

With these remarks we shall proceed to show how the electronic contribution to $\tilde{P}_3(t)$ as characterized by the parameter σ in Equation (4.1) can be uniquely determined by a combination of Kerr and ellipse rotation experimental data without having to know the explicit forms of the nuclear response functions $\tilde{a}(t)$ and $\tilde{b}(t)$.

Reproduced with permission of the copyright owner. Further reproduction prohibited without permission.

REFERENCES - CHAPTER IV

1. See for example, W. Voight, Ann. der Physik 4, 197 (1901); A. D. Buckingham and B. J. Orr, "Molecular Hyperpolarizabilities," Quarterly Review 21, 195 (1967).

2. See for example, P. Debye, Marx's Handbuch der Radiologie VI, Chap. V, (Akademische Verlagsgesellschaft, Leipzig, 1925); S. Kielich, "Optically Induced Birefringence," Acta Physica Polonica 30, 683 (1966).

3. A. R. Von Hippel, Dielectrics and Waves (M.I.T. Press, Cambridge, 1954), p. 93.

4. J. C. Slater, Quantum Theory of Matter (McGraw Hill Book Company, Inc., New York, 1968), Chap. 5.

5. H. A. Lorentz, The Theory of Electrons, 2nd ed., (Dover Publ., New York, 1952).

6. N. Bloembergen, Nonlinear Optics (W. A. Benjamin, Inc., New York, 1965), p. 5.

7. G. Duffing, Erzwungene Schwingungen bei veranderlicher Eigenfrequenz, (F. Vieweg u. Sohn, Braunschweig, 1918).

8. J. J. Stoker, Nonlinear Vibrations in Mechanical and Electrical Systems (Interscience Publ. Inc., New York, 1950), Chap. IV.

9. J. A. Armstrong, N. Bloembergen, J. Ducuing, and P. S. Pershan, "Interaction between Light Waves in a Nonlinear Dielectric," Phys. Rev. 127, 1918 (1962).

10. C. C. Wang and E. L. Baardsen, "Study of Third Harmonic Generation in Reflection," Phys. Rev. 185, 1079 (1969); Errata: Phys. Rev. B 1, 2827 (1970).

11. A. D. Buckingham and J. A. Pople, "Theoretical Studies of the Kerr Effect I: Deviation from a Linear Polarization Law," Proc. Phys. Soc. A, 68, 905 (1955).

Reproduced with permission of the copyright owner. Further reproduction prohibited without permission.

12. R. W. Hellwarth, "Theory of Light Scattering Spectra Using the Linear-Dipole Approximation," J. Chem. Phys. 52, 2128 (1970).

13. M. P. Bogaard, A. D. Buckingham, and G.L.D. Ritchie, "The Temperature-Dependence of Electric Birefringence in Gaseous Benzene and Carbon Disulphide," Mol. Phys. 18, 575 (1970).

14. S. L. Shapiro and H. P. Broida, "Light Scattering from Fluctuations in Orientations of CS_2 in Liquids," Phys. Rev. 154, 129 (1967).

15. R. R. Alfano and S. L. Shapiro, "Observation of Self-Phase Modulation and Small Scale Filaments in Crystals and Glasses," Phys. Rev. Lett. 24, 592 (1970).

16. C. Kittel, Introduction to Solid State Physics, Third Ed. (John Wiley and Sons, New York, 1953).

17. H. S. Gabelnick and H. L. Strauss, "Low-Frequency Motions in Liquid Carbon Tetrachloride. II. The Raman Spectrum," J. Chem. Phys. 49, 2234 (1968).

18. D. A. Jackson, M. J. Bird, H. T. A. Pentecost, and J. G. Powles, "Molecular Reorientation Rates in Crystals by Anisotropic Light Scattering," Phys. Lett. 35A, 1 (1971).

19. L. Boyer, R. Vacher, L. Cecchi, M. Adam, and P. Berge, "Rayleigh Scattering in a Plastic Crystal Due to Orientational Relaxation," Phys. Rev. Lett. 26, 1435 (1971).

20. P. Debye, Physik Z. 13, 97 (1912); Marx's Handbuch der Radiologie VI, Chap. V, Leipzig, 1925.

21. P. Debye, Polar Molecules (The Chemical Catalog Co., 1929). Reprinted by Dover Publications, Inc., New York.

22. J. Frenkel, Kinetic Theory of Liquids (Dover Publications, Inc., New York, 1955).

23. N. D. Foltz, C. W. Cho, D. H. Rank, and T. A. Wiggins, "Stimulated Rayleigh Scattering in Liquids," Phys. Rev. 165, 396 (1966).

Reproduced with permission of the copyright owner. Further reproduction prohibited without permission.

24. R. Y. Chiao and J. Godine, "Polarization Dependence of Stimulated Rayleigh-Wing Scattering and the Optical-Frequency Kerr Effect," Phys. Rev. 185, 430 (1969).

25. N. Bloembergen and P. Lallemand, "Complex Intensity Dependent Index of Refraction, Frequency Broadening of Stimulated Raman Lines, and Stimulated Rayleigh Scattering," Phys. Rev. Lett. 16, 81 (1966).

26. C.J.F. Bottcher, Theory of Electric Polarization (Elsevier Publishing Company, Amsterdam, 1952).

27. S. Flugge, Handbuch der Physik XVII, Dielectrics (Springer-Verlag, Berlin, 1956).

28. P. D. Maker, R. W. Terhune, and C. M. Savage, "Optical Third Harmonic Generation," in Quantum Electronics Vol. 2 (Columbia Univ. Press, New York, 1964), p. 1559.

29. E. B. Wilson, J. C. Decius, and P. C. Cross, Molecular Vibrations (McGraw-Hill Book Company, Inc., New York, 1955).

30. R. Loudon, "The Raman Effect in Crystals", Adv. Phys. 13, 423 (1964).

31. H. C. Tobin and T. Baak, "Raman Spectra of Some Low-Expansion Glasses," J. Opt. Soc. Am. 58, 1459 (1968).

32. G. Placzek, Marx Handbuch der Radiologie, E. Marx, ed., 2nd ed., (Akademische Verlagsgesellschaft, Leipzig, 1934), v.6, pt.II, p. 205.

33. R. W. Hellwarth, "Kerr Effect in Symmetric Molecule Liquids, in Proc. International School of Physics (Enrico Fermi), Vol. XLII, edited by R. J. Glauber, (Academic Press, New York, 1969), p. 563.

34. G. Hauchecorne, F. Kerherve, and G. Mayer, "Mesure des Interactions Entre Ondes Lumineuses dans Diverses Substances," Le Jour. de Physique 32, 47 (1971).

Reproduced with permission of the copyright owner. Further reproduction prohibited without permission.

35. S.P.S. Porto, "Angular Dependence and Depolarization Ratio of the Raman Effect," J. Opt. Soc. Am. 56, 1585 (1966).

36. M. Hass, "Raman Spectra of Vitreous Silica, Germania, and Sodium Silicate Glasses," J. Phys. Chem. Solids 31, 415 (1970).

37. W. Wadia and L. S. Ballomal, J. Phys. Chem. Glasses 9, 115 (1968).

38. G. J. Su, N. F. Borelli, and A. R. Miller, J. Phys. Chem. Glass 3, 167 (1962).

39. R. Shuker and R. W. Gammon, "Raman-Scattering Selection Rule Breaking and the Density of States in Amorphous Materials," Phys. Rev. Lett. 25, 222 (1970).

40. R. J. Bell and P. Dean, "Properties of Vitreous Silica: Analysis of Random Network Models," Nature 212, 1354 (1966).

41. R. J. Bell, N. E. Bird, and P. Dean, "The Vibrational Spectra of Vitreous Silica, Germania, and Beryllium Fluoride," J. Phys. Chem (Proc. Phys. Soc.) Ser. 2, 1, 229 (1968).

42. P. Debye, Phys. Z. [illegible] 100 (1935).

43. V. S. Starunov, "Scattering of Light Due to Anisotropy Fluctuations in Low Viscosity Liquids," Opt. Spectrosc. 18, 165 (1965).

44. R. Polloni, C. A. Sacchi, and O. Svelto, "Self-Trapping with Picosecond Pulses and 'Rocking' of Molecules," Phys. Rev. Lett. 23, 690 (1969).

45. R. Cubeddu, R. Polloni, C. A. Sacchi, and O. Svelto, "Self-Phase Modulation and 'Rocking' of Molecules in Trapped Filaments of Light with Picosecond Pulses," Phys. Rev. A2, 1955 (1970).

46. O. Rahn, M. Maier, and W. Kaiser, "Stimulated Raman, Librational, and Brillouin Scattering in Water," Optics Comm. 1, 109 (1969).

47. R. W. Hellwarth, "Effect of Molecular Redistribution on the Nonlinear Refractive Index of Liquids," Phys. Rev. 152, 156 (1966).

48. W. S. Gornal, H. E. Howard-Lock, and B. P. Stoicheff, "Induced Anisotropy and Light Scattering in Liquids," Phys. Rev. A1, 1288 (1970).

Reproduced with permission of the copyright owner. Further reproduction prohibited without permission.

49. J. P. McTague and G. Birnbaum, "Collision Induced Light Scattering in Gaseous Argon and Krypton," Phys. Rev. Lett. 21, 661 (1968).

50. J. P. McTague, P. A. Fleury, and D. B. Dupre, "Intermolecular Light Scattering in Liquids," Phys. Rev. 188, 303 (1969).

51. See for example, V. Volterra, J. A. Bucaro, and T. A. Litovitz, "Two Mechanisms for Depolarized Light Scattering from Gaseous Argon," Phys. Rev. Lett. 26, 55 (1971).

52. J. A. Stratton, Electromagnetic Theory (McGraw-Hill Book Company, Inc., New York, 1941).

53. R. Y. Chiao, E. Garmire, and C. H. Townes, "Self-Trapping of Optical Beams," Phys. Rev. Lett. 13, 479 (1964).

54. Y. R. Shen, "Electrostriction, Optical Kerr Effect, and Self Focusing of Laser Beams," Phys. Lett. 20, 378 (1966).

55. Y. R. Shen and Y. J. Shaham, "Self Focusing and Stimulated Raman and Brillouin Scattering in Liquids," Phys. Rev. 163, 224 (1967).

56. Ya. B. Zel'dovich and Yu. P. Raizer, "Self Focusing of Light. Role of Kerr Effect and Striction," Sov. Phys. JETP Lett. 3, 86 (1966).

57. K. A. Brueckner and S. Jorna, "Linearized Theory of Laser-Induced Instabilities in Liquids and Gases," Phys. REv. 164, 182 (1967).

58. E. L. Kerr, "Laser-Beam Self Focusing and Glass Damage Caused by Electrostrictively Driven Acoustic Waves," in Proc. of the ASTM Symposium on Damage in Laser Glass, Boulder, Colorado, June 20, 1969, ASTM Special Technical Publ. No. 469, p. 22.

59. E. L. Kerr, "Transient and Steady State Electrostrictive Laser Beam Trapping," IEEE J. Quant. Electr. QE-6, 616 (1970).

60. E. L. Kerr, "Filamentary Tracks Formed in Transparent Optical Glass by Laser Beam Self Focusing II. Theoretical Analysis," Phys. Rev. A4, 1195 (1971).

Reproduced with permission of the copyright owner. Further reproduction prohibited without permission.

CHAPTER V

INTERPRETATION OF THE NONLINEAR POLARIZATION

5.0 Interpreting the Model for $\tilde{P}_3(t)$

In Chapter IV we gave a phenomenological basis for stating that the third order nonlinear polarization in any isotropic medium may be expressed by the relation

$$\tilde{P}_3(t) = \frac{\sigma}{2}\tilde{E}(t)\cdot\tilde{E}(t)\tilde{E}(t) + \int \tilde{a}(t-\tau)\tilde{E}(\tau)\cdot\tilde{E}(\tau)d\tau\ \tilde{E}(t) + \int \tilde{b}(t-\tau)\tilde{E}(\tau)\cdot\tilde{E}(t)\tilde{E}(\tau)d\tau \qquad (5.1)$$

when all frequencies involved are much lower than any electronic absorptions. Here σ is the parameter which characterizes direct electronic distortion nonlinearities and the response functions $\tilde{a}(t)$ and $\tilde{b}(t)$ characterize those nonlinearities which result from nuclear rearrangement.

We shall in this section use the model to derive a general expression for the nonlinear susceptibility tensor $\chi_3^{ijk\ell}(-\omega,\omega_1,\omega_2,\omega_3)$. This nonlinear susceptibility expression will then serve as a basis for the interpretation of the experimental determinations which were described in Chapter 3.

Looking first at the electronic contribution to the nonlinear polarization, it is clear from both Equation (5.1) and Equation (4.7) that in the dispersionless approximation, the nonlinear electronic response tensor takes the form

Reproduced with permission of the copyright owner. Further reproduction prohibited without permission.

$$\chi_{3e}^{ijk\ell}(\tau_1,\tau_2,\tau_3) = \frac{\sigma}{6}\,(\delta_{ij}\delta_{k\ell} + \delta_{i\ell}\delta_{jk} + \delta_{ik}\delta_{j\ell})\delta(\tau_1)\delta(\tau_2)\delta(\tau_3) \quad (5.2)$$

Here the subscript "e" denotes the fact that we are only considering the electronic portion of the nonlinear response. This expression is readily transformed into the frequency domain where we find

$$\chi_{3e}^{ijk\ell}(-\omega;\omega_1,\omega_2,\omega_3) = \frac{\sigma}{24}\,(\delta_{ij}\delta_{k\ell} + \delta_{i\ell}\delta_{jk} + \delta_{ik}\delta_{j\ell}) \quad (5.3)$$

Clearly Equations (5.2) and (5.3) give a characterization of the electronic contribution to the nonlinear polarization in the case where all frequencies involved in the nonlinear process are far from the frequency of the electronic transition. The more general expressions for the nonlinear response and nonlinear susceptibility which included dispersion were previously given in Equations (4.7) and (4.8).

Going on to examine the nuclear portion of the nonlinear polarization given by Equation (5.1) we see from Equation (2.6) that the nuclear nonlinear response function is given by

$$\begin{aligned}
\chi_{3n}^{ijk\ell}(\tau_1,\tau_2,\tau_3) = {} & \{\tfrac{1}{3}\,a(\tau_3)\delta(\tau_1)\delta(\tau_2-\tau_3) + \tfrac{1}{6}\,b(\tau_1)\delta(\tau_3)\delta(\tau_1-\tau_2) \\
& + \tfrac{1}{6}\,b(\tau_3)\delta(\tau_2)\delta(\tau_1-\tau_3)\}\,\delta_{ij}\delta_{k\ell} \\
& + \{\tfrac{1}{3}\,a(\tau_2)\delta(\tau_2)\delta(\tau_1-\tau_2) + \tfrac{1}{6}\,b(\tau_3)\delta(\tau_2)\delta(\tau_1-\tau_3) \\
& + \tfrac{1}{6}\,b(\tau_2)\delta(\tau_1)\delta(\tau_2-\tau_3)\}\,\delta_{i\ell}\delta_{jk} \\
& + \{\tfrac{1}{3}\,a(\tau_1)\delta(\tau_2)\delta(\tau_1-\tau_3) + \tfrac{1}{6}\,b(\tau_2)\delta(\tau_1)\delta(\tau_2-\tau_3) \\
& + \tfrac{1}{6}\,b(\tau_1)\delta(\tau_3)\delta(\tau_1-\tau_2)\}\,\delta_{ik}\delta_{j\ell} \quad (5.4)
\end{aligned}$$

Reproduced with permission of the copyright owner. Further reproduction prohibited without permission.

which has been symmetrized with respect to the interchanges of the pairs $j,\tau_1 \leftrightarrow k,\tau_2 \leftrightarrow \ell,\tau_3$ in accordance with the discussion of Equation (2.13). Employing the transformation of Equation (2.9) and dividing by a factor of 4 to conform to the more common definition of $\chi_3^{ijk\ell}$ given in Equation (2.20), we obtain

$$\chi_{3n}^{ijk\ell}(-\omega,\omega_1,\omega_2,\omega_3) = \frac{1}{24}\{2a(\omega_2+\omega_3) + b(\omega_1+\omega_2) + b(\omega_1+\omega_3)\}\delta_{ij}\delta_{k\ell}$$

$$+ \frac{1}{24}\{2a(\omega_1+\omega_2) + b(\omega_1+\omega_3) + b(\omega_2+\omega_3)\}\delta_{i\ell}\delta_{jk}$$

$$+ \frac{1}{24}\{2a(\omega_1+\omega_3) + b(\omega_2+\omega_3) + b(\omega_1+\omega_2)\}\delta_{ik}\delta_{j\ell} \quad (5.5)$$

Here $a(\omega) = \int_{-\infty}^{\infty} \tilde{a}(t)\, e^{i\omega t}\, dt$ and $b(\omega) = \int_{-\infty}^{\infty} \tilde{b}(t)\, e^{i\omega t}\, dt$. Thus these functions are equal to the Fourier transforms of the time functions $\tilde{a}(t)$ and $\tilde{b}(t)$ multiplied by a factor of 2π.

It is clear that a direct consequence of the nuclear response functions of Equation (5.1) is that the nonlinear susceptibility takes the form of a sum of terms which are functions of the sum (or difference) of two frequency arguments.

5.1 Interpretation of the Nonlinear Susceptibility

Having derived the forms of the electronic and nuclear contributions to the nonlinear susceptibility, we may combine Equations (5.3) and (5.5) to obtain

Reproduced with permission of the copyright owner. Further reproduction prohibited without permission.

$$\chi_3^{ijk\ell}(-\omega,\omega_1,\omega_2,\omega_3) =$$

$$\frac{1}{24}\{\sigma + 2a(\omega_2+\omega_3) + b(\omega_1+\omega_2) + b(\omega_1+\omega_3)\}\ \delta_{ij}\delta_{k\ell}$$

$$+ \frac{1}{24}\{\sigma + 2a(\omega_1+\omega_2) + b(\omega_1+\omega_3) + b(\omega_2+\omega_3)\}\ \delta_{i\ell}\delta_{jk}$$

$$+ \frac{1}{24}\{\sigma + 2a(\omega_1+\omega_3) + b(\omega_2+\omega_3) + b(\omega_1+\omega_2)\}\ \delta_{ik}\delta_{j\ell} \qquad (5.6)$$

This expression may be applied directly to interpret the physical significance of the nonlinear susceptibility elements which have been measured by the techniques which we have described in Chapter III. The results of this application of Equation (5.6) are tabulated in Table 5.1 where the assumption has been made that $a(\Delta)$ and $b(\Delta)$ are negligible compared to σ at optical frequencies (e.g., 14,000 cm^{-1}). This assumption is quite reasonable since most common Raman vibrations are resonant from approximately 100-5000 cm^{-1} and yield negligible contributions at optical frequencies. It will be noted however that the terms $a(\Delta)$ and $b(\Delta)$ in the TWM susceptibilities have been retained, since Δ in this experiment is often generated by a Raman laser[1] and could thus yield a resonant contribution to $\chi_3^{ijk\ell}$. Although some terms have been dropped for convenience in the table, we add a note of caution that reference should be made back to Equation (5.6) in any case in which the medium of interest has vibrational resonances which lie in the visible.

Table 5.1 clearly shows that third harmonic generation is the only experimental means of directly measuring the electronic contribution to $\chi_3^{ijk\ell}$. As we shall discuss in Chapter 7, however, THG

Reproduced with permission of the copyright owner. Further reproduction prohibited without permission.

Reproduced with permission of the copyright owner. Further reproduction prohibited without permission.

Experiment	Elements of χ_3^{ijkl} Determined	Interpretation	Reference Equations
Third Harmonic Generation	$\chi_3^{1111}(-3\omega,\omega,\omega,\omega)$	$\sigma/8$	(3.8 - 3.10)
Three-Wave Mixing	$\chi_3^{1111}(-(\omega+\Delta),\omega,\omega,-(\omega-\Delta))$	$\sigma/8 + (1/6)\{a(\Delta)+b(\Delta)\}$	(3.14)
	$\chi_3^{1221}(-(\omega+\Delta),\omega,\omega,-(\omega-\Delta))$	$\sigma/24 + \frac{1}{12}\, b(\Delta)$	
Kerr Effect	$\frac{1}{2}\{\chi_3^{1221}(-\omega,\omega,\Omega,-\Omega)+\chi_3^{1212}(-\omega,\omega,\Omega,-\Omega)\}$	$(\sigma+\beta)/24$	(3.21)
Direct Interferometric Measurement of $\delta n_{\parallel}$ Using Two Beams	$\chi_3^{1111}(-\omega,\omega,\Omega,-\Omega)$	$\frac{(3\sigma+2\alpha+2\beta)}{24}$	(3.20a)
Direct Interferometric Measurement of $\delta n_{\perp}$ Using Two Beams	$\chi_3^{1122}(-\omega,\omega,\Omega,-\Omega)$	$\frac{(\sigma+2\alpha)}{24}$	(3.20b)
Ellipse Rotation	$\chi_3^{1221}(-\omega,\omega,\omega,-\omega)$	$(\sigma+2\beta)/24$	(3.39)
Self Focusing Linear Polarization	$\chi_3^{1111}(-\omega,\omega,\omega,-\omega)$	$\frac{3\sigma+4\alpha+4\beta}{24}$	(3.23)
Self Focusing Circular Polarization	$\chi_3^{1122}(-\omega,\omega,\omega,-\omega)$	$\frac{\sigma+2\alpha+\beta}{24}$	(3.24)

TABLE 5.1

Here $\alpha = a(o)$ and $\beta = b(o)$

studies are extremely difficult to perform with any degree of precision and are virtually impossible to calibrate to any degree of accuracy.

Three-wave mixing studies offer a possible alternative means of measuring the electronic contribution to the nonlinear response if it can be established in any particular situation that $a(\Delta)$ and $b(\Delta)$ are negligible. Perhaps light scattering measurements along with measurements of the polarization dependence of the TWM signal[2] may be used to establish whether or not the nuclear contribution may be neglected in any given situation. However this measurement cannot in general be regarded as a means of measuring the purely electronic contribution to the nonlinear susceptibility without the aid of supplementary measurements to establish the validity of neglecting the nuclear dependence of the measurement.

Generally speaking the Kerr effect and ellipse rotation together offer the most experimentally promising means of determining the electronic parameter σ and also the nuclear parameter $\beta = b(0)$. The former technique gives a determination of $\sigma + \beta$ whereas the latter measurement yields $\sigma + 2\beta$. The application of these two techniques have the added advantage that they are both easily calibrated to the same very accurate absolute standard of calibration; see Section 6.7.

Clearly it may be inferred from Equation (5.1) and Table 5.1 that if σ and β are known, only α is needed to completely characterize an isotropic medium with respect to intensity dependent changes in refractive index. In the nuclear rearrangement models of Chapter IV it has been demonstrated that with the exception of electrostriction

Reproduced with permission of the copyright owner. Further reproduction prohibited without permission.

and possibly the Raman effect, the nuclear nonlinearities exhibit a ratio of $\beta/\alpha = -3$. In general, this ratio may be determined through the measurement of depolarization ratios in light scattering studies*.[3]

Upon further examination of Table 5.1 we note two additional possibilities for determining the intensity dependent refractive index which should not be overlooked. The first of these is a direct measurement of $\delta n_{||}$ and $\delta n_{\perp}$ using interferometric techniques. Previous attempts at performing such interferometric determinations in solids have not produced results which are consistent with any of the other measurements outlined in Table 5.1.[4] However, such measurements have been performed with some degree of success in liquid media.[5] An accurate interferometric determination of this type using a low frequency Kerr field (which is yet of a high enough frequency to rule out electrostrictive effects) would be of great value in verifying the assertions of the previous investigations. An examination of Table 5.1 will show that the quantities measured by such an experiment when combined with ellipse rotation and/or Kerr data will yield a unique determination of α, β and σ in addition to giving a check on the consistency of ellipse rotation and Kerr measurements. Indeed, in view of the difficulty of making accurate a.c. Kerr measurements (see Section 7.0) the interferometric measurements may well prove to be the most ideal data to use in conjunction with ellipse rotation data for the determination of α, β, and σ .

The second added scheme for determining α, β, and σ from Table 5.1 is suggested by the direct measurement of self-focusing thresholds[6] for plane and circularly polarized waves. Although

---

* See Appendix I.

Reproduced with permission of the copyright owner. Further reproduction prohibited without permission.

these measurements will in principle provide the same information which may be obtained by the interferometric techniques proposed above, this technique is not readily adaptable to accurate determinations of $\chi_3^{ijk\ell}$. The reasons are primarily twofold. Firstly, circularly polarized beams have been shown to be extremely unstable in the self-focusing process.[7,8] Secondly, the experimental implementation of such measurements, as discussed in Section 3.4, is extremely difficult being complicated by the facts that (1) self-trapping is highly dependent on beam profile, (2) trapping is a threshold process which eliminates the possibility of making the measurements over a large range of powers, and (3) trapping involves high intensities and rather large index changes which bring in the possibility of complications from damage phenomena in solids and other nonlinear optical phenomena.

In the light of the above facts, we conclude that until the interferometric determinations of $\delta n_{||}$ and $\delta n_{\perp}$ are shown to be practically feasible, ellipse rotation and the Kerr effect offer a unique means of determining the electronic contribution to the nonlinear polarization and estimating the nonlinear refractive index in any isotropic medium. Under certain conditions, three-wave mixing data may serve as an added check on the conclusions drawn from the ellipse rotation and Kerr data.

Reproduced with permission of the copyright owner. Further reproduction prohibited without permission.

REFERENCES - CHAPTER V

1. P. D. Maker and R. W. Terhune, "Study of Optical Effects Due to an Induced Polarization Third Order in the Electric Field Strength," Phys. Rev. 137, A801 (1965).

2. G. Hauchecorne, F. Kerherve, and G. Mayer, "Mesures des Interactions Entre Ondes Lumineuses Dans Diverses Substances," Le Journal de Physique 32, 47 (1971).

3. S. P. S. Porto, "Angular Dependence and Depolarization Ratio of the Raman Effect," J. Opt. Soc. Am. 56, 1585 (1966).

4. A. P. Veduta and B. P. Kirsanov, "Variation of the Refractive Index of Liquids and Glasses in a High Intensity Field of a Ruby Laser," Sov. Phys. JETP 27, 736 (1968).

5. M. Paillette, "Experimental Study of the Intensity-Dependent Variations of the Absolute Refractive Index in Liquids," J. Quantum Elect. QE-4, 350 (1968).

6. P. L. Kelley, "Self Focusing of Optical Beams," Phys. Rev. Lett. 15, 1005 (1965).

7. D. H. Close, C. R. Giuliano, R. W. Hellwarth, L. D. Hess, F. J. McClung, and W. G. Wagner, "The Self Focusing of Light of Different Polarizations," IEEE J. Quantum Elect. QE-2, 553 (1966).

8. W. G. Wagner, H. A. Haus, and J. H. Marburger, "Large Scale Self-Trapping of Optical Beams in the Paraxial Ray Approximation," Phys. Rev. 175, 256 (1968).

Reproduced with permission of the copyright owner. Further reproduction prohibited without permission.

CHAPTER VI

EXPERIMENTAL IMPLEMENTATION OF THE ELLIPSE ROTATION STUDY

6.0 Introduction

In this chapter we describe the implementation of an ellipse rotation experiment with which we have measured the ellipse rotation parameter $\chi_3^{1221}(-\omega,\omega,\omega,-\omega)$ in CCl_4 and obtained the first measurement of ellipse rotation in any solid, viz., fused quartz, BK-7 borosilicate crown glass, and SF-7 dense flint glass.

The first observation of ellipse rotation was performed by Maker, Terhune, and Savage in 1964[1] using a weakly focused multimode ruby laser. Wang[2] and McWane and Sealer[3] have performed subsequent ellipse rotation studies using unfocused multimode lasers. These latter results show that the earlier measurements had yielded values of χ_3^{1221} which were about an order of magnitude too small.

In the present study of ellipse rotation, several modifications have been made in the experimental technique which overcome difficulties encountered in previous studies. Firstly, the reproducibility of our results were assured by using a single (transverse and longitudinal) mode Q-spoiled ruby laser in our investigation. The independence of our results on the spatial profile of the laser was confirmed by complementary data obtained with the use of a multimode laser. Secondly, our investigation was conducted with a beam which was focused centrally into the sample under study so that the entire ellipse rotation process occurred within a focal volume which was entirely contained by the sample. It will be shown that this

Reproduced with permission of the copyright owner. Further reproduction prohibited without permission.

condition results in an ellipse rotation signal which is independent of the dimensions of the sample and the focal length of the input beam. This greatly facilitates a direct accurate comparison of ellipse rotation parameters for media of widely varying refractive indices. Additionally, focusing is particularly advantageous in the study of materials with extremely low ellipse rotation coefficients since it produces sufficiently high intensities within the samples to detect induced birefringence without the need for picosecond pulse techniques and also allows the intensities at all sample-air interfaces and at all of the other associated optical components to be much lower than that within the samples. This latter factor is extremely important in that it prevents the possibility of erroneous readings due to nondamaging absorbing plasmas being formed at sample-air interfaces or due to nonlinear phenomena induced within the polarizing optics of the experiment.

As a third point, the sensitivity of our apparatus was increased by measuring the ellipse rotation directly through monitoring the amount of light rotated into a polarization orthogonal to the input polarization. Previous experimental investigations inferred ellipse rotation by monitoring the relative change in two orthogonal linearly polarized components of the output beam after it had traversed the sample. Our "null" technique offers a major advantage not only in the increased sensitivity which is achieved but also in the fact that it provides a direct means of monitoring the amount of stray birefringence in the system at low input power levels where no ellipse rotation occurs. Consequently, we are provided with a means of determining the

Reproduced with permission of the copyright owner. Further reproduction prohibited without permission.

sensitivity of our ellipse rotation apparatus for small angles of rotation.

Finally, previous difficulties which were encountered in the calibration of ellipse rotation studies have been overcome in our investigation by calibrating all of the measurements to the ellipse rotation parameter $\sigma + 2\beta$ for CS_2 . This parameter we are able to determine to within 2% absolute accuracy using the very accurate d.c. Kerr measurements which are reported in the literature; see Section 6.6.

This chapter will be divided into seven sections. Firstly, a detailed description of the experimental arrangement is given in Section 6.1. The samples which we studied are then described in Section 6.2. In Section 6.3 the analysis of ellipse rotation which was given in Section 3.4 is generalized to the case of a focused Gaussian beam. These results are then employed in Section 6.4 to interpret the signal which is experimentally measured in our investigation of ellipse rotation. In Section 6.5 we describe the details of the data collection process and the means applied to reduce the data. The calibration standard for the experiment is discussed in Section 6.6. Finally the results of the ellipse rotation study are presented in Section 6.7.

6.1 The Experimental Arrangement

The experimental arrangement for our ellipse rotation measurement is schematically diagrammed in Figure 6.1. The sole purpose of the apparatus is to direct an elliptically polarized laser beam into the samples to be examined and to analyze the amount of light at the

Reproduced with permission of the copyright owner. Further reproduction prohibited without permission.

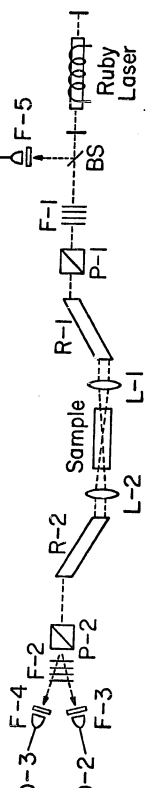

Figure 6.1

Reproduced with permission of the copyright owner. Further reproduction prohibited without permission.

sample exit face which is orthogonally polarized with respect to the input signal.

The Q-spoiled ruby laser is fired into a stack of Schott glass neutral density filters (F-1) to set the input intensity into the sample. One of the filters (N.D. = 0.1) is tilted to split off a portion of the beam for power monitoring in the photodiode D-1. The rest of the beam is coupled through a high power Rochon prism (P1) to define its plane of polarization. This is followed by a Fresnel rhomb (R1) which is oriented so as to produce elliptically polarized radiation of the desired eccentricity. The beam is then focused into the sample centrally by lens (L1) and then recollimated by lens (L2). A second Fresnel rhomb (R2) is oriented parallel to R1 so as to produce a linearly polarized output in the absence of ellipse rotation. This is followed by a Wollaston prism (P2) oriented to direct a maximum "transmitted" signal into the photodiode (D3) and a minimum "nulled" signal into D2 in the absence of ellipse rotation.

The laser power delivered to the sample is adjusted by moving the Schott neutral density filters from stack F-1 to F-2 thus ensuring a constant total power level into the monitoring diodes. Any rotation of the polarization ellipse during propagation through the sample thus reveals itself as a relative increase in the "nulled" signal at D2. Monitoring of the transmitted beam at D3 gives assurance that there are no changes in the transmission path or spatial profile of the laser which might give erroneous readings in D2.

Having given a general description of the experimental arrangement, we shall go on to give a more specific description of the

Reproduced with permission of the copyright owner. Further reproduction prohibited without permission.

various elements employed in the experiment and of the alignment procedures which were followed to ensure accurate repeatable results.

The Laser - The ruby laser which was employed in this work consisted of a 9/16" diam × 4" long 60°Czochralski grown ruby which is antireflection coated on both ends. The ruby is mounted in a Korad K-1 laser head which is water cooled to operate at approximately 65°F. In the course of our investigation of ellipse rotation, the laser was operated in two different modes as shown in Figure 6.2. In multimode operation a KDP Pockel's cell and quartz Brewster stack were employed as a means for Q-switching the laser. In this mode the beam diameter was apertured to 1/4" and the output was measured to be 0.6J in a 20 ns (FWHM) pulse as monitored on a TRG Model 100 ballistic thermopile and on the detector D1. Single mode operation was achieved by using a 2mm long cell of cryptocyanine in acetone as a saturable absorber and internally aperturing the output beam to 1/8" diameter. The dye cell was placed at Brewster's angle in front of the rear reflector of the laser. In this mode of operation, the output was approximately 0.05J in a 20 ns pulse.

In both modes of operation the length of the optical cavity was approximately 75 cm and longitudinal mode selection was performed by employing a Korad K-LMS sapphire etalon as the output reflector. The rear reflector in both modes of operation is a 99%+ reflectivity ruby laser mirror

The Neutral Density Attenuators - The filters in neutral density stacks F-1 and F-2 are Schott glass ND-41 filters totaling N.D. = 4.0 at 6943Å (2 - N.D. = 1.0, 5 - N.D. = 0.3, 5 - N.D. = 0.1). Attenuation

Reproduced with permission of the copyright owner. Further reproduction prohibited without permission.

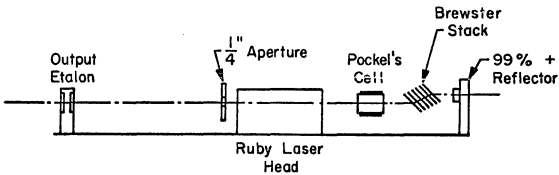

Figure 6.2a

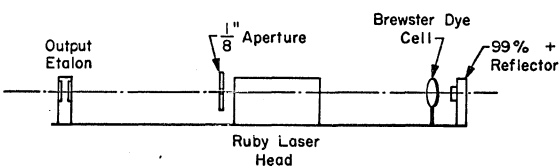

Figure 6.2b

Reproduced with permission of the copyright owner. Further reproduction prohibited without permission.

checks using the ruby laser source showed no detectable deviations from the specified values for these filters both individually and stacked. Examination of the filters on a Joyce Loebl double beam recording microdensitometer after the experimental investigation showed the filters to exhibit flat characteristics across their surface area with a relative density variation of no more than 0.025 density from one filter to another. During the ellipse rotation study the filters were numbered and moved in the same sequence to increase intensity on each experimental run. Thus each sample was examined under the same conditions.

The Detection System - The detectors D-1, D-2, and D-3 are all ITT FW 114A S-20 biplanar photodiodes with response times of approximately 1 ns. The input beam is apertured to 1/8" and expanded to fill the detection surface with a 20 mm f.1 negative lens. To prevent stray light from entering the detectors two 30% transmitting 200Å (FWHM) Optics Technology ruby laser filters are employed at D-1 and D-3 and a Spectrolab 68% transmitting 14Å (FWHM) ruby laser spike filter is employed at D-2. Input levels into the diodes are adjusted by using Kodak wratten neutral density filters.

The output signals from D-2 and D-3 are monitored on a Tektronix type 555 dual beam oscilloscope with type L plug-ins operating at a 100 ns/cm sweep rate. D-1 is monitored by a Tektronix type 585 oscilloscope with a 50 ns/cm sweep rate. The overall response times of the detection systems are thus approximately 7 ns for D-1 and 15 ns for D-2 and D-3.

Reproduced with permission of the copyright owner. Further reproduction prohibited without permission.

Fresnel Rhombs - The Fresnel rhombs used in this investigation were a pair of Isomet LMA 3000 glass rhombs. These were mounted in lucite holders which clamped the rhombs from the sides. Tension on the holders was adjusted for minimum birefringence at the detector D-2 and the rhombs were rotated so that the power into the sample consisted of 14.8% right circularly polarized and 85.2% left circularly polarized radiation, i.e., the rhomb was tilted at 22.5° with respect to the vertical; see Section 6.4.

Focusing Optics - The focusing lenses used in this study were 10 and 15 cm focal length biconvex pairs which were adjusted to focus the laser beam into the center of each sample and recollimate the transmitted laser radiation. The choice of these two sets of lenses was based on the fact that shorter focal length lenses would produce such high intensities as to damage the solid samples before an appreciable ellipse rotation could be observed; on the other hand, longer focal length lenses would tend to cause surface breakdown on the 4" long samples and also violate the condition that the sample completely contain the focal volume of the lens; see Section 6.3.

Alignment Optics - Since a 2 meter path exists between the laser and the detectors D-2 and D-3, a deviation of the beam by 1.5 m rad. at the laser output would cause the signal at the detectors to miss completely the 1/8" diameter detection aperture. This deviation could easily be produced by a slight wedge in the filters of stack F-1 which would be moved to F-2 to increase the intensity at the sample. It is thus vital to constantly check system alignment.

Reproduced with permission of the copyright owner. Further reproduction prohibited without permission.

The alignment scheme shown in Figure 6.3 was used to check alignment of the system after each shot and after each transfer of filters between F-1 and F-2. Essentially the scheme involves aligning a He-Ne laser collinear with the ruby laser beam and using it as a continuous monitor of proper alignment. Initial alignment is performed by aligning the He-Ne beam to coincide with burn spots produced on Polaroid film inserted at several positions along the optical path between the laser and detectors. The mirror M-1 in Figure 6.3 which serves to insert the He-Ne beam into the ruby laser cavity collinear to the ruby laser output beam is removed before each shot and replaced after pulsing the ruby laser with the aid of reference points in the ruby laser cavity. Exact alignment is assured since the output reflector of the He-Ne laser and the sapphire etalon of the ruby laser form an interferometer, the fringes of which may be viewed at the detector D-1 entrance aperture when exact alignment is attained.

6.2 Sample Selection and Preparation

Three glass samples and one symmetric molecule liquid were chosen for study in this work. The choice of glasses was primarily based upon the availability of other (a.c. Kerr, THG, and TWM) experimental data although an effort was made to examine silicate glasses of diverse densities. Glasses examined were fused quartz (suprasil), Schott BK-7 borosilicate crown glass, and Schott SF-7 dense flint glass. Carbon tetrachloride (CCl_4) was selected as the symmetric molecule liquid to be studied since accurate d.c. Kerr data is readily available on it and the relative sizes of electronic and nuclear

Reproduced with permission of the copyright owner. Further reproduction prohibited without permission.

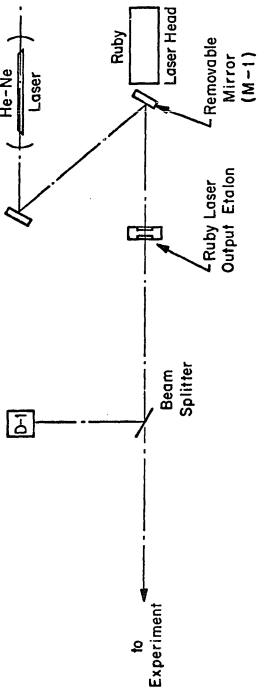

Figure 6.3

Reproduced with permission of the copyright owner. Further reproduction prohibited without permission.

rearrangement type contributions to its nonlinear refractive index is yet an unresolved question. Since the Kerr measurements on the liquid have been performed with much greater accuracy than any of the measurements in the solid media, they will serve as examples of the potential promise of ellipse rotation and Kerr measurements as tools for effectively separating electronic and nuclear nonlinearities in isotropic media.

The nominal length of the samples used in this study was 4". This choice is somewhat arbitrary, but was based on the fact that much longer samples might exhibit prohibitively high stray birefringence and much shorter samples would necessitate such high intensities (i.e., strong focusing) as to possibly result in breakdown of the sample before ellipse rotation is observed. All sample and cell surfaces were optically polished to minimize scattering and glass samples were Grade A for minimum scatter and birefringence. The CCl_4 used in the study was J. T. "Baker Analyzed" reagent photometric grade CCl_4.

Samples were examined under two sets of experimental conditions in this study. In the first case, the focusing and recollimating lenses were fixed at a constant separation and the samples were cut so as to maintain collimation of the beam upon its exit from the second lens. The lengths of the samples are obtained by keeping the parameter

$$K = L(1 - \frac{1}{n}) \tag{6.1}$$

constant. Here L is the sample length and n the refractive index. We note that this parameter is independent of the focal length of the lenses used. The details of this derivation and the equations for the

Reproduced with permission of the copyright owner. Further reproduction prohibited without permission.

lens spacing are given in Appendix J. A 4" long absorption cell with quartz windows selected for minimum birefringence was used to hold the CCl_4. The calculated lengths of the samples are shown in Table 6.1.

The second set of samples used in the study were all 4" in length. In this case the lenses were adjusted for each sample to maintain approximate collimation of the laser beam. This enabled us to check the assertion that our results should not depend on sample dimensions; see Section 6.3.

6.3 Ellipse Rotation Using Focused Gaussian Beams

Previous experimental studies of ellipse rotation have been performed using unfocused or weakly focused beams.[1-3] As discussed in Section 6.0 we believe that several major advantages may be achieved by using focused beams, especially for media with low ellipse rotation parameters.

Marburger and others have performed computer studies on the self focusing of linearly polarized beams.[4,5] They find that for pulse powers significantly below the critical powers for self focusing it is valid to assume that a Gaussian beam remains Gaussian as it propagates through the medium. The elliptically polarized beam is a much more complicated case which has not been studied fully. Preliminary studies show that such beams exhibit anomalous behavior in self focusing since the right and left circularly polarized components are cross coupled by the nonlinearity, and self focusing consequently progresses at a different rate for each component.[5,6] Nevertheless it is quite reasonable to assume that at the low powers at which we are conducting our ellipse rotation studies (see Section 6.5) changes

Reproduced with permission of the copyright owner. Further reproduction prohibited without permission.

TABLE 6.1

Sample	Refractive Index at 6943Å	Length L (inches)
CCl_4	1.46	4.0
Fused Quartz	1.455	4.0
BK-7 Glass	1.51	3.7
SF-7 Glass	1.63	3.24

Reproduced with permission of the copyright owner. Further reproduction prohibited without permission.

in the beam profile resulting from self-focusing effects should be negligible. Indeed, this is borne out by our experimental results. The effects of self focusing for higher input powers is still an unresolved question which is presently being studied by Marburger.[7]

Since our primary interest in this work is in making a comparison of ellipse rotation data between a standard reference sample and several other materials, we shall attempt to derive some qualitative results concerning ellipse rotation with focused beams which will aid us in interpreting the data. A rigorous consideration of the nonlinear propagation problem will be deferred until a more definitive treatment becomes available.

Perhaps one of the most basic estimates of the behavior of the ellipse rotation signal in a focused beam experiment would be obtained by considering the case of a focused Gaussian beam[8] in the limit where the power is low enough to permit the assumption that the spatial energy profile of the beam remains unaltered in propagating through the nonlinear medium. Since ellipse rotation experiments are generally carried out under the condition that the ellipse rotation signal is small compared to the total input power, the neglecting of self-focusing effects is quite reasonable. Although the spatial profile of the laser output in our own experimental investigation was not precisely determined, the Gaussian estimate should give some valuable insights for the interpretation of the results which we have obtained. The validity of our analysis concerning the dependence of the ellipse rotation signal on power input, focusing, and other parameters will be verified in the experimental investigation.

Reproduced with permission of the copyright owner. Further reproduction prohibited without permission.

The propagation of a Gaussian beam in a linear dielectric medium is described by the Rayleigh-Sommerfeld formulation of diffraction as applied to each transverse component of the incident electric field.[9] The axial component of the field is specified by the relation $\nabla \cdot \underline{E} = 0$. Although the field is normally separated into Cartesian components, right and left circularly polarized components are also admissible since the Helmholtz equation $\nabla^2 \underline{E} + k^2 \underline{E} = 0$ is a vector relation which may be separated into circular as well as Cartesian components. If it is assumed that the transverse components of the electric field possess a Gaussian distribution and that the beam is converging to a focus at the center of the sample $z = 0$, then the transverse components of the field are completely specified by the relation[8]

$$\underline{E}_{\pm}(r,z) = E'_{\pm}\, \hat{e}_{\pm}\, \frac{w_o}{w(z)} \exp\{i(kz-\gamma) - r^2\left(\frac{1}{w^2(z)} - \frac{ik}{2R(z)}\right)\} \qquad (6.2)$$

Here r is the radial distance outward from the axis of the beam; $E'_{\pm}/\sqrt{2}$ are the peak amplitudes of the right and left circularly polarized components of the beam at the focus $z = 0$; $\hat{e}_{\pm} = (\hat{e}_x \pm i\hat{e}_y)/\sqrt{2}$ are the right and left circularly polarized unit vectors defined in Equation (3.28); $w(z) = w_o(1+(\lambda z/(\pi w_o^2 n))^2)^{1/2}$ is the 1/e spot size with λ being the free space wavelength; $R(z) = z(1+(\pi w_o^2 n/(\lambda z))^2)$ is the radius of the wavefront; and the phase factor γ is given by $\gamma = \tan^{-1}(\lambda z/(\pi w_o^2 n))$. An examination of Equation (6.2) clearly shows that the Gaussian beam propagates with its surfaces of constant energy flux specified by a set of hyperboloids which obey the relation

Reproduced with permission of the copyright owner. Further reproduction prohibited without permission.

$$r^2 = \kappa w^2(z) = \kappa\left(w_o^2 + \left(\frac{\lambda z}{w_o \pi}\right)^2\right) \tag{6.3a}$$

Here κ parameterizes the set of hyperbolic surfaces across which there is no energy flow. In addition to κ, an orthogonal set of surfaces parameterized by the variable s may be defined which determines the surfaces of constant phase. Assuming γ to be negligibly small, these surfaces may be approximated by the relationship

$$s = z + \frac{r^2}{2R(z)} \tag{6.3b}$$

The lines of constant κ and s are shown in Figure 6.4. Clearly for the cylindrically symmetric beam a hyperboloidal surface is traces out by s for each value of κ thus suggesting a "ray" interpretation of the energy flow in the beam. Equation (6.3) and Figure 6.4 also show that κ and s provide an alternate system of coordinates by which the beam may be characterized. Specht has demonstrated that this system is identical to the prolate spheroidal coordinates in the limit where $(\lambda r)^2/(\pi w_o^2 n)^2 \ll 1$.[10] This condition is most certainly satisfied in the region of high intensity at optical wavelengths. In the analysis to follow, we shall adopt the ray approach to interpret the flow of energy in the beam. It should be borne in mind however that the preceding developments have been based upon the assumption that only the transverse components of the electric field are significant. The f-number of the beam should thus be kept high enough to merit the dropping of axial components of the field in estimating the energy flow and induced refractive index changes. Thus we shall assume that

Reproduced with permission of the copyright owner. Further reproduction prohibited without permission.

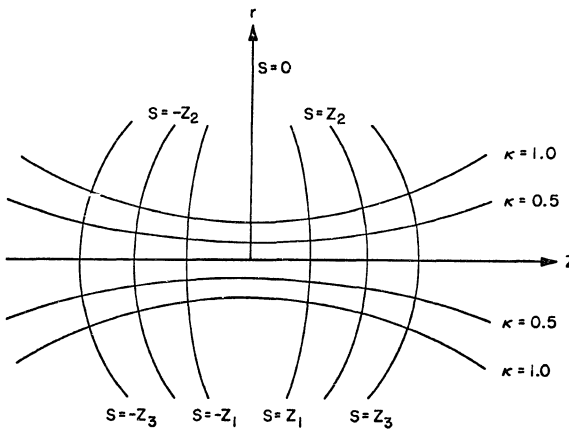

Figure 6.4

Reproduced with permission of the copyright owner. Further reproduction prohibited without permission.

$R(z)/w(z) >> 1$.

Under the assumption that the power in the beam is such that the spatial energy distribution given by Equation (6.2) is unperturbed by the induced change in refractive index, the field of Equation (6.2) may be substituted into Equation (3.36) to obtain an estimate of the induced change in the linear susceptibility. The results may then be substituted into the wave equation, Equation (3.3) to give an expression for the perturbed solution for the field. Putting the results in terms of the circularly polarized modes of Equation (6.2) we find

$$\nabla^2 \underline{E}_{\pm}(r,z) + k^2 \underline{E}_{\pm}(r,z) = - \frac{4\pi k^2}{n^2} \{A|E_{\pm o}(r,z)|^2 + (A+B)|E_{\mp o}(r,z)\}^2 \underline{E}_{\pm}(r,z) \tag{6.4}$$

Here $\underline{E}_{\pm o}(r,z)$ are the right and left circularly polarized components of the field given by Equation (6.2) with the peak amplitudes $E'_{\pm}$ equal to $E'_{\pm o}$, and $\underline{E}_{\pm}(r,z)$ is the perturbed field.

Under the assumption that changes in the spatial profile of the beam due to self focusing will be negligible, we shall adopt a trial solution of the form

$$\underline{E}_{\pm}(r,z) = E'_{\pm}(s,\kappa)\hat{e}_{\pm}U(r,z)$$

$$\text{where } U(r,z) = \frac{w_o}{w(z)} \exp i(kz-\gamma) - r^2\left(\frac{1}{w^2(z)} - \frac{ik}{R(z)}\right) \tag{6.5}$$

This form is essentially the same as the Gaussian of Equation (6.2) with the exception that what was previously the "peak amplitude" of

Reproduced with permission of the copyright owner. Further reproduction prohibited without permission.

the field is now allowed to vary as a function of s and κ, the two variables previously defining the ray paths in Figure 6.4.

Substituting Equation (6.5) into Equation (6.4) we obtain the form

$$U\nabla^2 E'(s,\kappa) + 2\nabla U(r,z)\cdot\nabla E'(s,\kappa) + E'(s,\kappa)\nabla^2 U(r,z) + k^2 E'(s,\kappa)U(r,z)$$

$$= -\frac{4\pi k^2}{n^2}\{A|E_{\pm o}(r,z)|^2 + (A+B)|E_{\mp o}(r,z)|^2\}E'_{\pm}(s,\kappa)U(r,z) \quad (6.6)$$

Upon examination of Equation (6.6) we note firstly that since $U(r,z)$ is a Gaussian beam, it satisfies the Helmholtz equation. Thus the last two terms on the left side of Equation (6.6) sum to zero. Secondly we note that since s defines the surfaces of constant phase for $U(r,z)$ and the amplitude of $U(r,z)$ changes slowly over distances of the order of a wavelength, we may make the approximation

$$2\nabla U(r,z)\cdot\nabla E'(s,\kappa) \simeq 2ik\frac{\partial E'_{\pm}(s,\kappa)}{\partial s}U(r,z) \quad (6.7)$$

Also since $E'_{\pm}(s,\kappa)$ is assumed to be constant over distances of the order of a wavelength, the first term in Equation (6.6) will be negligible compared to the term of Equation (6.7). Hence Equation (6.6) may be approximated by the relation

$$\frac{1}{E'_{\pm}(s,\kappa)}\frac{\partial E'_{\pm}(s,\kappa)}{\partial s} = \frac{2\pi ik}{n^2}\{A|E_{\pm o}(r,z)|^2 + (A+B)|E_{\mp o}(r,z)|^2\} \quad (6.8)$$

Integration of Equation (6.8) with respect to s for various fixed values of κ will be a rather straightforward operation if $w(z)$ is approximated by $w(s)$ in the expression for $E_{\pm o}(r,z)$. This

Reproduced with permission of the copyright owner. Further reproduction prohibited without permission.

is justified since $R(z)/w(z) >> 1$. Hence assuming A and B to be real as we have done in Section 3.4, we recognize that Equation (6.8) merely predicts that the nonlinearity will produce a differential phase shift $\phi_K(L) = \phi_{K+}(L) - \phi_{K-}(L)$ between the right and left circular components of the input beam. Explicitly, we find for a sample of length L with the focal region of the beam centered in the sample, the phase shift takes the form

$$\phi_K(L) = \phi_{K+}(L) - \phi_{K-}(L)$$
$$= \int_{-L/2}^{L/2} \frac{2\pi\omega}{cn} B\{|E'_{-o}|^2 - |E'_{+o}|^2\} \frac{w_o^2}{w^2(s)} e^{-2K} ds \qquad (6.9)$$

Clearly, the exponential dependence of the differential phase shift on $K = r^2/w^2(z)$ shows that it takes on the Gaussian profile of the input beam. Performing the integration of Equation (6.9) and expressing the result in terms of the ellipse rotation angle for the set of rays parameterized by K we find

$$\theta_K(L) = \frac{\phi_K(L)}{2} = \frac{\pi\omega}{2c}(\sigma+2\beta)\{|E'_{-o}|^2 - |E'_{+o}|^2\} \frac{\pi w_o^2 e^{-2K}}{\lambda} \qquad (6.10)$$

$$\times \tan^{-1}\left(\frac{L\frac{\lambda}{2\pi w_o^2 n}}{1 - \frac{L^2}{4}(\lambda/(\pi w_o^2 n))^2}\right)$$

Here we have used the relation $B = 6\chi_3^{1221}(-\omega,\omega,\omega,-\omega) = \frac{1}{4}(\sigma+2\beta)$ from Equation (3.26) and Table 5.1. It should be noted that in the limit where the length of the sample L is large enough to encompass the focal region of the beam, the $\tan^{-1}$ factor in Equation (6.10) will

Reproduced with permission of the copyright owner. Further reproduction prohibited without permission.

take on its $L \to \infty$ limit of π .

It is often convenient to specify the rotation angle in terms of a quantity other than the field strength which is directly measurable. Since the total time averaged power $\langle P \rangle_{av}$ in the Gaussian beam is related to the peak amplitudes of the field by the expression

$$\langle P \rangle_{av} = \frac{w_o^2 cn}{16} \{ |E'_{+o}|^2 + |E'_{-o}|^2 \} \tag{6.11}$$

Equation (6.10) may be rewritten in the form

$$\theta_K = \frac{2\pi^2 \omega^2}{c^3 n} (\sigma+2\beta) \langle P \rangle_{av} \cos(2u) e^{-2K} \tag{6.12}$$

Here $\tan u = |E'_{+o}/E'_{-o}|$ gives the relative field strength in the right and left circularly polarized modes and we have taken the limit where L is large compared to the focal region of the beam.

Equation (6.12) clearly shows that the degree of ellipse rotation of each group of rays characterized by K is linearly proportional to the total power input and completely independent of focal and sample dimensions provided that the sample completely contains the focal volume of the beam. In order to prevent the sample from being subjected to unnecessarily high field intensities, the experimental investigations of ellipse rotation should be conducted with the longest possible sample which is free of optical birefringence and the longest focal length lens which is consistent with the restriction that the sample completely contain the focal volume of the beam. It should be noted that the invariance of θ_K with respect to sample and

Reproduced with permission of the copyright owner. Further reproduction prohibited without permission.

focal dimensions permits the interchanging of various samples in the investigation without making any correction for focusing in the comparison of the recorded ellipse rotation data. Furthermore, it should be recalled that the focused beam experiment also offers an advantage in that only the sample is subject to the high power densities of the focused beam. As noted earlier, this is a major advantage in the examination of materials with low ellipse rotation coefficients.

In summary, we have considered the generalization of ellipse rotation to the case of a focused Gaussian beam in the approximation that self-focusing effects are negligible for small ellipse rotation angles. A ray optics approach has been used to calculate the induced ellipse rotation in various portions of the beam. It is found that the resulting expression for the differential phase shift which is given by Equation (6.9) is effectively identical to the plane wave result of Equation (3.39) with the exception that $E^2 z$ is not replaced by $\int E^2 ds$ for each ray of the beam.

The final result given in Equation (6.12) demonstrates the linear dependence of the ellipse rotation angle on the input power $\langle P \rangle_{av}$ for the Kth set of rays. In order to obtain the total amount of power which is rotated into a polarization state orthogonal to that of the input beam, an integral of the input intensity must be taken over its cross sectional area weighted by the ellipse rotation angle for each ray. This analysis will be carried out in the section which follows.

Reproduced with permission of the copyright owner. Further reproduction prohibited without permission.

6.4 Interpretation of the Ellipse Rotation Signal

Having expressed the ellipse rotation angle for each ray in a Gaussian input beam as a function of the parameter κ, which is effectively a specification of the radial distance from the beam axis normalized to the spot size, we shall continue in this section to express this result in terms of a directly measurable quantity, the power measured by the diode D-2 in Figure 6.1. In contrast to previous ellipse rotation measurements which measured the relative amounts of power in two perpendicularly polarized directions, it is to be recognized that our experimental configuration measures directly the amount of power which is rotated into a polarization which is orthogonal to that of the input polarization of the elliptically polarized radiation. Hence at low input levels there would ideally be no signal observed at D-2 and the presence of any signal would represent a source of "noise" which would arise as a result of stray birefringence in the system and would place a limit on the minimum detectable amount of ellipse rotation.

In order to interpret the results expressed by Equation (6.12) in terms of the measured power at D-2 we shall employ the schematic representation of our experiment which is shown in Figure 6.5. At the input to the sample the electric field of the beam may be represented by the form

$$\underline{E}(r,-L/2) = E_+(r,-L/2)\hat{e}_+ + E_-(r,-L/2)\hat{e}_- \qquad (6.13)$$

Reproduced with permission of the copyright owner. Further reproduction prohibited without permission.

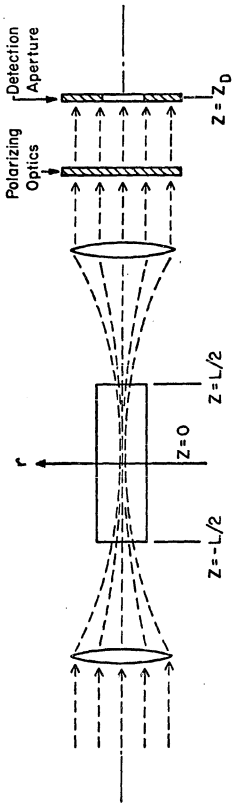

Figure 6.5

Reproduced with permission of the copyright owner. Further reproduction prohibited without permission.

Upon traversing the sample the two components of the beam will have experienced a differential phase shift resulting in the rotation of the polarization ellipse. Hence the field may be written in the form

$$\underline{E}(r,L/2) = E_+(r,L/2)e^{i\phi_{K+}(L)}\hat{e}_+ + E_-(r,L/2)e^{i\phi_{K-}(L)}\hat{e}_-$$

$$= \{E_+(r/L/2)e^{i2\theta_K(L)}\hat{e}_+ + E_-(r,L/2)\hat{e}_-\}\, e^{i\phi_{K-}(L)} \qquad (6.14)$$

where we must employ Equations (6.9) - (6.12) to write the phase shifts which are produced by the nonlinear polarization.

Upon exiting from the sample, the field expressed by Equation (6.14) continues to propagate as a Gaussian beam in a linear medium. The ellipse rotation angle which has been assumed to be small, should not affect the propagation of the beam appreciably (i.e., self focusing neglected). Hence the second lens will recollimate the beam and direct it to the detection aperture of the diode D-2, where it may be expressed in the form

$$\underline{E}(r,z_D) = \{E_+(r,z_D)e^{i2\theta_K(L)}\hat{e}_+ + E_-(r,z_D)\hat{e}_-\}\, e^{i\phi_{K-}(L)} \qquad (6.15)$$

Here $E_\pm(r,z_D)$ take the form which the Gaussian input beam would have at the detection aperture were the nonlinear behavior of the sample negligible. Hence $E_\pm(r,z_D)$ are Gaussian beams of the form given in Equation (6.2) with a spot size which we shall denote by w'. The size of w' is determined by the focal lengths of the two lenses in the experiment.[8]

Reproduced with permission of the copyright owner. Further reproduction prohibited without permission.

Using Equation (6.15) it is seen that the fraction $f(\theta_K)$ of power which is orthogonally polarized to the input polarization for the Kth set of rays in the beam may be expressed in the form

$$f(\theta_K) = \frac{(E_+(r,z_D)e^{i2\theta_K}\hat{e}_+ + E_-(r,z_D)\hat{e}_-) \cdot (E_+(r,z_D)\hat{e}_+ - E_-(r,z_D)\hat{e}_-)}{|E_+(r,z_D)|^2 + |E_-(r,z_D)|^2} \tag{6.16}$$

It is significant to note here that our experimental apparatus shown in Figure 6.1 does in fact read the fractional power directly since the total attenuation in the optical path of the experiment is kept constant, i.e., the power to the sample is increased by moving neutral density filters from stack F-1 to F-2. By substituting $\tan u = |E_+(r,z_D)/E_-(r,z_D)|$ into Equation (6.16) and using Equation (3.30) it is seen that

$$f(\theta_K) = (\sin(2u) \sin \theta_K)^2 \tag{6.17}$$

For small rotation angles $\sin \theta_K \simeq \theta_K$. Hence substituting Equation (6.12) into Equation (6.17) for small values of θ_K, one finds

$$f(\theta_K) = \left(\frac{2\pi^2\omega^2}{c^3 n} (\sigma+2\beta) \langle P \rangle_{av} e^{-2K}\right)^2 \left(\frac{\sin 4u}{2}\right)^2 \tag{6.18}$$

In order to obtain a value for the total fraction F of orthogonally polarized light reaching D-2, the fraction $f(\theta_K)$ must be integrated over the detection aperture after it is weighted by the Gaussian intensity distribution of the field in Equation (6.15). Performing this operation we find

Reproduced with permission of the copyright owner. Further reproduction prohibited without permission.

$$F = \frac{4}{w'^2} \int_0^{r_o} \frac{\exp(-2r^2/w'^2)}{(1-\exp(-2r_o^2/w'^2))} \left\{\frac{\pi^2\omega^2}{nc^3}(\sigma+2\beta)\langle P\rangle_{av}\exp(-2r^2/w'^2)\right\}^2 r\,dr$$

$$= \frac{\pi^4\omega^4}{3c^6}\left(\frac{\sigma+2\beta}{n}\langle P\rangle_{av}\right)^2 \left\{\frac{1-\exp(-6r_o^2/w'^2)}{1-\exp(-2r_o^2/w'^2)}\right\} \qquad (6.19)$$

Here r_o is the radius of the detection aperture; w' is the spot size defined in Equation (6.15); κ has been re-expressed in the form r^2/w'^2 ; and u has been set equal to $22\text{-}1/2^o$ to maximize Equation (6.18) and give the maximum sensitivity. It should be noted that this last fact places 14.8% of the power into one of the circularly polarized modes of the input beam.

Equation (6.19) clearly demonstrates that the relative sizes of $\frac{(\sigma+2\beta)}{n}$ may be determined for any two samples by monitoring F as a function of the input power $\langle P\rangle_{av}$. The $F \propto \langle P\rangle_{av}^2$ dependence of Equation (6.19) will serve as a check on the range of validity of the experimental determination. Furthermore it is to be noted that F is maximized as r_o approaches zero. This is to be expected since the maximum rotation angle is attained where the beam intensity is maximum. Since the power reaching the detector also decreases with decreasing r_o however, the optimal aperture size will be limited by the sensitivity of the detection system.

6.5 Experimental Procedure and Data Reduction

In the experimental determination of F vs $\langle P\rangle_{av}$ using the apparatus described in Section 6.1, a rigid procedure was followed to

Reproduced with permission of the copyright owner. Further reproduction prohibited without permission.

insure the accuracy and repeatability of the results.

Having aligned the apparatus using the He-Ne alignment laser and having adjusted all of the polarizing elements for a minimal "null signal" at the diode D-2 in Figure 6.1, the ruby laser is fired several times with the neutral density stack F-1 full (i.e., minimum input to the sample); this assures proper nulling of the system at D-2 and will also yield an estimate of the sensitivity of the system. Generally this "null signal" at D-2 is less than 0.002 of the transmitted power in the laser beam which is detected at D-3.

Once the null level of the system is determined for the sample under study, the power is increased gradually until a detectable change is produced in the signal at D-2. The laser is fired repeatedly at a rate of one shot every 6 minutes to insure repeatability of the laser output. As the signal at D-2 begins to increase, the power to the sample is increased in steps of 0.1 density and the signals produced at the three diodes are recorded with each successive laser shot. Since the signal-to-noise ratio is low for small ellipse rotation angles due to stray birefringence, it is difficult to obtain accurate results at low input powers. Likewise, results obtained at extremely high input levels will be affected by the self focusing of the beam or by other nonlinear phenomena such as stimulated light scattering. Hence it is to be expected that the range in which the measurements would give accurate results would be that in which the $F \propto \langle P \rangle_{av}^2$ dependence which is predicted by Equation (6.19) is strictly adhered to. Subsequent estimates of the critical powers for self focusing using the data from our experimental determinations show that

Reproduced with permission of the copyright owner. Further reproduction prohibited without permission.

our results are obtained from data for which the input power is less than 25% of the critical power.[5] Hence the results are self consistent and it is not surprising that the experimental data would adhere closely to the $F \propto \langle P \rangle_{av}^2$ dependence which we predicted.

After gathering the data for several samples, a normalization procedure must be followed to correct the readings obtained at D-2 for fluctuations in laser power and also for the finite "null signal" measured at the beginning of each run. Hence F may be written in the form

$$F_{rel} = \frac{(\text{signal at D-2})(\frac{\text{mean signal at D-1}}{\text{signal at D-1}}) - (\text{null signal at D-2})}{(\frac{\text{mean signal at D-3}}{\text{mean signal at D-1}})} \qquad (6.20)$$

Here Equation (6.20) gives a relation for the relative increase in F as a function of increasing signal at D-2 rather than an absolute reading of the fraction F. This is to say that F_{rel} is equal to F multiplied by some constant factor. In Equation (6.20) the factor in the denominator serves to normalize the results in the event that the transmission of the samples differ. This factor was found to be constant from sample to sample. The first term in the numerator possesses a factor which serves to normalize the signal at D-2 to a constant laser output level, whereas the second term in the numerator subtracts out the "null signal" so that $F_{rel} = 0$ at low levels of input to the sample.

The results of plotting the relative measurements of F vs $\langle P \rangle_{av}$ are shown in Figures 6.6 and 6.7 where the data for the four

Reproduced with permission of the copyright owner. Further reproduction prohibited without permission.

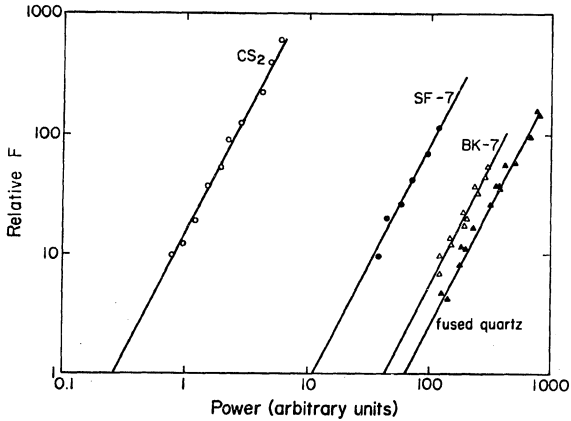

Figure 6.6

Reproduced with permission of the copyright owner. Further reproduction prohibited without permission.

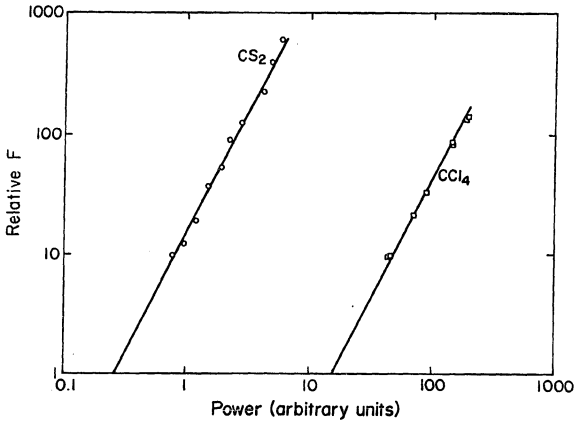

Figure 6.7

Reproduced with permission of the copyright owner. Further reproduction prohibited without permission.

materials which we are studying have been plotted. Since carbon-disulphide, CS_2 , has been selected as the normalization standard, an ellipse rotation plot of this material has been included for comparison. The plotted points on the figures are actual data points which were obtained by direct application of Equation (6.20), whereas the solid lines are the best fit $F_{rel} \propto \langle P \rangle_{av}^2$ lines through the data. On these graphs $\langle P \rangle_{av} = 1$ corresponds to an input power of roughly 0.6 kW and $F_{rel} = 10$ corresponds to an approximate fraction $F = 1/1500$ (roughly an equivalent rotation of 2^o for an incident plane wave). Most of the experimental runs in this investigation were carried out by using the single mode laser configuration described in Section 6.1 since this mode of operation was most repeatable and excluded the possibility of multimode effects; however the results displayed on Figures 6.6 and 6.7 were all repeatable to within $\pm$ 10% independent of the laser mode used, the focal length of the lens system (10-15 cm f.l), or the sample lengths.

During the data collection process, several additional restrictions were imposed which helped to improve the repeatability of the measurements. The alignment of the optical components and detectors was extremely important. Hence the alignment scheme of Figure 6.3 was employed to check the alignment of the system after each shot.

Changes in the intensity profile of the laser output during an experimental run will naturally change the ellipse rotation signal and thus produce a "scatter" in the plotted data. Errors from laser fluctuations were minimized firstly by periodically checking the near and

Reproduced with permission of the copyright owner. Further reproduction prohibited without permission.

far field patterns produced by the laser on a piece of exposed Polaroid film. Changes in the laser output would also show up in a variation of the signal at the diode D-1 or in the ratio of signals at diodes D-1 and D-3. This is reasonable since a variation in the spatial energy distribution of the laser pulse would not only have different propagation characteristics, but also produce a varying response on the photocathodes of the detectors. Hence any shots which produced a variation in signal at D-1 or in the ratio of signals D-1/D-3 of greater than $\pm$ 10% from their mean values were rejected as "bad shots". Such fluctuations in laser output are a consequence of temperature variations in the laser system or fluctuations in the flashlamp voltage.

As a final, very important, precaution the experimental data on any given sample are not considered to be meaningful unless parallel data on a sample of some other material are obtained and plotted without a realignment of the laser system. Since the investigation involves the comparison of ellipse rotation data for several samples to infer their relative values, it is imperative that each sample be examined under exactly the same experimental conditions.

In conclusion we observe that the largest ellipse rotation signals shown in Figures 6.6 and 6.7 are signals of less than 15^{o} equivalent rotation for an incident plane wave. It is thus quite reasonable that the results obtained would not be appreciably affected by any self focusing. Although it is conceivable that electrostrictive self focusing could affect the results of our experiment by producing self focusing without an increase in the ellipse rotation,

Reproduced with permission of the copyright owner. Further reproduction prohibited without permission.

this may be seen to be most improbable by comparing the power levels which are employed in Figures 6.6 and 6.7 with the response times and power levels predicted for electrostrictive self focusing in Section 4.2.5. Indeed, the assertion that electrostrictive self focusing is absent is borne out by the adherence of the data to the $F \propto \langle P \rangle_{av}^2$ fit predicted by Equation (6.19) and the constancy of the ratio of signals D-1/D-3 which was maintained in the experimental investigation.

6.6 Calibration Standard for Ellipse Rotation

One of the major limitations on the accurate determination of nonlinear optical susceptibilities is the lack of an absolute standard to which relative measurements may be calibrated. The calibration of previous ellipse rotation studies was achieved by attempting to estimate the total power output and spatial intensity profile of the laser directly.[1-3] A recent study by McAllister, Mann, and DeShazer, however, indicates that the output of a single mode Q-spoiled laser will exhibit "hot spots" and irregular time behavior which are not detectable by the usual means of monitoring the laser output on film (a time integrating process) or by measuring the total output of the laser on a photodetector (a spatial integration of the output).[11] Such irregularities in laser output are only eliminated by meeting stringent requirements on the design of the optical cavity and by extremely careful alignment.[12] Multimode lasers such as those employed in previous ellipse rotation studies would clearly be even more difficult to characterize.

Reproduced with permission of the copyright owner. Further reproduction prohibited without permission.

In view of the difficulties of a direct calibration procedure, we have chosen to calibrate our measurements of ellipse rotation to the ellipse rotation parameter for carbon disulphide, CS_2, which we are able to determine to within 2% at 23°C and $\lambda = 6943\text{Å}$ through the use of very accurate d.c. Kerr constant measurements reported in the literature.[13] Thus the repeatability of the laser output is all that is necessary to insure accurate and reproducible results.

The use of the Kerr measurements to calibrate ellipse rotation may be understood by an examination of Table 5.1 which shows that a Kerr determination will yield a value of $\sigma+\beta$ for a sample whereas $\sigma+2\beta$ is measured by ellipse rotation. Hence the medium to be used for a calibration standard should be one in which either electronic or nuclear mechanisms dominate so that either σ or β is negligible. In this case the d.c. Kerr measurement may be corrected by employing the Lorentz local field factors to obtain the a.c. Kerr constant from which the ellipse rotation parameter may be inferred directly.

In this investigation our choice of CS_2 for the standard of calibration was based on the above condition in addition to the fact that its Kerr constant is the best known of any substance. A recent measurement by Volkova et al. shows that this constant is found to be $B_o(CS_2) = 3494 \pm 4 \times 10^{-10}$ esu at 546 nm and 23°C.[13] By correcting this value to 6943Å using the dispersion measurements of $B_o(CS_2)$ performed by McComb,[14] we find that $B_o(CS_2) = 253 \pm 5 \times 10^{-9}$ esu at 6943Å and 23°C.

Since CS_2 is a highly anisotropic molecule, one would be led to expect that molecular reorientation effects would greatly overshadow

Reproduced with permission of the copyright owner. Further reproduction prohibited without permission.

any contributions to the nonlinear polarization arising from direct electronic distortion. Recent attempts have been made by Mayer[15] and Hauchecorne et al.[16] to measure the electronic parameter σ in CS_2 using two completely independent techniques: (1) second harmonic generation in the presence of a d.c. electric field, and (2) three-wave mixing. Both of these studies indicate that $\sigma < 0.015\beta$ for CS_2 ; see Appendix K for further details.

Neglecting the size of σ compared to that of β it is seen that the ellipse rotation parameter is given by the relation

$$\chi_3^{1221}(-\omega,\omega,\omega,-\omega) = \frac{\sigma+2\beta}{24} = \frac{B_o n\lambda}{24\pi} = 378 \pm 7 \times 10^{-15} \text{ esu}$$

at 6943Å and 23°C with $n = 1.62$. Since the dielectric constant of CS_2 is equal to the square of its refractive index to within less than 1/2%, it is felt that local field corrections may be neglected in the above estimate.

As a final note we should like to point out that the choice of CS_2 as a standard of calibration holds an added advantage other than those outlined above in that it is also employed as the standard of calibration in the a.c. and d.c. Kerr measurements with which we shall compare our data in Chapter VII.

6.7 Results of Ellipse Rotation Measurements

The ellipse rotation data presented in Figures 6.7 and 6.8 may be interpreted with the aid of Equation (6.19) to yield an estimate of $\chi_3^{1221}(-\omega,\omega,\omega,-\omega)$. As suggested by Equation (6.19), F obeys the relation

Reproduced with permission of the copyright owner. Further reproduction prohibited without permission.

$$F = J\left(\frac{\sigma+2\beta}{n}\langle P\rangle_{av}\right)^2 \qquad (6.21)$$

where J is constant depending on the laser beam profile. Thus a knowledge of the refractive index n for each material will allow us to infer $\sigma+2\beta$ from the graphs using $\frac{\sigma+2\beta}{24} = 378 \pm 7\times 10^{-15}$ esu for CS_2 as the standard of calibration. The results are shown in Table 6.2.

As we have already noted in Section 6.5, the uncertainty in the ellipse rotation results should be no greater than 10% relative accuracy since the various experimental runs over a large range of experimental conditions invariably yielded results which were well within this range. Hence the absolute accuracy of these determinations should be better than ±11%.

Reproduced with permission of the copyright owner. Further reproduction prohibited without permission.

TABLE 6.2

Material	$\chi_3^{1221}(-\omega,\omega,\omega,-\omega) \times 10^{15}$ esu
CS_2	378 ± 7
Fused Quartz	1.5
BK-7 Glass	2.3
SF-7 Glass	9.9
CCl_4	6.08

All values within ± 10% of CS_2 standard.

Reproduced with permission of the copyright owner. Further reproduction prohibited without permission.

REFERENCES - CHAPTER VI

1. P. D. Maker, R. W. Terhune, and C. M. Savage, "Intensity Dependent Changes in the Refractive Index of Liquids," Phys. Rev. Lett. 12, 507 (1964).

2. C. C. Wang, "Nonlinear Susceptibility Constants and Self Focusing of Optical Beams in Liquids," Phys. Rev. 152, 149 (1966).

3. P. D. McWane and D. A. Sealer, "New Measurements of Intensity-Dependent Changes in the Refractive Index of Liquids," Appl. Phys. Lett. 8, 278 (1966).

4. E. L. Dawes and J. H. Marburger, "Computer Studies in Self Focusing," Phys. Rev. 179, 862 (1969).

5. W. G. Wagner, H. A. Haus and J. H. Marburger, "Large Scale Self-Trapping of Optical Beams in the Paraxial Ray Approximation," Phys. Rev. 175, 256 (1968).

6. D. H. Close, C. R. Giuliano, R. W. Hellwarth, L. D. Hess, F. J. McClung, and W. G. Wagner, "The Self Focusing of Light of Different Polarizations," IEEE J. Quant. Elect. QE-2, 553 (1966).

7. E. L. Dawes and J. H. Marburger, "Self Focusing of Elliptically Polarized Beams," (abstract) J. Opt. Soc. Amer. 61, 670 (1971).

8. H. Kogelnik, "On the Propagation of Gaussian Beams of Light through Lenslike Media Including Those with a Loss or Gain Variation," Appl. Opt. 4, 1562 (1965).

9. E. Wolf and E. W. Marchand, "Comparison of the Kirchhoff and the Rayleigh-Sommerfeld Theories of Diffraction at an Aperture," J. Opt. Soc. Amer. 54, 587 (1964).

10. W. A. Specht, Jr., "Rotational Modes in Spherical-Mirror Resonators," Calif. Institute of Technology, Quantum Electronics Laboratory Sc. Report No. 2, AFOSR Contr. No. AF49(638)-1322, June 1964.

Reproduced with permission of the copyright owner. Further reproduction prohibited without permission.

11. G. L. McAllister, M. M. Mann, and L. G. DeShazer, "Transverse-Mode Distortions in Giant-Pulse Laser Oscillators," IEEE J. Quantum Electronics QE-6, 44 (1970).

12. B. E. Newman and L. G. DeShazer, private communication.

13. Y. A. Volkova, V. A. Zamkoff, and L. V. Nalbandoff, Zhurnal Optika i Spectroscopia XXX, 556 (1971).

14. See K. H. Hellwege and A. M. Hellwege, Landolt-Bornstein Zahlenwerte und Funktionen, II/8 (Springer-Verlag, Berlin, 1962), pp. 849-860.

15. G. Mayer, "Rayonnement de l'harmonique Pair d'une Onde Lumineuse par des Molecules Soumises a un Champ Electrique Statique," Compt. Rend. B267, 54 (1968).

16. G. Hauchecorne, F. Kerherve, and G. Mayer, "Mesure des Interactions Entre Ondes Lumineuses Dans Diverses Substances," Le Jour. de Physique 32, 47 (1971).

Reproduced with permission of the copyright owner. Further reproduction prohibited without permission.

CHAPTER VII

INTERPRETATION OF THE NONLINEAR SUSCEPTIBILITY MEASUREMENTS IN ISOTROPIC MEDIA

7.0 The Accuracy of Experimental Determinations of $\chi_3^{ijk\ell}$

In this chapter we shall use the nonlinear susceptibility relations which are summarized in Table 5.1 to interpret the presently available experimental measurements of $\chi_3^{ijk\ell}$ in CCl_4 and the optical glasses which we have studied in the hope of inferring the sizes of the electronic and nuclear contributions to the intensity-dependent refractive indices of these materials. Since the validity of our analysis will depend upon the accuracy with which each of the experimental investigations have been conducted, we shall first discuss the merits and weaknesses of each of the experimental techniques.

Third Harmonic Generation Measurements

The third harmonic generation coefficient $\chi_3^{1111}(-3\omega,\omega,\omega,\omega)$ was measured by Wang and Baardsen in BSC glass.[1] As we have noted in Section 3.1, the short coherence length involved in this process makes surface scattering measurements the only practical means of implementing this determination. The measurement was thus adversely affected by (1) the possibility of surface impurities[2] and (2) the low signal yield, which resulted in the need to use photon counting techniques. Since this latter fact necessitated repetitive pulsing of the laser, a loss in mode control and repeatability was inevitable. It is thus not at all surprising that the value obtained for $\chi_3^{1111}(-3\omega,\omega,\omega,-\omega)$ had a relative accuracy of approximately 30%. Since the only means of

Reproduced with permission of the copyright owner. Further reproduction prohibited without permission.

calibrating THG data is through a direct estimation of the laser output power and beam profile, the difficulties which have already been discussed with regard to this technique in the case of the ellipse rotation studies also apply here. The requirement of repetitive pulsing, however, complicated this determination to an even greater extent and the absolute accuracy was thus assessed to be a factor of 3. In the light of such a large uncertainty, it would be highly artificial to attempt to draw any conclusions from the THG data; rather it is to be recognized that the value of THG determinations lies in their ability to give relative determinations of the electronic contribution σ to the nonlinear polarization. Hence we merely note that the findings of these investigations are in excellent agreement (20%) with our ellipse rotation measurements on borosilicate crown glass, but recognize that this agreement should not be considered to be extremely significant in view of the large uncertainty in the data.

Three-Wave Mixing Measurements

The three-wave mixing (TWM) studies which determine $\chi_3^{1111}(-(\omega+\Delta),\omega,\omega,-(\omega-\Delta))$ were first reported by Maker and Terhune in a number of crystalline solids in addition to fused quartz and BSC glass.[3] In a more recent study Hauchecorne, Kerherve, and Mayer[4] reported TWM determinations in CCl_4, CS_2, fused quartz, and a number of optical glasses. In this latter work a study of second harmonic generation in the presence of a strong static electric field in CS_2 and CCl_4 vapor is also reported. This technique might be considered to be a very special case of three-wave mixing in which the difference in

Reproduced with permission of the copyright owner. Further reproduction prohibited without permission.

frequency Δ is equal to ω. Thus $\chi_3^{1111}(-2\omega,\omega,\omega,0)$ is determined. From Table 5.1 it is clear that this technique provides a means of measuring σ since $a(\omega)$ and $b(\omega)$ would clearly be negligible at optical frequencies.

Considering first the use of TWM to determine $\chi_3^{1111}(-(\omega+\Delta),\omega,\omega,-(\omega-\Delta))$ we note that the frequency components taking part in the mixing process are usually generated by employing a ruby laser as the fundamental frequency source and directing the beam through a Raman laser cell to generate a Stokes shifted beam at frequency $\omega-\Delta$. Since this scheme involves two simultaneous nonlinear processes, stimulated Raman scattering and three-wave mixing, one would expect that any fluctuations in the laser output would be grossly amplified in the output signal of the experiment. Even so, the experimenters were able to obtain repeatable results with a relative uncertainty of approximately 20% by splitting the beams involved in the mixing process into two separate paths and making TWM measurements on two samples simultaneously. One of the samples could then serve as a standard of calibration to which all of the other materials could be referenced.

The absolute calibration of the two TWM studies were achieved in quite distinct manners which shall be discussed separately. In the original investigation by Maker and Terhune[3] a benzene cell was used as the Raman source thus resulting in a Stokes shift of 992 cm^{-1}. Calibration was quite ingeneously achieved by making TWM measurements on a sample of benzene. Since the 992 cm^{-1} Stokes shift is then resonant with a Raman active molecular vibration of the sample, it is

Reproduced with permission of the copyright owner. Further reproduction prohibited without permission.

argued that the TWM susceptibility is related to the Raman susceptibility by the relation

$$3|\chi_3^{1111}(-(\omega+\Delta),\omega,\omega,-(\omega-\Delta))| \simeq 6|\chi_3^{1111}(-(\omega-\Delta),\omega,\omega-\Delta,-\omega)| \qquad (7.1)$$

where $\chi_3^{1111}(-(\omega-\Delta),\omega,\omega-\Delta,-\omega)$ is the Raman susceptibility which may be calculated from direct measurements of the spontaneous Raman scattering cross section. Although this result may have been inferred by "ignoring dispersion" due to the frequency change Δ and including the degeneracy factors D from Equation (2.20), a better idea of what this approximation really involves may be obtained by substituting the laser and Stokes waves into Equation (5.6) to find that the Raman susceptibility may be expressed in the form

$$\chi_3^{1111}(-(\omega-\Delta),\omega,\omega-\Delta,-\omega) = \frac{1}{8}\sigma + \frac{1}{12}(a(-\Delta)+b(-\Delta)) + \frac{1}{12}(\alpha+\beta) \qquad (7.2)$$

Here we note that $\alpha = a(0)$, $\beta = b(0)$ and the rapidly varying optical terms of the nuclear response have been dropped since they are negligibly small. A measurement of the total spontaneous Raman scattering cross section and linewidth will yield a measurement of

$$\text{Im}\ \chi_3^{1111}(-(\omega+\Delta),\omega,\omega-\Delta,-\omega) = \frac{1}{12}\{a''(-\Delta)+b''(-\Delta)\} \qquad (7.3)$$

where it is recalled that $a''(-\Delta)$ and $b''(-\Delta)$ are the imaginary parts of $a(-\Delta)$ and $b(-\Delta)$ respectively; see Appendix I. From Section 4.2.2 it will be recalled that $a(\Delta)$ and $b(\Delta)$ for the case of a Raman vibration are pure imaginary quantities when $\pm\Delta$ lies on a vibrational line center and that $a''(\Delta)$ and $b''(\Delta)$ are odd functions

Reproduced with permission of the copyright owner. Further reproduction prohibited without permission.

of Δ. Hence Equation (7.1) is seen to be valid if the contributions σ, α, and β are negligible compared to the nuclear functions $a(\Delta)$ and $b(\Delta)$. The fact that this condition is satisfied is attested by the manner in which the TWM power drops off in a benzene sample when any medium other than benzene is employed as a Raman source.[5] Employing the determination of the Raman cross section at 6943Å obtained by McClung,[6] it is found that

$$|\chi_3^{1111}(-(\omega+\Delta),\omega,\omega-\Delta,-\omega)| = 35 \pm 7 \times 10^{-14} \text{ esu}$$

for benzene. Using this as the standard of calibration we estimate that the absolute accuracy of the original TWM studies should be approximately ±35%.

In the more recent study by Hauchecorne et al. two alternate Raman sources, hydrogen and methane, were employed to produce Stokes shifts of 4150 cm^{-1} and 2914 cm^{-1} respectively. Performing the TWM studies with two different sets of mixing frequencies permitted the researchers to estimate the degree to which the nuclear functions $a(\Delta)$ and $b(\Delta)$ were possibly contributing to the TWM susceptibility. Absolute calibration of the TWM studies in the glass samples studied was based on the second harmonic generation susceptibility of crystalline quartz. The focal intensity of the laser beam at the sample was calibrated by a measurement of the second harmonic power generated with a quartz sample. The focal intensity of the Stokes beam was measured by measuring the power generated in the $E_\omega, E_{\omega-\Delta}$ mixing process in quartz. Although no absolute uncertainties were quoted, it is to be expected that the measurements could certainly be no more accurate than

Reproduced with permission of the copyright owner. Further reproduction prohibited without permission.

the 35% obtained by Maker and Terhune since the calibration involves both a determination of the average laser field intensities and the second harmonic generation susceptibility.

The experimental studies of TWM and electric field induced second harmonic generation in CS_2 and CCl_4[4] were calibrated in an entirely different manner. The relevant nonlinear susceptibilities were measured both directly through an estimate of the laser output power and beam profile and also by the calibration method of Maker and Terhune applied to hydrogen rather than benzene.[3] Again, the absolute uncertainties in the calibration are not quoted; it is noteworthy however that the d.c. Kerr measurements of gaseous argon and hydrogen obtained by Buckingham et al. yield an electronic contribution to the nonlinear susceptibility which is twice the size of that used in the calibration of these measurements.[7,8]

A.C. Kerr Measurements in Glasses

The a.c. Kerr measurements in glasses and fused quartz were reported by Duguay and Hansen in 1970.[9-11] The ultra-short laser pulse Kerr techniques which were employed in this work were first reported in a study of the response time of induced birefringence in benzene.[12] More specifically, a mode locked Nd:glass laser emitting pulses at 1.06μ, 4-5 ps in duration was employed to produce a Kerr birefringence in the glass samples which was detected by monitoring the polarization of a weaker second harmonic beam in transmission through the sample.

The implementation of an a.c. Kerr study using picosecond laser pulses is an extremely difficult piece of experimental work to perform

Reproduced with permission of the copyright owner. Further reproduction prohibited without permission.

accurately due to the necessity of obtaining repeatable pulses from sample to sample and the rigid requirement of having the two trains of 5 ps pulses coincide precisely as they enter the Kerr cell. Each pulse in the train is approximately 1.5 mm in length and thus any change in the relative overlap of the two pulses from one specimen to the next would completely invalidate the results. The fact that the glasses possess a Kerr coefficient two orders of magnitude lower than that of CS_2 made the study even more difficult. In view of these facts it is not at all surprising that the relative accuracy of the a.c. Kerr measurements are 35-50%.

In an attempt to calibrate a relative measurement of this type a specification of the beam character and direct calculation of the Kerr constant would be highly artificial. Fortunately, the Kerr studies are normalized using CS_2 as a standard of calibration. The choice of this common standard in the calibration of a.c. Kerr and ellipse rotation measurements make their comparison particularly meaningful.

Kerr Measurements in CCl_4

The most precise determination of the Kerr constant of CCl_4 is the d.c. measurement reported by George et al.[13,14] Using cw laser techniques the Kerr constant of liquid CCl_4 was determined relative to CS_2 with a relative accuracy of better than 1% at $\lambda = 6328\text{Å}$ and 23°C. The determined ratio of $B_o(CS_2)/B_o(CCl_4) = 41.6$ may be corrected using the dispersion measurements of McComb for CS_2 and of Szivessy and Dierkesmann for CCl_4.[15] Hence we find

$$\frac{B_o(CS_2)}{B_o(CCl_4)} = 40.8 \pm 0.8$$

Reproduced with permission of the copyright owner. Further reproduction prohibited without permission.

at $\lambda = 6943\text{Å}$ and 23°C.

Ellipse Rotation Studies

It has already been noted that the absolute accuracy of the ellipse rotation study which we have undertaken should be approximately ±11%. The degree of accuracy is partially due to the fact that a nanosecond Q-spoiled laser without mode-locking is sufficient for the implementation of this study. Hence mode control and repeatability are vastly increased.

From the theoretical considerations of Chapter V and the foregoing discussion, it is evident that ellipse rotation and the Kerr effect are two techniques which are particularly well suited for the comparison and interpretation of the electronic contribution to the nonlinear refractive index changes in isotropic media. Of all of the third order nonlinear phenomena which have been studied in glasses only third harmonic generation depends on no other parameters than the two which are determined by ellipse rotation and the Kerr effect. Additionally, these phenomena are easily calibrated to the same, very accurate, standard of calibration, the Kerr constant of CS_2. Hence a direct comparison is especially meaningful.

As we proceed to interpret the Kerr and ellipse rotation data the results of the three-wave mixing studies should not be overlooked. Although these data have a dependence on the nuclear rearrangement parameters $a(\Delta)$ and $b(\Delta)$, they may still be used as a valuable check on the conclusions which are drawn from Kerr and ellipse rotation measurements, especially when the nuclear contributions to the TWM data can be shown to be negligible through studies of the polarization

Reproduced with permission of the copyright owner. Further reproduction prohibited without permission.

dependence of the mixing process and through light scattering measurements.

7.1 Conclusions Concerning Optical Glasses

The results of the experimental investigations into ellipse rotation, the a.c. Kerr effect, and three-wave mixing in glasses are summarized in Table 7.1. As evidenced in the table, the data is calibrated according to the discussions of Sections 6.6 and 7.0 and presented in terms of parameters which would all be equal for any given material if all nuclear contributions could be neglected.

Comparison of the a.c. Kerr and ellipse rotation data for fused quartz and BK-7 glass in the first two columns indicate that β is nominally zero for both materials since it must take on a positive (or zero) value in order to produce a negative perturbation in the total energy of the medium in the field. It is easily shown however that a worst case estimate of the nuclear contribution to the Kerr constant of fused quartz may yield a value as large as 100%, whereas a maximum value of 45% is obtained for BK-7 glass. It has been suggested in Appendix I that absolute Raman scattering spectra may yield new estimates of the nuclear contributions to the intensity-dependent refractive indices. However, since the only currently available light scattering data on glasses all involve relative measurements, such conclusions will have to be deferred to a future date.[16,17]

In any attempt to use TWM data to infer the size of electronic contributions to the nonlinear susceptibility, the possibility of nuclear contributions $a(\Delta)$ and $b(\Delta)$ shown in Table 5.1 should not be ignored without careful consideration. As noted previously, light

Reproduced with permission of the copyright owner. Further reproduction prohibited without permission.

Reproduced with permission of the copyright owner. Further reproduction prohibited without permission.

Material	Ellipse Rotation $(\sigma+2\beta)/24$	Kerr Effect $(\sigma+\beta)/24$	Three-Wave Mixing $\frac{\sigma}{24} + \frac{1}{18}(a(\Delta) + b(\Delta))$		$n_{6943\text{Å}}$
CS_2	378	189	-	-	1.62
Fused Quartz	1.5(1.5)	1.7(9)	2.0(4)	1.75	1.455
BK-7 BSC Glass	2.3(2)	2.6(9)	3.8(8)	-	1.513
SF-7 Flint Glass	9.9(10)	-	-	-	1.631
LaSF-7 Glass	-	13.3(40)	-	-	1.91
WG-1 Glass	-	-	-	12.3	1.7
D2129 Glass	-	-	-	12.5	1.71
FED Glass	-	-	-	28.4	1.95
References		(11)	(3)	(4)	

TABLE 7.1

All data in units of 10^{-15} esu

Values in parentheses denote the uncertainty in the last digit relative to the calibration standard employed in each investigation.

scattering measurements will prove to be of great value here when they become available. For the present, a comparison of the TWM data in Table 7.1 for fused quartz seems to indicate that the measurements of Maker and Terhune[3] which employ a 992 cm^{-1} Stokes shift are affected by nuclear contributions whereas studies conducted by Hauchecorne et al.[4] where a Stokes shift of 4150 cm^{-1} was used derives a smaller contribution from nuclear nonlinearities. In view of the accuracy of these measurements however, we feel that such strong conclusions are premature without further investigation. Along these lines, it is felt that TWM measurements of both χ_3^{1111} and χ_3^{1221} involving Stokes shifts of several values along with Raman scattering data would certainly settle the question of electronic versus nuclear contributions to TWM.

If in fact the measurements of Hauchecorne et al. are accurately calibrated, and the TWM susceptibility which they measure is primarily electronic in nature, these measurements would clearly back our assertion that the electronic nonlinearities are dominant in producing nonlinear refractive index changes in glasses. In examining their data it is interesting to note that the values for WG-1 Schott glass and D-2129 glass whose linear refractive indices fall between those of SF-7 and LaSF-7 both have nonlinear parameters which also fall between those of SF-7 and LaSF-7. Likewise the parameter measured for FED glass is the highest of all glasses measured in correspondence to its high linear refractive index.

Reproduced with permission of the copyright owner. Further reproduction prohibited without permission.

The Nonlinear Refractive Index of Glasses

With the presently available data it is worthwhile to calculate the nonlinear refractive index n_2. The index change resulting in the self focusing of a linearly polarized beam is given by Equation (3.23) and Table 5.1 to be

$$\delta n_\ell = \frac{2\pi}{n}\left(\frac{3\sigma + 4\alpha + 4\beta}{8}\right)|E_\omega|^2 \tag{7.4}$$

where $|E_\omega|^2 = 2\langle E^2(t)\rangle_{av}$. Thus n_2 is defined by $\delta n_\ell = n_2|E_\omega|^2/2$ giving[18]

$$n_2 = \frac{2\pi}{n}\left(\frac{3}{4}\sigma + (\alpha+\beta)\right) \tag{7.5}$$

It is important to recognize that this value of n_2 is different from that which is commonly defined in Kerr experiments and arises from the $\delta n_{||}$ of Equation (3.20). Using the data in Table 5.1, this "Kerr nonlinear index" may be written in the form

$$n_2' = \frac{2\pi}{n}\left(\frac{3}{2}\sigma + (\alpha+\beta)\right) \tag{7.6}$$

which is indeed equal to n_2 if σ is negligible as in most Kerr liquids. However, $n_2' \neq n_2$ if σ is dominant, a fact which is often overlooked in the literature[11,19].

Suppose (in accordance with our nominal results) that this electronic contribution σ is assumed to dominate in Equation (7.5). In this case we may write $n_2 \simeq \frac{3\pi\sigma}{2n}$ and infer the value of σ using our ellipse rotation data (i.e., $\chi_3^{1221} \simeq \sigma/24$). This estimate gives values of $n_2 = 1.18, 1.69, 6.85 \times 10^{-13}$ esu for fused quartz, BK-7 glass,

Reproduced with permission of the copyright owner. Further reproduction prohibited without permission.

and SF-7 glass respectively. Moreover an estimate of the critical powers for self focusing given by[20]

$$P_{cr} = \frac{(1.22\lambda_o)^2 c}{128\, n_2} \tag{7.7}$$

yields approximate values of 0.25, 1, and 1.4 MW for SF-7, BK-7, and fused quartz respectively. Had the a.c. Kerr data been used to find n_2 assuming $\sigma >> \beta$, values approximately 10% higher would have been obtained for n_2.

In order to obtain an estimate of how great an error might be made by assuming $\sigma >> \beta$ it is instructive to assume the worst case estimate that $\beta = 0.45\ (\sigma+\beta)$ for BK-7 and $\beta \simeq (\sigma+\beta)$ for fused quartz. Using these worst case estimates with the upper limits of our data for χ_3^{1221} (which were used to obtain these estimates) one finds that $n_2 = 0.6$ and 1.2×10^{-13} esu for fused quartz and BK-7 glass respectively (assuming $\beta = -3\alpha$). These estimates are somewhat lower than those (more likely) estimates where β is assumed negligible; however both estimates clearly give critical powers for self focusing which are lower than the powers which are generated by mode locked solid state lasers. This suggests the possibility of self-focusing processes occurring in the laser oscillators, a contention which would merit further investigation since such phenomena would profoundly affect the output characteristics of these devices.

7.2 Conclusions Concerning CCl_4

The conclusions which were drawn concerning optical glasses were necessarily limited by the availability of accurate a.c. Kerr data. In

Reproduced with permission of the copyright owner. Further reproduction prohibited without permission.

order to bring out the value of comparing ellipse rotation and Kerr data for separating electronic and nuclear nonlinearities in isotropic media, we shall examine our results on CCl_4 .

The relative value of the Kerr constants of CS_2 and CCl_4 were measured by Hellwarth and George.[14] As noted in Section 7.0 the results of this determination may be expressed in the form

$$\frac{(\sigma+\beta)/n \text{ of } CS_2}{(\sigma+\beta)/n \text{ of } CCl_4} = 40.8 \pm 0.8 \tag{7.8}$$

at 6943Å and 23°C.

The results of our ellipse rotation measurements on CCl_4 were given in Table 6.2 in the form $\chi_3^{1221}(-\omega,\omega,\omega,-\omega) = 6.08 \pm 0.6 \times 10^{-15}$ esu. In terms of Equation (6.21) and Figure 6.8 we may write this result in the form

$$\frac{(\sigma+2\beta)/n \text{ of } CS_2}{(\sigma+2\beta)/n \text{ of } CCl_4} = 56 \pm 6 \tag{7.9}$$

It should be noted here that two previous measurements of this ratio obtained by Maker, et al.[21] and Wang[22] reported values of 32 and 34 respectively. These latter results however, claimed a relative accuracy of 25% and were achieved with the use of unfocused or weakly focused multimode lasers. The existence of such a discrepancy in the data is thus not at all surprising especially in view of the fact that CCl_4 has a relatively low ellipse rotation coefficient (compared to CS_2 for example) thus making this measurement particularly difficult to perform with an unfocused beam apparatus. Both the small ellipse rotation signal and the necessity of subjecting other components in the

Reproduced with permission of the copyright owner. Further reproduction prohibited without permission.

experiment to high intensities are liable to contribute to erroneous conclusions in such an experiment.

By combining the results of Kerr and ellipse rotation data as given in Equations (7.8) and (7.9) and employing the CS_2 Kerr constant normalizations previously discussed in Section 6.6, it is found that

$$\sigma + \beta = 100 \pm 4 \times 10^{-15} \text{ esu} \tag{7.10}$$

and that

$$\frac{\beta}{\sigma+\beta} = 0.46 \pm 0.17 \tag{7.11}$$

for CCl_4 at 6943Å and 23°C. Employing Equation (7.5) to calculate n_2 with $\beta = -3\alpha$ [23] one finds that

$$n_2 = (3.06 \pm .3) \times 10^{-13} \tag{7.12}$$

which corresponds to a critical power of approximately 550 kW. This figure is well within the limits of the 600 ± 300 kW critical power measured directly by Wang.[22]

Having established that both electronic and nuclear nonlinearities play a significant role in contributing to the intensity dependent refractive index, it is worthwhile to examine and compare other techniques which may be applied to separating electronic and nuclear nonlinearities in CCl_4.

Attempts to distinguish such contributions to the Kerr constants of symmetric molecule liquids by studying the temperature dependence of the effect have proved inconclusive, primarily due to the lack of a good theoretical model which describes this dependence.[13]

Reproduced with permission of the copyright owner. Further reproduction prohibited without permission.

Although one might hope that the nuclear response might be "frozen out" and thus distinguished by conducting experiments with picosecond laser pulses, the linewidth of the main central component of the depolarized light scattering spectrum indicates that the nuclear response time is appreciably shorter than a picosecond;[23] see Appendix I. Even in media where the nonlinearities producing the central spectral component may be frozen out by picosecond laser pulses, one must still deal with Raman type nonlinearities which would result in a much faster responding contribution.

Three alternative methods, d.c. Kerr measurements on CCl_4 vapor, TWM, and static field induced second harmonic generation have all been employed to obtain estimates of the second hyperpolarizability γ of CCl_4 molecules in the vapor phase. Since γ is defined by the expression $p = \alpha_o E_L + (\frac{1}{6})\gamma E_L^3$ where p is the dipole moment of the molecule, α_o the linear polarizability, and E_L the local field, an application of Equations (3.21) and (4.10) along with Table 5.1 clearly shows that the electronic contribution to the Kerr constant may be written in the form

$$B_{o\ elec} = \frac{2\pi}{n\lambda}\sigma = \frac{2\pi}{n\lambda}\left(\frac{n^2+2}{3}\right)^4 \frac{N\gamma}{3} \tag{7.13}$$

Here N is the number density of molecules in the liquid and the refractive index, n in the Lorentz local field factor is assumed to be constant over the optical range of the experiment.

The d.c. Kerr measurement of CCl_4 vapor was performed by Buckingham.[24] A value of $\gamma = 9.96 \pm 0.32 \times 10^{-36}$ esu was determined by extrapolation of the Kerr data to infinite values of

Reproduced with permission of the copyright owner. Further reproduction prohibited without permission.

temperature.[25] From Equation (7.13) with $N = 6.242 \times 10^{21} cm^{-3}$ we find that this hyperpolarizability corresponds to a value of $\sigma = 75 \times 10^{-14}$ esu.

The three-wave mixing and field induced second harmonic generation studies were both performed in gaseous CCl_4 by Hauchecorne et al. using a Q-spoiled ruby laser.[4] Both of these investigations yield a value of $\gamma = 4.2 \times 10^{-36}$ esu in the case where a hydrogen cell is used as a Raman source. This corresponds to a value of $\sigma = 31.6 \times 10^{-36}$ esu. When methane is employed as a Raman source for the TWM study however, a value of $\gamma = 7.4 \times 10^{-36}$ esu is obtained. A study of the polarization dependences of TWM showed that the ratio of power emitted at the TWM frequency for the case where the Stokes wave was polarized parallel to the fundamental wave compared to the case where they were perpendicularly polarized is 10 for the case of a hydrogen Raman source and 14 for the case of a methane Raman source. It is seen from Equation (3.14) and Table 5.1 that this ratio should be 9 for a purely electronic contribution. Hence it is suggested that the hydrogen Raman cell measurement gives the more accurate of the two estimates. This comparison also suggests the wide range of frequencies over which nuclear mechanisms may play a role in contributing to the nonlinear susceptibility.

Although neither of the two values obtained by the two groups agree well with one another, it is to be noted that the apparent disagreement lies in the absolute calibration of the data rather than the relative determinations. (It will be recalled that the value obtained by Buckingham for the hyperpolarizability of Ar is twice that which was used by Hauchecorne et al. in their calibration of the TWM and second

Reproduced with permission of the copyright owner. Further reproduction prohibited without permission.

harmonic generation data.[4,7]) Nevertheless, we recognize that our result $\sigma = 54 \pm 17 \times 10^{-15}$ esu clearly falls between results obtained by the other workers.

Although it is interesting to make the comparisons above and to speculate on the implications of the various determinations, it should be borne in mind that the calculation of liquid phase Kerr constants from vapor phase data may commonly err by a factor of two or more. Hence our result which asserts that the Kerr constant of liquid CCl_4 is $46 \pm 17\%$ nuclear provides the most accurate determination of this parameter to date.

7.3 Summary

Nonlinear refractive index changes in isotropic media have been considered as a special case of nonlinear optical phenomena involving a polarization cubic in the electric field strength. By modeling this polarization in the form proposed in Chapter IV

$$\underset{\sim}{\tilde{P}}_3(t) = \frac{\sigma}{2}\,\underset{\sim}{\tilde{E}}(t)\cdot\underset{\sim}{\tilde{E}}(t)\underset{\sim}{\tilde{E}}(t) + \int \tilde{a}(t-\tau)\underset{\sim}{\tilde{E}}(\tau)\cdot\underset{\sim}{\tilde{E}}(\tau)d\tau\ \underset{\sim}{\tilde{E}}(t) + \int \tilde{b}(t-\tau)\underset{\sim}{\tilde{E}}(\tau)\cdot\underset{\sim}{\tilde{E}}(t)\underset{\sim}{\tilde{E}}(\tau)d\tau$$

where σ is the parameter of "electronic distortion" and $\tilde{a}(t)$ and $\tilde{b}(t)$ are the time response functions for "nuclear rearrangement", we have established a basis for interrelating the various elements of the nonlinear susceptibility tensor $\underset{\sim}{\chi}_3$.

The above expression has been applied to interpret several nonlinear optical phenomena including optical frequency mixing and optically induced refractive index changes. The results of this analysis have been summarized in Table 5.1 which lists each phenomenon, the

Reproduced with permission of the copyright owner. Further reproduction prohibited without permission.

nonlinear susceptibility elements involved, and the interpretation of these tensor elements in terms of σ, a, and b. In Appendices H and I further relationships between $\tilde{a}(t)$ and $\tilde{b}(t)$ and spontaneous and stimulated light scattering parameters are established.

The analysis suggests that most† nonlinear refractive index changes in isotropic media may be characterized in terms of the electronic parameter σ and the nuclear parameters $\alpha = \int \tilde{a}(t)dt$ and $\beta = \int \tilde{b}(t)dt$. For this reason the Kerr effect experiments which measure the tensor elements $\frac{1}{2}\{\chi_3^{1221}(-\omega,\omega,\Omega,\Omega) + \chi_3^{1212}(-\omega,\omega,\Omega,\Omega)\} = \frac{\sigma+\beta}{24}$ for $|\Omega-\omega|$ sufficiently large and the measurements of the intensity dependent rotation of the polarization ellipse of a monochromatic optical beam which determines $\chi_3^{1221}(-\omega,\omega,\omega,-\omega) = \frac{\sigma+2\beta}{24}$ show particular promise for the study of nonlinear index changes. Together these experiments yield a determination of both the electronic parameter σ and the nuclear parameter β. Thus they provide a means of completely determining the electronic contribution to nonlinear index changes. Also, since α may be inferred from β using spontaneous light scattering measurements, a means is also provided to characterize the nuclear nonlinearities; see Appendix I.

The practicability of this technique has been demonstrated through a <u>focused</u> beam investigation of "ellipse rotation" which is particularly well suited to media exhibiting small nonlinearities. Values of $\chi_3^{1221}(-\omega,\omega,\omega,-\omega) = 1.5$, 2.3, 9.9 and 6.08×10^{-15} esu have been obtained for fused quartz, BK-7 borosilicate crown glass, SF-7

†Those which do not involve components in the spectrum of $\tilde{E}^2(t)$ which are resonant with a vibrational mode of the medium.

Reproduced with permission of the copyright owner. Further reproduction prohibited without permission.

dense flint glass, and carbon tetrachloride (CCl_4) respectively at 23^oC and $\lambda = 6943\text{Å}$. These measurements constitute the first observations of ellipse rotation in any solid and (with an absolute accuracy of 11%) are the most accurately known of any nonlinear optical constant in glasses.

Although our results when interpreted with a.c. Kerr and three-wave mixing data suggest that electronic contributions may dominate nonlinear index changes in glasses, we have been hesitant to rule out possible nuclear contributions until the uncertainty in the Kerr measurements can be reduced. If a purely electronic mechanism is assumed, however, we would obtain a nonlinear refractive index n_2 of 1.2, 1.7, and 6.9×10^{-13}esu for fused quartz, BK-7, and SF-7 glasses respectively. Even if nuclear contributions are found to be significant, these estimates would not err by much more than 50%, clearly suggesting that these "fast responding" nonlinearities are sufficiently large to produce self focusing in glasses with critical powers in the 1 MW range.

In contrast the case of CCl_4 for which very accurate Kerr data is available demonstrates the power of the proposed method for separating electronic from nuclear nonlinearities. With $\frac{\sigma}{\sigma+\beta} = 0.54 \pm 0.17$ both electronic and nuclear nonlinearities are significant and a value of the "fast responding" part of the nonlinear index (which excludes electrostrictive effects) is found to be $n_2 = (3.06 \pm 0.3) \times 10^{-13}$esu.

Reproduced with permission of the copyright owner. Further reproduction prohibited without permission.

REFERENCES - CHAPTER 7

1. C. C. Wang and E. L. Baardsen, "Study of Optical Third-Harmonic Generation in Reflection," Phys. Rev. 185, 1079 (1969); Phys. Rev. B1, 2827 (1970).

2. D. L. Rousseau and G. E. Leroi, "Charged-Particle Emission upon Ruby-Laser Irradiation of Transparent Dielectric Materials," J. Appl. Phys. 39, 3328 (1968).

3. P. D. Maker and R. W. Terhune, "Study of Optical Effects Due to an Induced Polarization Third Order in the Electric Field Strength," Phys. Rev. 137, A801 (1965).

4. H. Hauchecorne, F. Kerherve and G. Mayer, "Mesures Des Interactions Entre Ondes Lumineuses Dans Diverses Substances," Le Jour. de Physique 32, 47 (1971).

5. R. W. Terhune and P. D. Maker, "Nonlinear Optics", in Lasers, Vol. 2, ed. A. K. Levine (M. Dekker, Inc. New York, 1968), Chap. 4.

6. F. J. McClung, Hughes Research Labs Report No. 306.

7. A. D. Buckingham and D. A. Dunmur, "Kerr Effect in Inert Gases and Sulphur Hexafluoride," Trans. Faraday Soc. 64, 1776 (1968).

8. A. D. Buckingham and B. J. Orr, "Electric Birefringence in Molecular Hydrogen," Proc. Roy. Soc. A.305, 259 (1968).

9. M. A. Duguay and R. W. Hansen, Spring Meeting of the Optical Soc. of Amer., Philadelphia, Pa., April 7-10, 1970. Phys. Abst. 73, No. 72308.

10. M. A. Duguay and J. W. Hansen, Symposium on Damage in Laser Materials, Boulder, Colorado, June 24-25, 1970, NBS Special Publ. 341, pp.45-50.

11. M. A. Duguay, J. W. Hansen, and S. L. Shapiro, "Nd:Glass Laser Radiation," IEEE J. Quant. Electr. QE-6, 725 (1970).

Reproduced with permission of the copyright owner. Further reproduction prohibited without permission.

12. M. A. Duguay and J. W. Hansen, "An Ultrafast Light Gate," Appl. Phys. Lett. 15, 192 (1969).

13. N. George, R. W. Hellwarth, and C. R. Cooke, "Kerr Constant Measurements Using a Laser Polarimeter," Electron Technology 2, 229 (1969).

14. R. W. Hellwarth and N. George, "Nonlinear Refractive Indices of CS_2-CCl_4 Mixtures," Jour. Opto-Electronics 1, 213 (1969).

15. See Landolt-Bornstein Zahlenwerte und Funktionen, II/8 (Springer-Verlag, Berlin, 1962), pp. 849-860.

16. M. Hass, "Raman Spectra of Vitreous Silica, Germania, and Sodium Silicate Glass," J. Phys. Chem. Solids 31, 415 (1970).

17. M. C. Tobin and T. Baak, "Raman Spectra of Some Low-Expansion Glasses," J. Opt. Soc. Amer. 58, 1459 (1968).

18. R. Y. Chiao, E. Garmire, and C. H. Townes, "Self-Trapping of Optical Beams," Phys. Rev. Lett. 13, 479 (1964).

19. R. R. Alfano and S. L. Shapiro, "Direct Distortion of Electronic Clouds of Rare-Gas Atoms in Intense Electric Fields," Phys. Rev. Lett. 24, 1217 (1970).

20. P. L. Kelley, "Self Focusing of Optical Beams," Phys. Rev. Lett. 15, 1005 (1965).

21. P. D. Maker, R. W. Terhune, and C. M. Savage, "Intensity-Dependent Changes in the Refractive Index of Liquids," Phys. Rev. Lett. 12, 507 (1964).

22. C. C. Wang, "Nonlinear Susceptibility Constants and Self Focusing of Optical Beams in Liquids," Phys. Rev. 152, 149 (1966).

23. H. S. Gabelnick and H. L. Strauss, "Low-Frequency Motions in Liquid Carbon Tetrachloride. II. The Raman Spectrum," J. Chem. Phys. 49, 2334 (1968).

24. A. D. Buckingham, private communication.

25. A. D. Buckingham and B. J. Orr, "Molecular Hyperpolarizabilities," Quart. Rev. (London) 21, 195 (1967).

Reproduced with permission of the copyright owner. Further reproduction prohibited without permission.

APPENDIX A

Electron Oscillator Model for $\tilde{P}_2(t)$

As an example of how the nonlinear polarization second order in the electric field strength may take on the time dependence suggested by Equation (2.6), let us consider the Lorentz electron oscillator model of an atomic system[1] in which the usual harmonic potential is perturbed by the presence of a small anharmonicity. Hence expanding the anharmonic potential in a power series about its minimum value and keeping only the first order nonlinearity one finds that the equation of motion of the electron may be written in the form[2]

$$\frac{d^2\tilde{r}(t)}{dt^2} + \gamma \frac{d\tilde{r}(t)}{dt} + \omega_o^2 \tilde{r}(t) + \delta\tilde{r}^2(t) = -\frac{e\tilde{E}(t)}{m} \tag{A.1}$$

where ω_o is the resonant frequency of the electron oscillator, γ the linewidth of the transition being modeled, $\tilde{r}(t)$ the displacement of the electron from its equilibrium position, $-e$ the electron charge, m the reduced mass of the electron, $\tilde{E}(t)$ the applied electric field, and δ the anharmonic coefficient. We shall assume that $\delta\tilde{r}(t)$ is much smaller than ω_o^2 so that the anharmonicity merely presents a small correction to the linear solution in which $\delta \to 0$. Adopting an approximation to $\tilde{r}(t)$ in the form of a power series in δ we write

$$\tilde{r}(t) = \tilde{r}_o(t) + \delta\tilde{r}_1(t) + \delta\tilde{r}_2(t) + \cdots \tag{A.2}$$

where $\tilde{r}_o(t)$ is the solution of Equation (A.1) with $\delta = 0$ and the succeeding terms present small corrections to this linear approximation.

Reproduced with permission of the copyright owner. Further reproduction prohibited without permission.

Substituting this trial solution into Equation (A.1) and equating powers of δ one finds for the first two terms

$$\tilde{r}_o(t) = -\int_{-\infty}^{\infty} \tilde{z}(t-\tau)\,\frac{e\tilde{E}(\tau)}{2\pi m}\,d\tau \tag{A.3}$$

$$\delta\tilde{r}_1(t) = \frac{-\delta}{2\pi}\int \tilde{z}(t-\tau)\,\tilde{r}_o^2(\tau)\,d\tau \tag{A.4}$$

where $\tilde{z}(t)$ is the inverse Fourier transform of the linear oscillator response function $z(\omega) = [\omega_o^2 - \omega^2 - i\omega\gamma]^{-1}$.

Since the polarization of the dielectric medium is defined by the relation $\tilde{P}(t) = -Ne\,\tilde{r}(t)$ where N is the number density of electrons, the linear polarization is given by $\tilde{P}_1(t) = -Ne\,\tilde{r}_o(t)$ and the nonlinear polarization quadratic in the electric field strength is clearly given by $\tilde{P}_2(t) = -Ne\,\delta\tilde{r}_1(t)$ which may be written in the form

$$\tilde{P}_2(t) = \frac{Ne\delta}{2\pi}\int_{-\infty}^{\infty} \tilde{z}(t-\tau)\,\tilde{r}_o^2(\tau)\,d\tau$$

$$= \int_{-\infty}^{\infty} \tilde{\chi}_2(t-\tau, t-\tau_2)\tilde{E}(\tau_1)\tilde{E}(\tau_2)d\tau_1 d\tau_2 \tag{A.5}$$

where Equation (A.3) was employed to define

$$\tilde{\chi}_2(t_1,t_2) = \frac{Ne^3\delta}{(2\pi)^3 m^2}\int_{-\infty}^{\infty} \tilde{z}(\tau)\,\tilde{z}(t_1-\tau)\,\tilde{z}(t_2-\tau)\,d\tau \tag{A.6}$$

which clearly takes the form given in Equation (2.6).

Reproduced with permission of the copyright owner. Further reproduction prohibited without permission.

APPENDIX B

Expanded Form for $\underline{P}_3(\omega)$

In Section 2.3 the i^{th} component of the nonlinear polarization $\underline{P}_3(\omega)$ was examined at a specific frequency ω_s which is the sum frequency of three monochromatic field components, i.e., $\omega_s = \omega_a + \omega_b + \omega_c$; see Equation (2.17). For the sake of completeness we note here for the case of a field whose Fourier spectrum is given by

$$\underline{E}(\omega) = \frac{1}{2} \underline{E}_{\omega_a} \{\delta(\omega-\omega_n) + \delta(\omega+\omega_a)\}$$

$$+ \frac{1}{2} E_{\omega_b} \{\delta(\omega-\omega_b) + \delta(\omega+\omega_b)\}$$

$$+ \frac{1}{2} E_{\omega_c} \{\delta(\omega-\omega_c) + \delta(\omega+\omega_c)\} \qquad \text{(B.1)}$$

the complete expression for the nonlinear polarization $P_{3,i}(\omega)$ which is given by

$$P_{3,i}(\omega) = \iiint_{-\infty}^{\infty} \chi_3'^{ijk\ell}(\omega_1,\omega_2,\omega_3) E_j(\omega_1) E_k(\omega_2) E_\ell(\omega_3)$$

$$\times \delta(\omega-\omega_1-\omega_2-\omega_3) d\omega_1 d\omega_2 d\omega_3 \qquad \text{(B.2)}$$

takes the form

Reproduced with permission of the copyright owner. Further reproduction prohibited without permission.

$$P_{3i}(\omega) = \frac{1}{8} \sum_{n=\{s\}} \chi_3^{ijk\ell}(\omega_n,\omega_n,\omega_n) E_j(\omega_n) E_k(\omega_n) E_\ell(\omega_n)\ \delta(\omega-3\omega_n)$$

$$+ \frac{3}{8} \sum_{\substack{n=\{s\} \\ m=\{s\} \\ n\neq m}} \chi_3^{ijk\ell}(\omega_n,\omega_n,\omega_m) E_j(\omega_n) E_k(\omega_n) E_\ell(\omega_m)\ \delta(\omega-2\omega_n-\omega_m)$$

$$+ \frac{3}{4} \sum_{c\{s\}} \chi_3^{ijk\ell}(\omega_n,\omega_m,\omega_p) E_j(\omega_n) E_k(\omega_m) E_\ell(\omega_p) \delta(\omega-\omega_n-\omega_m-\omega_p) \quad \text{(B.3)}$$

Here $\{s\}$ denotes the set of subscripts (a,b,c,a^*,b^*,c^*) where $\omega_{n^*} = -\omega_n$; sums are assumed to be taken over the spatial indices j, k, and ℓ; and the notation $c\{s\}$ denotes the fact that the third sum is to be taken over all <u>combinations</u> of the indices in $\{s\}$, i.e., $n \neq m \neq p$. It is seen that Equation (B.3) consists of a total of 56 terms (six terms in the first sum, thirty in the second and twenty in the final sum) corresponding to all possible combinations of the indices $\{s\}$ taken three at a time (including combinations in which two and all three of the indices are degenerate such as (a,a,a) or (a,a,b)).

Reproduced with permission of the copyright owner. Further reproduction prohibited without permission.

APPENDIX C

The Ellipse Rotation Angle

Given an elliptically polarized wave of the form

$$\tilde{\underline{E}}(t) = \text{Re}\ \{(E_+\hat{e}_+ + E_-\hat{e}_-)\ e^{-i\omega t}\} \qquad (C.1)$$

a schematic representation of the wave may be given in terms of the two counter-rotating vectors as shown in Figure C.1. Clearly, the major axis of the ellipse of polarization is oriented along the x-axis. Now if a phase shift ϕ is produced between the right and left circularly polarized components of the wave, the schematic representation is changed to that shown in Figure C.2. Since the two counter-rotating components are of the same frequency, they clearly sum to produce a maximum in the polarization ellipse at an angle $\phi/2$ with respect to the x-axis. Hence the ellipse rotation angle is $\phi/2$.

Reproduced with permission of the copyright owner. Further reproduction prohibited without permission.

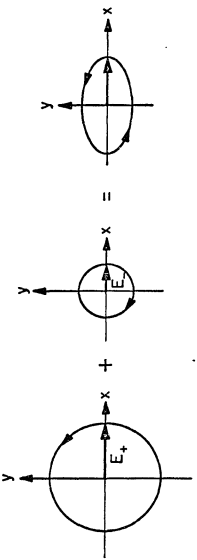

Figure C.1

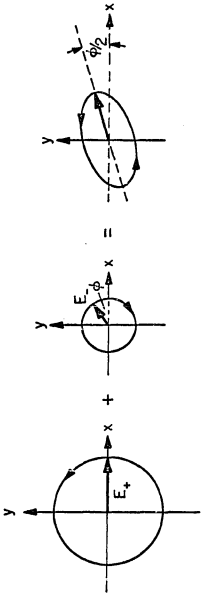

Figure C.2

Reproduced with permission of the copyright owner. Further reproduction prohibited without permission.

APPENDIX D

Local Field Corrections for $\chi_3^{ijk\ell}$

In a dense medium the electric field $\underline{E}_{\mathcal{L}}$ seen by individual electrons in the medium is affected by the dipolar fields of surrounding atoms or molecular groups. Hence the macroscopic susceptibility cannot be obtained by simply multiplying the average polarizability of individual molecules by the number density of molecules. Rather, the susceptibility of the medium must be corrected to include terms which will express the local field in terms of the macroscopic field.

For the case of a dielectric medium where the electron states are localized in space, Lorentz[1] has chosen to express the local field in the form

$$\underline{E}_{\mathcal{L}}(\omega) = \underline{E}(\omega) + \phi\underline{P}(\omega) \tag{D.1}$$

This expression may be shown to hold exactly in cubic ionic solids and approximately in isotropic liquid media where $\phi = 4\pi/3$.[3] Hence, using the definition $\underline{P}(\omega) = \chi^{\mathcal{L}}(\omega)\underline{E}_{\mathcal{L}}(\omega)$ where $\chi^{\mathcal{L}}$ is the "local linear susceptibility" (i.e., that which is obtained for $\phi = 0$), one finds that

$$\underline{E}_{\mathcal{L}}(\omega) = \frac{1}{1 - \phi\chi^{\mathcal{L}}(\omega)}\underline{E}(\omega) \equiv L(\omega)\ \underline{E}(\omega) \tag{D.2}$$

where $L(\omega)$ is defined to be the "Lorentz local field correction factor".

Using the relation $\varepsilon(\omega) - 1 = 4\pi L(\omega)\chi^{\mathcal{L}}(\omega)$ with $\phi = 4\pi/3$ in Equation (D.2) one finds

Reproduced with permission of the copyright owner. Further reproduction prohibited without permission.

$$L(\omega) = \frac{\varepsilon(\omega)+2}{3} = \frac{n^2(\omega)+2}{3} \tag{D.3}$$

Hence the n^{th} order macroscopic nonlinear polarization with which we have been dealing in the text would presumably be written in the form

$$\underline{P}_n^{NL}(\omega) = L(\omega_1)\cdots L(\omega_n)\ \underline{\underline{\chi}}_n^{\mathcal{L}}(-\omega,\omega_1,\omega_2,\cdots,\omega_n):\underline{E}(\omega_1)\cdots\underline{E}(\omega_n) \tag{D.4}$$

Here the local field factors which are usually lumped into the definition of the nonlinear susceptibility tensor $\underline{\underline{\chi}}_n$ have been factored out and another nonlinear susceptibility tensor $\underline{\underline{\chi}}_n^{\mathcal{L}}$ defined which is essentially the nonlinear susceptibility which we have been modeling in Chapter IV since it <u>excludes</u> local field effects, i.e., $\phi = 0$. The colon ":" in Equation (D.4) is used to denote the dot products of the n field components $\underline{E}(\omega_i)$ with the n^{th} order nonlinear susceptibility tensor.

Although the nonlinear polarization given by Equation (D.4) appears to be that which we would substitute into Equation (3.3) as a nonlinear source term, this would be incorrect. To see this we write the total macroscopic polarization in the form

$$\underline{P}(\omega) = \underline{\underline{\chi}}^{\mathcal{L}}(\omega)\ \underline{E}_{\mathcal{L}}(\omega) + \underline{P}^{NL}(\omega) \tag{D.5}$$

where the local field $\underline{E}_{\mathcal{L}}(\omega) = \underline{E}(\omega) + \phi\underline{P}(\omega)$ and $\underline{P}^{NL}(\omega)$ is composed of terms of the form given in Equation (D.4). Substituting the local field into Equation (D.5) and solving for $\underline{P}(\omega)$ one finds that

$$\underline{P}(\omega) = L(\omega)\ \underline{\underline{\chi}}^{\mathcal{L}}(\omega)\ \underline{E}(\omega) + L(\omega)\ \underline{P}^{NL}(\omega) \tag{D.6}$$

Reproduced with permission of the copyright owner. Further reproduction prohibited without permission.

where $\underline{P}^{NL}(\omega)$ is given by the expression of Equation (D.4). From this relation it is clear that Equation (D.4) does not give the nonlinear susceptibility which is fully corrected for local fields, but that the true macroscopic nonlinear susceptibility must include an "extra" local field correction at the frequency ω. Hence the total polarization may be written in the form

$$\underline{P}(\omega) = \underline{\chi}(\omega)\cdot\underline{E}(\omega) + \sum_{n=2}^{\infty} \underline{\chi}_n(-\omega,\omega_1,\omega_2,\cdots,\omega_n):\underline{E}(\omega_1)\cdots\underline{E}(\omega_n) \qquad (D.7)$$

where $\underline{\chi}(\omega) = L(\omega)\underline{\chi}^{\mathscr{L}}(\omega)$ and

$$\underline{\chi}_n(-\omega,\omega_1,\omega_2,\cdots,\omega_n) = L(\omega)L(\omega_1)L(\omega_2)\cdots L(\omega_n)\underline{\chi}_n^{\mathscr{L}}(-\omega,\omega_1,\cdots,\omega_n)$$

for $n = 1,2,3,\cdots$.

Reproduced with permission of the copyright owner. Further reproduction prohibited without permission.

APPENDIX E

Dispersion Corrections for Electronic Nonlinearities

It will be recalled that in Section 4.1, the electronic portion of the nonlinear susceptibility was shown to take the form

$$\chi_{3e}^{ijk\ell}(-\omega,\omega_1,\omega_2,\omega_3) = \frac{-dm}{3N^3e^4}\chi(\omega)\chi(\omega_1)\chi(\omega_2)\chi(\omega_3)[\delta_{ij}\delta_{k\ell}+\delta_{i\ell}\delta_{jk}+\delta_{ik}\delta_{j\ell}] \tag{E.1}$$

which we choose to approximate by employing the dispersionless estimate

$$\chi(\omega)\chi(\omega_1)\chi(\omega_2)\chi(\omega_3) \approx \chi^4(\bar{\omega}) \tag{E.2}$$

for some mean value $\bar{\omega}$ of the frequencies involved in the mixing process.

In order to estimate the degree of dispersive error which might be expected to arise from the various frequency components used in the different experimental investigations, we may calculate the factor of Equation (E.2) for each case of experimental interest, assuming a purely electronic nonlinearity. Since $\chi(\omega) = (n^2(\omega)-1)/4\pi$, we need only to compare the dispersive effects of the factor

$$N \equiv \{n^2(\omega)-1\}\prod_{i=1}^{3}\{n^2(\omega_i)-1\} \tag{E.3}$$

Reproduced with permission of the copyright owner. Further reproduction prohibited without permission.

where the Π denotes a product of the terms in brackets which follow it.

It should be recalled that in addition to correcting for the dispersion on the nonlinear susceptibility a correction must also be made for local fields. This involves a factor of

$$L \equiv L(\omega_1)L(\omega_2)L(\omega_3)L(\omega)$$

where

$$L(\omega_i) = \frac{n^2(\omega_i) + 2}{3}$$

In Table E.1 we have tabulated the refractive indices for fused quartz and BK-7 glass at all wavelengths which are applicable to available experimental determinations. In Table E.2 the factor $81\,NL$ is tabulated for each case in which data is available for χ_3^{ijkl} in these media. Clearly the dispersion corrections are small enough to be negligible in all cases.

Reproduced with permission of the copyright owner. Further reproduction prohibited without permission.

TABLE E.1

Material	Fused Quartz Suprasil	BK-7 Schott Glass
λ (Å)		
3533	1.476	1.519
5300	1.46	
5490	1.46	
6500	1.457	
6943	1.455	1.513
7460	1.454	
9750	1.451	
1060	1.45	1.507

Reproduced with permission of the copyright owner. Further reproduction prohibited without permission.

TABLE E.2

Experiment	$81NL$ for Fused Quartz Suprasil	$81NL$ for BK-7 Schott Glass
Third Harmonic Generation $\lambda=1.06\mu$	453	
Ellipse Rotation $\lambda=6943\text{Å}$	448	936
a.c. Kerr Effect $\lambda_1=1.06\mu$ $\lambda_2=5300\text{Å}$	444	930
Three Wave Mixing $\lambda=6943\text{Å}$ $\Delta=992\text{cm}^{-1}$	451	
Three Wave Mixing $\lambda=6943\text{Å}$ $\Delta=4,150\ \text{cm}^{-1}$	445	

Reproduced with permission of the copyright owner. Further reproduction prohibited without permission.

APPENDIX F

The Polarizability Tensor $\underline{\alpha}(\theta,\phi)$

In Section 4.2.1 we considered a molecule whose polarizability tensor in its principal coordinate system was given by

$$\underline{\alpha} = \begin{pmatrix} \alpha_1 & 0 & 0 \\ 0 & \alpha_1 & 0 \\ 0 & 0 & \alpha_2 \end{pmatrix} \tag{F.1}$$

and is diagrammatically represented in Figure 4.1. Using the rotation matrix[4]

$$\underline{A} = \begin{pmatrix} -\cos\psi\sin\phi-\cos\theta\cos\phi\sin\psi & \cos\psi\cos\phi-\cos\theta\sin\phi\sin\psi & \sin\psi\sin\theta \\ \sin\psi\sin\phi-\cos\theta\cos\phi\cos\psi & -\sin\psi\cos\phi-\cos\theta\sin\phi\cos\psi & \cos\psi\sin\theta \\ \sin\theta\cos\phi & \sin\theta\sin\phi & \cos\theta \end{pmatrix} \tag{F.2}$$

where $\phi+\frac{\pi}{2}$, θ, and ψ are the Euler angles,† we find that $\underline{\alpha}$ may be written for a molecule oriented as shown in Figure 4.1. This gives

$$\underline{\alpha}(\theta,\phi) = \underline{A}^t\cdot\underline{\alpha}\cdot\underline{A} =$$

$$\begin{pmatrix} \alpha_1+(\alpha_2-\alpha_1)\sin^2\theta\cos^2\phi & (\alpha_2-\alpha_1)\sin^2\theta\sin\phi\cos\phi & (\alpha_2-\alpha_1)\cos\theta\sin\theta\cos\phi \\ (\alpha_2-\alpha_1)\sin^2\theta\sin\phi\cos\phi & \alpha_1+(\alpha_2-\alpha_1)\sin^2\theta\sin^2\phi & (\alpha_2-\alpha_1)\cos\theta\sin\theta\sin\phi \\ (\alpha_2-\alpha_1)\sin\theta\cos\theta\cos\phi & (\alpha_2-\alpha_1)\sin\theta\cos\theta\sin\phi & \alpha_1+(\alpha_2-\alpha_1)\cos^2\theta \end{pmatrix} \tag{F.3}$$

Here $\underline{A}^t$ is the transpose of $\underline{A}$ and the resultant polarizability is independent of ψ since $\underline{\alpha}$ is symmetric with respect to its x and y principal axes.

†This unusual definition of the Euler angles is chosen so that θ and ϕ correspond to the azimuthal and polar angles shown in Figure 4.1.

Reproduced with permission of the copyright owner. Further reproduction prohibited without permission.

When the molecules are randomly oriented in a medium, the total system will exhibit a polarizability per unit volume which is proportional to the orientationally averaged single molecule polarizability. Performing this average for a randomly oriented system of molecules we find that

$$\underline{\bar{\alpha}} = \frac{1}{4\pi} \int \underline{\alpha}(\theta,\phi)\, d\Theta = \begin{pmatrix} \alpha & 0 & 0 \\ 0 & \alpha & 0 \\ 0 & 0 & \alpha \end{pmatrix} \tag{F.4}$$

Here the integration is taken over the entire sphere of solid angles Θ and the average polarizability $\alpha = (\alpha_2 + 2\alpha_1)/3$. It is to be noted here that Trace $(\underline{\alpha})$ remains invariant as it must under a rotational operation. As expected the averaging operation reduces $\underline{\alpha}$ to a scalar since the medium of molecules is macroscopically isotropic.

Another useful average for the molecule of Equation (F.1) is the quantity $\overline{\alpha_{ij}\Theta\,\alpha_{k\ell}(\Theta)}$, for this average determines the value of the nonlinear susceptibility and response tensor; see Equation (4.21) for the case of molecular reorientation. One would expect that since the tensor is modelling the nonlinear response in an <u>isotropic</u> medium, it may be characterized by a maximum of three independent tensor elements. Indeed, performing the averages, it is found that

$$\overline{\alpha_{ij}\alpha_{k\ell}} = \begin{cases} \frac{4}{45}(\alpha_2-\alpha_1)^2 + \alpha^2 & \text{for } i=j=k=\ell \\ \alpha^2 - \frac{2}{45}(\alpha_2-\alpha_1)^2 & \text{for } i=j\neq k=\ell \\ \frac{(\alpha_2-\alpha_1)^2}{15} & \text{for } i=k\neq j=\ell \\ & \text{or } i=\ell\neq j=k \end{cases} \tag{F.5}$$

Thus we may write these results in the form

Reproduced with permission of the copyright owner. Further reproduction prohibited without permission.

$$\overline{\alpha_{ij}\alpha_{k\ell}} - \alpha^2\delta_{ij}\delta_{k\ell} = \frac{2}{45}(\alpha_2-\alpha_1)^2\{\frac{3}{2}(\delta_{ik}\delta_{j\ell}+\delta_{i\ell}\delta_{jk})-\delta_{ij}\delta_{k\ell}\} \quad \text{(F.6)}$$

Both $\overline{\alpha_{ij}}$ and $\overline{\alpha_{ij}\alpha_{k\ell}}$ are considered for the more general case where

$$\underline{\alpha} = \begin{pmatrix} \alpha_1 & 0 & 0 \\ 0 & \alpha_2 & 0 \\ 0 & 0 & \alpha_3 \end{pmatrix} \quad \text{(F.7)}$$

in the book by Wilson, Decius, and Cross.[15] Our results may be generalized to this case by replacing our α by $\alpha = (1/3)(\alpha_1+\alpha_2+\alpha_3)$ and our $(\alpha_2-\alpha_1)^2$ by $(1/2)\{(\alpha_1-\alpha_2)^2+(\alpha_2-\alpha_3)^2+(\alpha_1-\alpha_3)^2\}$.

Reproduced with permission of the copyright owner. Further reproduction prohibited without permission.

APPENDIX G

The Distribution Function for Molecular Reorientation

In Section (4.2.1) we showed that the distribution function $\tilde{f}(t)$, which describes the orientational distribution of an ensemble of polarizable cigar shaped molecules as described by Equation (4.13) obeys the relation (Equation (4.18))

$$\frac{\zeta}{kT}\frac{\partial \tilde{f}}{\partial t} = \frac{1}{\sin\theta}\frac{\partial}{\partial\theta}\left\{\sin\theta\frac{\partial \tilde{f}}{\partial\theta} + \tilde{f}\frac{(\alpha_2 - \alpha_1)\tilde{E}^2(r,t)\sin 2\theta}{2kT}\right\} \quad (G.1)$$

for a field polarized along the z axis.

We shall undertake the solution of this equation in two steps. First we shall consider the case of an applied d.c. field which is shut off at $t = 0$. This will establish the concept of the relaxation time of the system and give us a general form for a trial solution for the case where $\tilde{E}(r,t)$ varies arbitrarily in time.

Consider a field of the form

$$\tilde{E}(t) = \begin{cases} E_0 & t < 0 \\ 0 & t \geq 0 \end{cases} \quad (G.2)$$

where $\tilde{E}(t)$ is directed along the z axis. For $t < 0$ we know that the system must take on a Maxwell-Boltzman distribution, hence

$$f = \frac{e^{-U/kT}}{\int e^{-U/kT} d\Omega} , \quad (G.3)$$

Reproduced with permission of the copyright owner. Further reproduction prohibited without permission.

$$= \frac{\exp\{\frac{1}{2kT}((\alpha_2-\alpha_1)\cos^2\theta+\alpha_1)E_o^2\}}{\int\exp\{\frac{1}{2kT}((\alpha_2-\alpha_1)\cos^2\theta+\alpha_1)E_o^2\}d\Omega}$$

$$\simeq \frac{1+\frac{1}{2kT}\{(\alpha_2-\alpha_1)\cos^2\theta+\alpha \quad E_o^2+\ldots\}}{4\pi(1+\frac{1}{6kT}(\alpha_2-\alpha_1)E_o^2+\ldots)}$$

$$\simeq \frac{1}{4\pi}+\frac{(\alpha_2-\alpha_1)E_o^2(\cos^2\theta-1/3)}{8\pi kT}+\ldots$$

Here we have used the relation $U = -(1/2)\alpha_{zz}(\theta)E_z^2$ from Equations (4.14) and (4.16). The dropping of all higher order terms is justified since α is typically of the order 10^{-23} cm^3 so that even for a power density of 10^{10} W/cm^2 ($E^2 = 8.4 \times 10^7$ esu) we have $\alpha|E|^2/kT \simeq 10^{-2}$ at 300°K. This power density is well above the optical breakdown intensity for liquids and is typical for breakdown in glasses. It is also to be noted that the factor "1/3" in the second term is maintained so that the normalization $\int\bar{f}d\Omega = 1$ is preserved.

For $t \geq 0$ Equation (G.1) becomes

$$\frac{\zeta}{kT}\frac{\partial\bar{f}}{\partial t} = \frac{1}{\sin\theta}\frac{\partial}{\partial\theta}\{\sin\theta(\frac{\partial\bar{f}}{\partial\theta})\} \qquad (G.4)$$

Since $\bar{f}(t=0)$ must match the Maxwell-Boltzman distribution of Equation (G.3) we choose a trial solution of the form

Reproduced with permission of the copyright owner. Further reproduction prohibited without permission.

$$\tilde{f}(t) = \tilde{A}(t) + \tilde{B}(t)\cos^2\theta \tag{G.5}$$

which, when substituted into Equation (G.4), yields

$$\frac{\zeta}{kT}\left(\frac{\partial\tilde{A}}{\partial t} + \frac{\partial\tilde{B}}{\partial t}\cos^2\theta\right) = -6\,\tilde{B}(t)\cos^2\theta + 2\tilde{B}(t) \tag{G.6}$$

By matching the angular varying terms of Equation (G.6) we find the two conditions:

$$\frac{\partial\tilde{A}}{\partial t} = \frac{2kT}{\zeta}\tilde{B}(t) \tag{G.7}$$

and

$$\frac{\partial\tilde{B}}{\partial t} = -\frac{6kT}{\zeta}\tilde{B}(t) \tag{G.8}$$

Solving Equations (G.7) and (G.8) $\tilde{f}$ is found to take on the form

$$\tilde{f}(t) = (Ce^{-t/\tau_R} + D)\cos^2\theta - \frac{C}{3}e^{-t/\tau_R} + \frac{D}{3\tau_R}t + F \tag{G.9}$$

Here C, D, and F are constants and the orientational relaxation time τ_R is given by

$$\tau_R = \frac{\tau_D}{3} = \frac{\zeta}{6kT}$$

where τ_D is the Debye relaxation time.[5] As t becomes very large we must have an isotropic distribution. Thus D = 0. Matching the initial conditions we find the solution

Reproduced with permission of the copyright owner. Further reproduction prohibited without permission.

$$\tilde{f}(t) = \frac{1}{4\pi} + \frac{(\alpha_2-\alpha_1)E^2}{8\pi kT} \left(\cos^2\theta - \frac{1}{3}\right) e^{-t/\tau_R} \qquad (G.10)$$

Thus the distribution function is seen to decay exponentially to a uniform distribution with a characteristic time $\tau_R = \zeta/6kT$.

The form of Equation (G.10) suggests that we adopt a trial solution of the form

$$\tilde{f}(t) = A\{1 + \beta(\cos^2\theta - \tfrac{1}{3})\tilde{\Phi}(t)\} \qquad (G.11)$$

in considering the solution of Equation (G.1) for the more general case of an arbitrary but linearly polarized $\tilde{E}(t)$. Substituting Equation (G.11) into Equation (G.1) we obtain,

$$6\tau_T A\{\beta(\cos^2\theta - \tfrac{1}{3})\Phi'(t)\} = \frac{1}{\sin\theta}\frac{\partial}{\partial\theta}\{\beta A\tilde{\Phi}(t)\sin\theta\sin(2\theta) + \beta\phi E^2 A \sin(2\theta)\{1+\beta(\cos^2\theta - \tfrac{1}{3})\tilde{\Phi}(t)\}\}$$

where $\beta \equiv (kT)^{-1}$ and $\phi \equiv (\alpha_2-\alpha_1)/2$ (G.12)

Expanding Equation (G.12), employing several trigonometric identities, and keeping terms up to first order in $\beta = (kT)^{-1}$ we find that Equation (G.12) reduces to the simple form

$$\tilde{\Phi}'(t) = -\frac{\tilde{\Phi}(t)}{\tau_R} + \phi\frac{\tilde{E}^2(t)}{\tau_R} \qquad (G.13)$$

Clearly the problem of solving for $\tilde{f}$ has been reduced to the form of a first order linear equation for $\tilde{\Phi}(t)$. Writing $\tilde{\Phi}(t)$ in the form of

Reproduced with permission of the copyright owner. Further reproduction prohibited without permission.

a convolution and substituting into Equation (G.11) we find that

$$\tilde{f}(t) = \frac{1}{4\pi}\left\{1 + \left(\frac{\alpha_2-\alpha_1}{2kT}\right)\left(\cos^2\theta - \frac{1}{3}\right)\int_{-\infty}^{t} \frac{\tilde{E}^2(\tau)}{\tau_R} e^{\frac{\tau-t}{\tau_R}} d\tau \right\} \quad (G.14)$$

This solution for a linearly polarized field $\tilde{E}(t)$ is clearly seen to take the form of a uniform distribution $f = \frac{1}{4\pi}$ which is perturbed by an anisotropic term which takes on the form of a linear response function driven by the force $\tilde{E}^2(t)$. It is easily seen that for $\tilde{E}(t)$ = constant the solution reduces to the approximate Maxwell-Boltzmann equilibrium distribution given in Equation (G.3). For an arbitrary linearly polarized $\tilde{E}(t)$ the system is seen to average out oscillations in $\tilde{E}^2(t)$ which are faster than the response time τ_R, but respond readily to slower oscillations. It is this reorientational relaxation mechanism which is responsible for the phenomenon of Rayleigh wing scattering of light.[6] See Appendix H .

It is clear that Equation (G.14) must represent the solution for $\tilde{f}(t)$ for any linearly polarized field since the medium is isotropic and thus the form of $\tilde{f}(t)$ should be independent of the orientation of the medium (or the coordinate system). Examining the d.c. case given by Equation (G.3) we recognize that $\tilde{f}$ may be written in the form

$$\tilde{f} = \frac{1}{4\pi}\left\{1 - \frac{U(\theta) - \overline{U(\theta)}}{kT}\right\} \quad (G.15)$$

Reproduced with permission of the copyright owner. Further reproduction prohibited without permission.

where the "bar" denotes an orientational average. For the a.c. case given in Equation (G.14), this expression is virtually unchanged except that now $U(\Theta) = -\frac{1}{2}\alpha_{zz}E_z^2$ is replaced by,

$$\langle\tilde{U}(\Theta)\rangle = -\frac{\alpha_{zz}}{2}\int_{-\infty}^{t}\frac{\tilde{E}_z^2(t)}{\tau_R}e^{\frac{\tau-t}{\tau_R}}d\tau \qquad (G.16)$$

which, for the specific case of a monochromatic optical field, is seen to be the time averaged energy. Since this quantity must clearly be independent of the direction of $\tilde{E}(t)$, we may write $\langle\tilde{U}(\Theta)\rangle$ in the form

$$\langle\tilde{U}(\Theta)\rangle = -\frac{\alpha^{ij}(\Theta)}{2}\int_{-\infty}^{t}\frac{\tilde{E}_i(\tau)\tilde{E}_j(\tau)}{\tau_R}e^{\frac{\tau-t}{\tau_R}}d\tau \qquad (G.17)$$

where $\alpha^{ij}(\Theta)$ is given in Equation (4.14) and we sum over the repeated indices i and j. Thus for any linearly polarized wave we would expect that

$$\tilde{f}(\Theta,t) = \frac{1}{4\pi}\left\{1 - \frac{\alpha^{ij}(\Theta) - \overline{\alpha^{ij}(\Theta)}}{2kT}\int_{-\infty}^{\infty}\tilde{E}_i(\tau)\tilde{E}_j(\tau)\tilde{\rho}(t-\tau)d\tau\right\} \qquad (G.18)$$

where

$$\tilde{\rho}(t) = \begin{cases} \frac{e^{-t/\tau_R}}{\tau_R} & t > 0 \\ 0 & t \leq 0 \end{cases} \qquad (G.19)$$

Reproduced with permission of the copyright owner. Further reproduction prohibited without permission.

The solution in Equation (G.18) was derived for a linearly polarized wave of arbitrary time dependence and direction of polarization. We would argue, however, that this solution is valid for a field whose direction of polarization varies in time. To see this on physical grounds we simply recognize that a reorientational nonlinearity is dependent upon the induced alignment of molecules along the direction of the applied field and that the time constant associated with this process is not dependent upon whether or not there is a change in the direction of the field. This may be shown mathematically by constructing the input field in the form of a step function series of vectors which sum to yield a continuously varying vector field $\underset{\sim}{\tilde{E}}(t)$ in the limit where the interval between the steps is vanishingly small. Since the solution for $\tilde{\Phi} \propto (\tilde{f} - \frac{1}{4\pi})$ involves the solution of a linear equation, the results for each step interval in the field may be added to obtain the total solution for $\tilde{\Phi}(t)$. This step function representation of $\underset{\sim}{\tilde{E}}(t)$ and the resulting series solution is seen to be independent of the direction of $\underset{\sim}{\tilde{E}}(t)$ since $\langle \tilde{U}(0) \rangle$ is independent of the direction of $\underset{\sim}{\tilde{E}}(t)$ in Equation (G.17). Thus Equation (G.18) is seen to be generally applicable to a field which varies in direction as well as amplitude.

Reproduced with permission of the copyright owner. Further reproduction prohibited without permission.

APPENDIX H

Stimulated Scattering of Light and the Polarization Properties of $\tilde{\underline{P}}_3(t)$

H.0 Stimulated Light Scattering Processes

It has been demonstrated in Chapter IV that any isotropic medium exhibits a nonlinear polarization cubic in the electric field strength which may be written in the form

$$\tilde{\underline{P}}_3(t) = \sigma\tilde{\underline{E}}(t)\cdot\tilde{\underline{E}}(t)\tilde{\underline{E}}(t) + \int \tilde{a}(t-\tau)\tilde{\underline{E}}(\tau)\cdot\tilde{\underline{E}}(\tau)\,d\tau\ \tilde{\underline{E}}(t) + \int \tilde{b}(t-\tau)\tilde{\underline{E}}(\tau)\cdot\tilde{\underline{E}}(\tau)\cdot\tilde{\underline{E}}(t)\tilde{\underline{E}}(\tau)\ d\tau \qquad (H.1)$$

where σ is the parameter of electronic distortion and $\tilde{a}(t)$ and $\tilde{b}(t)$ characterize the nuclear nonlinearity. Thus far in this work we have been dealing with nonlinear interactions which involve sum and difference frequencies which are either very large or very small compared to the molecular vibrational resonances of the medium. This has permitted us to assume that $a(\omega)$ and $b(\omega)$ take on real values in the experimental studies which have been considered.[7] In this section we shall extend our consideration of nonlinear processes to include the cases in which $a(\omega)$ and $b(\omega)$ are complex valued and hence result in an induced gain (or loss) in the nonlinear medium. This gain results in what is commonly known as the "stimulated scattering of light".[8] Physically such a process involves the coupling of a strong electromagnetic wave onto the molecular vibrations of the

Reproduced with permission of the copyright owner. Further reproduction prohibited without permission.

medium which in turn couple energy back into a wave at a different frequency and result in gain. In Section H.1 we shall use the model of Equation (H.1) to examine the dependence of both stimulated scattering of light and induced refractive index changes on the polarization and frequency separation of the incident fields involved in the interaction.

In order to assess the role of $\tilde{\underline{P}}_3(t)$ in the processes described above we again employ Maxwell's equations to arrive at the wave equation (Equation (3.3))

$$\nabla^2 \underline{E}'_\omega(\underline{r}) + \frac{\omega^2 n^2(\omega)}{c^2} \underline{E}'_\omega(\underline{r}) = -\frac{4\pi\omega^2}{c^2} \underline{P}'_{3,\omega}(\underline{r}) \tag{H.2}$$

Since the primary interest is now in light scattering processes and induced changes in refractive index, we choose to write the field in the form of two monochromatic components; thus,

$$\tilde{\underline{E}}(t) = \mathrm{Re}\left\{\underline{E}_\Omega\, e^{i(\underline{K}\cdot\underline{r}-\Omega t)} + \underline{E}_\omega\, e^{i(\underline{k}\cdot\underline{r}-\omega t)}\right\} \tag{H.3}$$

Employing Equation (H.3) in Equation (2.20) we find that $\underline{P}_{3,\omega}(\underline{r})$ may be written symbolically in the form

$$\underline{P}_{3,\omega}(\underline{r}) = 6\underline{\underline{\underline{\chi}}}_3(-\omega,\omega,\Omega,-\Omega) \vdots \underline{E}_\omega \underline{E}_\Omega \underline{E}^*_\Omega \tag{H.4}$$

Here $\underline{\underline{\underline{\chi}}}_3(-\omega,\omega,\Omega,-\Omega)$ is the fourth rank tensor whose components are $\chi_3^{ijk\ell}(-\omega,\omega,\Omega,-\Omega)$ and the three dots indicate that the dot product is taken between the fields and the susceptibility tensor $\underline{\underline{\underline{\chi}}}_3$. Substituting Equations (H.3) and (H.4) into Equation (H.2) we may solve for $k^2(\omega)$ to find that

Reproduced with permission of the copyright owner. Further reproduction prohibited without permission.

$$k^2(\omega) = \frac{\omega^2 n^2(\omega)}{c^2}\left\{1 + \frac{24\pi}{n^2}\,\hat{e}^*_\omega \cdot \underline{\chi}_3(-\omega,\omega,\Omega,-\Omega) : \hat{e}_\omega \underline{E}_\Omega \underline{E}^*_\Omega\right\} \qquad (H.5)$$

where $\hat{e}_\omega = \underline{E}_\omega / |\underline{E}_\omega|$ is the unit vector specifying the polarization of $\underline{E}_\omega$.

Assuming that the nonlinearity is small, we may expand Equation (H.5) to find that the nonlinearity produces a real index change at frequency ω which is given by

$$\delta n(\omega) = \frac{12\pi}{n(\omega)}\,\hat{e}^*_\omega \cdot \underline{\chi}'_3 : \hat{e}_\omega \underline{E}_\Omega \underline{E}^*_\Omega \qquad (H.6)$$

and an intensity gain corresponding to an imaginary index change

$$g(\omega) = \frac{-24\pi\omega}{cn(\omega)}\,\hat{e}^*_\omega \cdot \underline{\chi}''_3 : \hat{e}_\omega \underline{E}_\Omega \underline{E}^*_\Omega \qquad (H.7)$$

Here $\underline{\chi}'_3$ and $\underline{\chi}''_3$ are the real and imaginary parts of the nonlinear susceptibility tensor $\underline{\chi}_3$ and $g(\omega)$ is defined by the relation

$$|\underline{E}_\omega|^2 = |\underline{E}_\omega|^2_{z=0}\, e^{gz} \qquad (H.8)$$

for a wave vector $\underline{k}$ along the z axis.

It is noteworthy to recognize that Equation (H.5) yields the exact solution for $k^2(\omega)$ and the induced index change whereas Equation (H.6) gives the same estimate which was obtained through Equations (3.5) and (3.20). The gain (or loss) defined by Equations (H.7) and (H.8) forms the basis for stimulated light scattering processes.[6,8]

Both the induced refractive index change and the induced gain are functions of $\Delta = \Omega - \omega$ and of the polarization properties of $\underline{E}_\Omega$ and $\underline{E}_\omega$. In Section H.1 we shall consider this polarization and the

Reproduced with permission of the copyright owner. Further reproduction prohibited without permission.

frequency dependence as it is determined by the model of Equation (H.1).

H.1 The Dispersion and Polarization Properties of $\tilde{P}_3(t)$

Since the nonlinear polarization cubic in the electric field strength is characterized by Equation (H.1) we would expect that this relation along with the physical models of Chapter IV which yield specific forms for σ , $\tilde{a}(t)$ and $\tilde{b}(t)$ would completely determine the manner in which the medium would react to the field of Equation (H.3). Since the medium is assumed to be isotropic, the third order nonlinear polarization is specified by the three susceptibility tensor elements χ_3^{1122}, χ_3^{1221}, and χ_3^{1212}, which may be shown through Equation (5.6) to be given by

$$\chi_3^{1122}(-\omega,\omega,\Omega,-\Omega) = \frac{1}{24}\,(\sigma + 2\alpha + b(-\Delta)) \tag{H.9}$$

$$\chi_3^{1221}(-\omega,\omega,\Omega,-\Omega) = \frac{1}{24}\,(\sigma + \beta + b(-\Delta)) \tag{H.10}$$

$$\chi_3^{1212}(-\omega,\omega,\Omega,-\Omega) = \frac{1}{24}\,(\sigma + 2a(-\Delta) + \beta) \tag{H.11}$$

where, in contrast to Table 5.1, we have retained the nuclear terms of frequency $-\Delta = \omega - \Omega$, but again dropped optical terms of higher frequency.

Substitution of Equations (H.9) through (H.11) into Equations (H.6) and (H.7) characterizes the polarization properties for induced gain and refractive index changes. The results of this substitution have been tabulated for four special cases in Table H.1: (1) $\underline{E}_\Omega$ linearly polarized with $\underline{E}_\omega \| \underline{E}_\Omega$, (2) $\underline{E}_\Omega$ linearly polarized with $\underline{E}_\omega \perp \underline{E}_\Omega$, (3) $\underline{E}_\Omega$ circularly polarized with $\underline{E}_\omega$ circularly polarized in the same direction, and (4) $\underline{E}_\Omega$ circularly polarized with $\underline{E}_\omega$

Reproduced with permission of the copyright owner. Further reproduction prohibited without permission.

Reproduced with permission of the copyright owner. Further reproduction prohibited without permission.

	$\frac{\delta\chi(\omega)}{\lvert\underline{E}_\Omega\rvert^2}$	$g(\omega) \times \frac{cn(\omega)}{4\pi\omega\lvert\underline{E}_\Omega\rvert^2}$	$\delta n(\omega) \times \frac{n(\omega)}{2\pi\lvert\underline{E}_\Omega\rvert^2}$
$\underline{E}_\Omega \parallel \underline{E}_\omega$ Linearly Polarized	$6\chi_3^{1111}(-\omega,\omega,\Omega,-\Omega)$	$-\frac{1}{12}\{a''(-\Delta)+b''(-\Delta)\}$	$\frac{1}{24}\{3\sigma+2(\alpha+\beta)+2(a'(-\Delta)+b'(-\Delta))\}$
$\underline{E}_\Omega \perp \underline{E}_\omega$ Linearly Polarized	$6\chi_3^{1122}(-\omega,\omega,\Omega,-\Omega)$	$\frac{-b''(-\Delta)}{24}$	$\frac{1}{24}\{\sigma+2\alpha+b'(-\Delta)\}$
$\underline{E}_\Omega$ same as $\underline{E}_\omega$ Circularly Polarized	$6\chi_3^{1122}(-\omega,\omega,\Omega,-\Omega)+6\chi_3^{1212}(-\omega,\omega,\Omega,-\Omega)$	$-\frac{1}{24}\{2a''(-\Delta)+b''(-\Delta)\}$	$\frac{1}{24}\{2\sigma+2\alpha+\beta+2a'(-\Delta)+b'(-\Delta)\}$
$\underline{E}_\Omega$ opposite $\underline{E}_\omega$ Circularly Polarized	$6\chi_3^{1122}(-\omega,\omega,\Omega,-\Omega)+6\chi_3^{1221}(-\omega,\omega,\Omega,-\Omega)$	$\frac{-b''(-\Delta)}{12}$	$\frac{1}{24}\{2\sigma+2\alpha+\beta+2b'(-\Delta)\}$

TABLE H.1

$a(\Delta) = a'(\Delta) + ia''(\Delta)$ $\quad b(\Delta) = b'(\Delta) + ib''(\Delta)$

circularly polarized in the opposite direction.

In examining the table, it is difficult to obtain a full understanding of the gain and refractive index change relations independently of the specific forms of $a(-\Delta)$ and $b(-\Delta)$ for the various nuclear rearrangement mechanisms. Hence these forms already given in Chapter IV are again tabulated in Table H.2 in terms of the real and imaginary parts of $a(\Delta)$ and $b(\Delta)$ for each mechanism.

Clearly many conclusions may be drawn from Tables H.1 and H.2 concerning the polarization and spectral behavior of the induced refractive index changes and induced gain which are a result of each of the mechanisms. We shall not discuss all of the implications of these results but rather note several interesting and important consequences of these results.

Firstly, we note that σ , $\alpha = a(0)$ and $\beta = b(0)$ are all real quantities. Hence the gain is always zero for $\Delta = 0$.[9] It is also interesting to note that the gain function obeys the same symmetry restrictions held by the spontaneous light scattering cross section. For example, in the common case of "depolarized scattering"[+] it is noted that the ratio of spontaneous light scattering intensities polarized parallel and perpendicular to the input polarization respectively is given by $I_{||}/I_{\perp} = 4/3$. Indeed we see that for this case $\tilde{b}(t) = -3\tilde{a}(t)$ and thus $g_{||}/g_{\perp} = 4/3$. It will be shown in Appendix I that the induced gain functions bear a proportionality relationship to the spontaneous light scattering cross sections. This suggests the

[+]Scattering is depolarized if (in a plane perpendicular to the input polarization) the light scattered parallel to the input polarization I_{μ} divided by the light scattered perpendicular to the input polarization attains its maximum possible value, 4/3.

Reproduced with permission of the copyright owner. Further reproduction prohibited without permission.

Reproduced with permission of the copyright owner. Further reproduction prohibited without permission.

	Stimulated Scattering Process	$a(\Delta) = a'(\Delta) + ia''(\Delta)$	$b(\Delta) = b'(\Delta) + ib''(\Delta)$
Reorientation	Stimulated Rayleigh Wing Scattering	$\frac{-N(\alpha_2-\alpha_1)^2}{45(1+\Delta^2\tau_R^2)}(1+i\Delta\tau_R)$	$\frac{N(\alpha_2-\alpha_1)^2}{15(1+\Delta^2\tau_R^2)}(1+i\Delta\tau_R)$
Raman Effect	Stimulated Raman Scattering	$\frac{N(45\xi^2-2\psi^2)}{90\mu((\Omega_o^2-\Delta^2)^2+\Delta^2\Gamma^2)}(\Omega_o^2-\Delta^2+i\Delta\Gamma)$	$\frac{3N\psi^2}{45\mu((\Omega_o^2-\Delta^2)^2+\Delta^2\Gamma^2)} \times (\Omega_o^2-\Delta^2+i\Delta\Gamma)$
Libration	Stimulated Librational Scattering	$-\frac{2N(\alpha_2-\alpha_1)^2}{15((G-I\Delta^2)^2+\Delta^2\Lambda^2)} \times (G-I\Delta^2+i\Delta\Lambda)$	$\frac{2N(\alpha_2-\alpha_1)^2}{5((G-I\Delta^2)^2+\Delta^2\Lambda^2)}(G-I\Delta^2+i\Delta\Lambda)$

TABLE H.2

ability to determine $a(\Delta)$ and $b(\Delta)$ through light scattering studies.

The cases of circular polarization in Table H.1 are of particular interest. Assuming $\tilde{b}(t) = -3\tilde{a}(t)$ it is seen that $g_{same}/g_{opp} = 1/6$. Consequently a circularly polarized "pump beam" will produce stimulated light scattering into a polarization which is circularly polarized in the opposite direction. This is in marked contrast to the linearly polarized case where the gain is highest in a direction parallel to that of the incident polarization.

Examining the real refractive index change induced by the circularly polarized wave we find that

$$\frac{n_{same}}{n_{opp}} = \frac{2\sigma + 2\alpha + \beta + 2a'(-\Delta) + b'(-\Delta)}{2\sigma + 2\alpha + \beta + 2b'(-\Delta)} \qquad \text{(H.12)}$$

Hence in contrast to the case of the perpendicularly polarized linear polarization case, the induced refractive index change is equal if the difference frequency $\Delta = \Omega - \omega$ is such that $a'(-\Delta)$ and $b'(-\Delta)$ are negligibly small compared to the other terms in Equation (H.12). This suggests the interesting possibility of measuring the nuclear contributions $a'(-\Delta)$ and $b'(-\Delta)$ as a function of Δ by performing an a.c. Kerr effect experiment with a circularly polarized Kerr field $\underline{E}_{\Omega}$ inducing the refractive index change. A linearly polarized probe field $\underline{E}_{\omega}$ will then experience no rotation in the absence of a contribution from $a'(-\Delta)$ and $b'(-\Delta)$, however, a rotation of the field will yield a direct measurement of the quantity $2a'(-\Delta) - b'(-\Delta)$.

It has already been shown for the case of two perpendicularly polarized plane waves that $\delta n_{\parallel} / \delta n_{\perp}$ is very much different for the two cases $\Delta = 0$ and $\Delta \neq 0$. Likewise for the case where $\Delta = 0$

Reproduced with permission of the copyright owner. Further reproduction prohibited without permission.

for two circularly polarized components

$$\frac{\delta n_{same}}{\delta n_{opp}} = \frac{\chi_3^{1122}(-\omega,\omega,\omega,-\omega) + \chi_3^{1212}(-\omega,\omega,\omega,-\omega)}{\chi^{1122}(-\omega,\omega,\omega,-\omega)+\chi_3^{1212}(-\omega,\omega,\omega,-\omega)+2\chi_3^{1221}(-\omega,\omega,\omega,-\omega)}$$

$$= \frac{\sigma + 2\alpha + \beta}{2\sigma + 2\alpha + 3\beta} \qquad \text{(H.13)}$$

which is clearly different from the result of Equation (H.12). This illustrates the importance of recognizing and keeping track of the terms which arise due to degeneracies in the field components when making calculations of induced gain and refractive index changes.

Reproduced with permission of the copyright owner. Further reproduction prohibited without permission.

APPENDIX I

Relating the Scattering Cross Section to the Nonlinear Polarization

I.0 Photon Representation of Light Scattering

In Appendix H we derived a classical expression for the gain which is induced in an isotropic medium by an intense optical field $\underline{E}$. The classical treatment was fully justified on the basis that the intense optical fields involved in the interaction assured that each radiation mode was well populated.[10] By employing this formalism to calculate the forward gain in the stimulated scattering of a linearly polarized beam $\underline{E}_\omega$ pumped by another linearly polarized beam $\underline{E}_\Omega$ which is polarized parallel to it, we find from Equation (H.7) that the intensity gain $g_{||}(\omega)$ may be written in the form

$$g_{||}(\omega) = \frac{-4\pi\omega}{cn(\omega)} \chi''_{R_{||}} |\underline{E}_\Omega|^2 \tag{I.1}$$

Here the imagi$g_{||}(\omega) = \frac{-4\pi\omega}{cn(\omega)} \chi''_{R_{||}} |\underline{E}_\Omega|^2$susceptibility $\chi''_{R_{||}}$ for scattering into this mode is given by $6\ \mathrm{Im}\{\chi_3^{1111}(-\omega,\omega,\Omega,-\Omega)\}$ and the Stokes shift Δ is $\Omega - \omega$. In fact it should be noted that this expression is valid not only for forward scattering in the direction of the pump beam, but for any direction in which the polarization of the scattered wave is parallel to that of the pump $\underline{E}_\Omega$, i.e., for $\underline{k}$ in the y-z plane of Figure I.1. Since the time averaged pump intensity I_Ω may be written as

$$I_\Omega = \frac{c\langle n_\Omega \rangle \hbar\Omega}{n(\Omega)V} = \frac{cn(\Omega)|\underline{E}_\Omega|^2}{8\pi} \tag{I.2}$$

Reproduced with permission of the copyright owner. Further reproduction prohibited without permission.

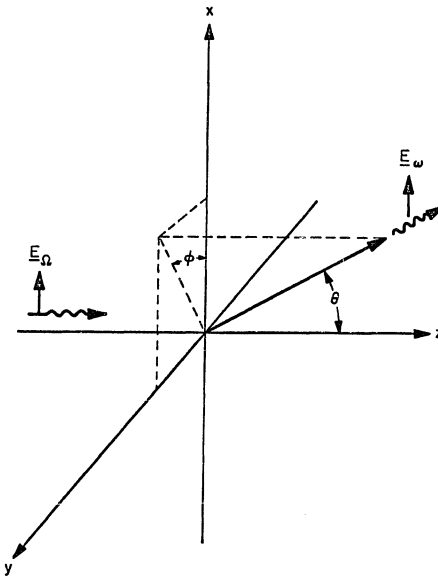

Figure I.1

Reproduced with permission of the copyright owner. Further reproduction prohibited without permission.

where $\langle n_\Omega \rangle$ is the number of incident photons in the mode volume V and $n(\Omega)$ is the refractive index at frequency Ω, we may express the gain in terms of the pump photon population and write

$$g_{||}(\omega) = \frac{-128\pi^4 \hbar c \langle n_\Omega \rangle \chi''_{R||}}{\lambda_\Omega \lambda_\omega n^2(\Omega)\, n(\omega)\, V} \tag{I.3}$$

where $\lambda_\omega = 2\pi c/\omega$. The growth equation for the Stokes intensity may then be written in the form

$$\frac{d\langle n_\omega \rangle}{dz} = \kappa_{\omega||} \langle n_\Omega \rangle \langle n_\omega \rangle \tag{I.4}$$

where

$$\kappa_{\omega||} = \frac{-128\pi^4 \hbar c \chi''_{R||}}{\lambda_\Omega \lambda_\omega n^2(\Omega)\, n(\omega)\, V}$$

Although Equation (I.4) expresses a classical model for the induced gain in the Stokes wave, it is suggestive of an equivalent relation which may be derived for the interaction of a system of harmonic oscillators (phonons) with an electromagnetic field.[11,12] Since each of the nuclear mechanisms proposed in Chapter IV may be modelled in terms of the vibration of some coordinate of nuclear rearrangement, we may develop a quantum mechanical model for the medium by quantizing each coordinate of vibration to give a phonon-like representation of the medium.[13] The growth equation for $\langle n_\omega \rangle$ then takes the form

$$\frac{d\langle n_\omega \rangle}{dz} = \frac{1}{c}\{W_{\text{emission}} - W_{\text{absorption}}\}$$

Reproduced with permission of the copyright owner. Further reproduction prohibited without permission.

$$= \kappa_{\omega_{||}} \{ | \langle n_\Omega - 1, n_\omega + 1, n_p + 1 | a_\Omega a_\omega^+ a_p^+ | n_\Omega, n_\omega, n_p \rangle |^2$$

$$- | \langle n_\Omega + 1, n_\omega - 1, n_p - 1 | a_\Omega^+ a_\omega a_p | n_\Omega, n_\omega, n_p \rangle |^2 \}$$

$$= \kappa_{\omega_{||}} \{ \langle n_\Omega \rangle (\langle n_\omega \rangle + 1)(\langle n_p \rangle + 1) - (\langle n_\Omega \rangle + 1)\langle n_\omega \rangle \langle n_p \rangle \} \qquad \text{(I.5)}$$

Here the emission and absorption rates for Stokes photons, $W_{emission}$ and $W_{absorption}$, are given in terms of raising "a^+" and lowering "a" operators for the photon and phonon modes which are initially in a state $\langle n_\Omega, n_\omega, n_p \rangle$ where the three arguments denote the occupancy of pump, Stokes, and phonon states respectively. The constant of proportionality for the scattering process $\kappa_{\omega_{||}}$ was obtained classically in Equation (I.4) which is seen to be equal to Equation (I.5) in the classical limit where $\langle n_\omega \rangle >> 1$ and $\langle n_\Omega \rangle >> 1$. It is particularly noteworthy that $\kappa_{\omega_{||}}$ is the same constant applied both to the emission and absorption processes in Equation (I.5). This is necessary to satisfy the condition that $d\langle n_\omega \rangle / dt = 0$ in thermal equilibrium. The processes which are described by Equation (I.5) are shown diagrammatically in Figure I.2 which is intended to give a pictorial visualization of the operation of raising and lowering operators. It is clearly seen that the "Stokes scattering" process represented by the first term of Equation (I.5) involves the "annihilation" of a pump photon and results in the "creation" of a Stokes photon and an added phonon (represented by the dot moving to the upper state). Conversely, the anti-Stokes scattering process described by the second term of Equation (I.5) involves the "annihilation" of a Stokes photon and a phonon to "create" a pump photon. The factors of "1" which distinguish Equation (I.5) from

Reproduced with permission of the copyright owner. Further reproduction prohibited without permission.

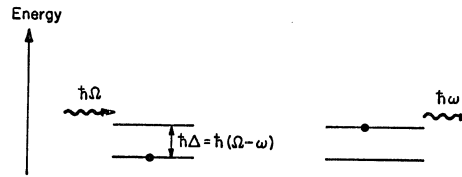

Stokes Scattering

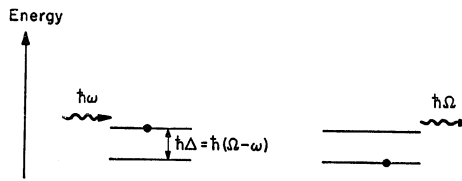

Anti-Stokes Scattering

Figure I.2

Reproduced with permission of the copyright owner. Further reproduction prohibited without permission.

Equation (I.4) are seen to account for the spontaneous emission terms in the quantized field and in the phonon mode.[11] Hence Equation (I.5) is seen to be a generalization of Equation (I.4) which includes terms in the quantum limit, i.e., spontaneous emission terms.

In order to see the relationship of the Raman susceptibility $\chi_{R_{||}}$ to the light scattering process, we take the limit of Equation (I.5) where only the incident field E_Ω is appreciably populated. This yields the relationship for the case of spontaneous Raman scattering of light†. Hence we may write

$$\frac{d\langle n_\omega\rangle}{dz} = \kappa_{\omega_{||}} \langle n_\Omega\rangle(\langle n_p\rangle + 1) \qquad \text{(I.6)}$$

Since the source of energy for the scattering process described by Equation (I.6) must come from the "pump mode" $\langle n_\Omega\rangle$, one would expect that we may write an expression analogous to Equation (I.6) which describes the attenuation of the incident field. For the sake of completeness, we could include in this new expression a term which would describe scattering into the pump mode $\langle n_\Omega\rangle$ from the mode at $\omega' = \Omega + \Delta$. Hence following an argument analogous to that which was used to obtain Equation (I.4) we find that the population of the pump mode $\langle n_\Omega\rangle$ is characterized by the relation

$$\frac{d\langle n_\Omega\rangle}{dz} = -\kappa'_{\Omega_{||}} \langle n_\Omega\rangle\langle n_\omega\rangle + \kappa_{\Omega_{||}}\langle n_{\omega'}\rangle\langle n_\Omega\rangle \qquad \text{(I.7)}$$

---

†Here the term Raman scattering is used in its more general sense where it refers to any light scattering process involving a frequency shift.

Reproduced with permission of the copyright owner. Further reproduction prohibited without permission.

where

$$\kappa'_{\Omega_{||}} = \frac{-128\pi^4 \hbar c\ \chi''_{R_{||}}}{\lambda_\Omega \lambda_\omega n^2(\omega)\ n(\Omega)\ V}$$

and

$$\kappa_{\Omega_{||}} = \frac{-128\pi^4 \hbar c\ \chi''_{R_{||}}}{\lambda_\Omega \lambda_{\omega'} n^2(\omega')\, n(\Omega) V}$$

Here we note that the same $\chi''_{R_{||}}$ may be used to express $\kappa_{\omega_{||}}$, $\kappa'_{\Omega_{||}}$ and $\kappa_{\Omega_{||}}$ since $\mathrm{Im}\ \chi_3^{1111}(-\omega,\omega,\Omega,-\Omega)$ is only a function of the difference frequency $\Delta = \Omega - \omega$ and is odd in Δ since the nonlinear response tensor must be real; see Section 2.1.

In a manner analogous to that used to arrive at Equation (I.5) we may obtain a quantum mechanical equivalent of Equation (I.7). Developing this relationship and specializing it to the case of spontaneous Raman scattering from the incident wave $\underline{E}_\Omega$ whence $\langle n_\Omega \rangle >> \langle n_\omega \rangle$ and $\langle n_{\omega'} \rangle$, we find that

$$\frac{d\langle n_\Omega \rangle}{dz} = -\kappa'_{\Omega_{||}} (\langle n_p \rangle + 1)\ \langle n_\Omega \rangle - \kappa_{\Omega_{||}} \langle n_p \rangle \langle n_\Omega \rangle \qquad \text{(I.8)}$$

Here the first term describes spontaneous scattering into the Stokes mode at frequency ω and the latter term describes scattering into the anti-Stokes mode at frequency $\omega' = \Omega + \Delta$. Integrating this relation directly to obtain $\langle n_\Omega \rangle$ we find that

$$\langle n_\Omega \rangle = \langle n_\Omega \rangle|_{z=0}\ e^{-\Pi z} \qquad \text{(I.9)}$$

where $\Pi = \kappa'_{\Omega_{||}} (\langle n_p \rangle + 1) + \kappa_{\Omega_{||}} \langle n_p \rangle$. If it is assumed that the thermal

Reproduced with permission of the copyright owner. Further reproduction prohibited without permission.

equilibrium of the system remains undisturbed by the incident field, a Bose-Einstein distribution may be employed to specify $\langle n_p \rangle$ in which case we find that[14]

$$\Pi = \kappa'_{\Omega||} \left\{ \frac{1}{1 - e^{-\frac{\hbar\Delta}{kT}}} \right\} \quad \kappa_{\Omega||} \left\{ \frac{1}{e^{\frac{\hbar\Delta}{kT}} - 1} \right\} \tag{I.10}$$

Recalling that the definition of the scattering cross section σ for scattering into the Stokes and anti-Stokes modes polarized parallel to the input wave is given by the expression

$$\langle n_\Omega \rangle = \langle n_\Omega \rangle \Big|_{z=0} e^{-N_v \sigma z} \tag{I.11}$$

where N_v is the number density of scatterers, we see immediately that the scattering cross sections for these two modes may be written in the form

$$\sigma_{||s} = \frac{\kappa'_\Omega}{N_v} \left(\frac{1}{1 - e^{-\frac{\hbar\Delta}{kT}}} \right) = \frac{-128\pi^4 \hbar c \, \chi''_R(\Omega,\Delta)}{N_v \lambda_\Omega \lambda_{\Omega-\Delta} n^2(\Omega-\Delta) n(\Omega) V} \left\{ 1 - e^{-\frac{\hbar\Delta}{kT}} \right\}^{-1}$$

$$\sigma_{||as} = \frac{\kappa_\Omega}{N_v} \left(\frac{1}{e^{\frac{\hbar\Delta}{kT}} - 1} \right) = \frac{-128\pi^4 \hbar c \chi''_R(\Omega,\Delta)}{N_v \lambda_\Omega \lambda_{\Omega+\omega} n^2(\Omega+\Delta) n(\Omega) V} \left\{ e^{\frac{\hbar\Delta}{kT}} - 1 \right\}^{-1} \tag{I.12}$$

Here the subscripts denote the Stokes and anti-Stokes cross sections respectively. Clearly Equation (I.12) yields a relationship between the scattering cross sections into a single radiation mode polarized parallel to the incident field and having a frequency shift of Δ and the Raman susceptibility $\chi''_{R||} = 6 \, \mathrm{Im}(\chi_3^{1111}(-\omega,\omega,\Omega,-\Omega))$. By a

Reproduced with permission of the copyright owner. Further reproduction prohibited without permission.

completely parallel development, relations which are equivalent to Equations (I.11) and (I.12) may be derived to relate the scattering cross sections $\sigma_{\perp s}$ and $\sigma_{\perp as}$ to the Raman susceptibility $\chi''_{R_\perp} = 6\ \mathrm{Im}\{\chi_3^{1122}(-\omega,\omega,\Omega,-\Omega)\}$ for scattering into a single mode which is polarized perpendicular to the polarization of the incident field. Examination of the gain relation, Equation (H.7) indicates that these expressions for scattering into the perpendicularly polarized modes are valid not only for forward scattering, but for scattering in any direction in space.

I.1 Relating the Total Light Scattering Cross Section to the Nonlinear Susceptibility

Theoretically Equation (I.12) along with Equations (H.9) through (H.11) which relate the nonlinear susceptibility to the nuclear response functions establishes a direct relationship between the light scattering cross sections for the parallel and perpendicular modes of scattering and nuclear response functions $a(\Delta)$ and $b(\Delta)$. Hence information regarding these functions may be obtained by measuring the scattered intensities. Experimentally however it is useful to obtain a knowledge of the variation of the scattered intensity with the direction of scattering and also to integrate Equation (I.12) over a finite frequency band since the scattered intensity which is actually measured will invariably be into more than one radiation mode.

The angular integration for the modes which are polarized perpendicular to the input polarization are straightforwardly treated since these modes exhibit a scattering cross section which is independent of the direction of scattering, as was previously noted. Hence

Reproduced with permission of the copyright owner. Further reproduction prohibited without permission.

the scattering cross section is obtained by replacing the symbol "$\|$" with the symbol "$\perp$" in Equation (I.12). In contrast it may be seen from Equation (H.7) that scattering into the modes which exhibit a component of polarization parallel to the direction of polarization of the incident beam exhibit a scattering cross section which is maximum in the plane perpendicular to the incident field (y-z plane in Figure I.1) and drops off as $\cos^2\xi$ when the direction of scattering deviates from this plane by an angle ξ. The radiation pattern may thus be interpreted as that which is produced by an induced dipole along the direction of polarization of the incident field.[15,16]

In considering the spectral integral over all of the frequency modes into which scattering may occur, we first recognize that the density of radiation modes per unit solid angle per unit frequency in the volume V is given by[11]

$$\frac{dp(\omega)}{d\Theta\, d\omega} = \frac{V\omega^2 n^3(\omega)}{(2\pi c)^3} \tag{I.13}$$

Hence the total scattering cross sections per unit solid angle for Stokes and anti-Stokes scattering are given by

$$\frac{d\sigma_{T\|s}}{d\Theta} = \int_0^\infty \sigma_{\|_s}(\Omega,\Delta)\, \frac{dp(\Omega-\Delta)}{d\Theta\, d(\Omega-\Delta)}\, d\Delta \tag{I.14}$$

and

$$\frac{d\sigma_{T\|as}}{d\Theta} = \int_0^\infty \sigma_{\|as}(\Omega,\Delta)\, \frac{dp(\Omega+\Delta)}{d\Theta d(\Omega+\Delta)}\, d\Delta \tag{I.15}$$

Equivalent relations for scattering into the perpendicularly polarized modes are obtained by simply replacing $\|$ with $\perp$ in Equations (I.14) and (I.15).

Reproduced with permission of the copyright owner. Further reproduction prohibited without permission.

Generally $\sigma_{||_s}(\Omega,\Delta)$ and $\sigma_{||_{as}}(\Omega,\Delta)$ will exhibit a number of resonances which arise as a result of the various nuclear contributions which were modeled in Section 4.2. For the sake of simplicity we shall consider the case where the single mode scattering cross section exhibits only a single resonant frequency at $\Delta = \Delta_o$. In the case where more resonances exist in the cross section, we recognize that the results are additive. Practically speaking, however, χ''_R will be most strongly affected by the mechanism which produces a resonance in the cross section in closest proximity to the Stokes shift $\Delta = \Omega - \omega$ of interest.

In order to evaluate Equations (I.14) and (I.15) we first recall that the single mode scattering cross sections are related to the Raman susceptibility by Equation (I.12). Hence the relations (see Equations (H.9) through (H.11))

$$\chi''_{R_{||}}(\Omega,\Delta) = 6\ \mathrm{Im}\ \chi_3^{1111}(-\omega,\omega,\Omega,-\Omega) = \frac{1}{2}\{a''(-\Delta) + b''(-\Delta)\} \tag{I.16}$$

$$\chi''_{R_{\perp}}(\Omega,\Delta) = 6\ \mathrm{Im}\ \chi_3^{1122}(-\omega,\omega,\Omega,-\Omega) = \frac{1}{4}\, b''(-\Delta) \tag{I.17}$$

may be employed to evaluate Equations (I.14) and (I.15) for specific forms of $a(-\Delta)$ and $b(-\Delta)$. It is immediately evident from these relations that the "depolarization ratio"[16] is given by the relation

$$T \equiv \frac{\sigma_{||_s}}{\sigma_{\perp_s}} = \frac{2\{a''(-\Delta) + b''(-\Delta)\}}{b''(-\Delta)} \tag{I.18}$$

Since $T = \frac{4}{3}$ for a "depolarized scatterer", we must have $b''(-\Delta) = -3a''(-\Delta)$ for this case. It is also evident from a comparison of Equation (I.18) to Table H.1 that T is also given by the ratio of

Reproduced with permission of the copyright owner. Further reproduction prohibited without permission.

Raman gains

$$T = \frac{g_{||}(\omega)}{g_{\perp}(\omega)} \tag{I.19}$$

as we had claimed in Appendix H.

The explicit evaluation of Equations (I.14) and (I.15) are particularly simple in two cases of experimental importance.

Case 1. $\hbar\Delta_o >> kT \quad \Omega >> \Delta_o >> \delta\Delta_o$

In the first case the resonant frequency Δ_o at which $|a''(-\Delta)|$ and $|b''(-\Delta)|$ attain their maximum values is such that $\hbar\Delta_o >> kT$, the pump frequency Ω is much greater than the resonance frequency Δ_o, and the linewidth of the resonance $\delta\Delta_o$ is much smaller than the resonant frequency Δ_o.

We first note in this case that the equilibrium phonon population $\langle n_p \rangle$ is much greater than unity. Hence using Equation (I.16) in Equation (I.12) and taking the low temperature limit of the Bose-Einstein distribution one finds

$$\sigma_{||_s}(\Omega,\Delta) = \frac{-64\pi^4 \hbar c\{a''(-\Delta)+b''(-\Delta)\}}{N_v \lambda_\Omega \lambda_{\Omega-\Delta} n^2(\Omega-\Delta)\, n(\Omega)\, V}$$

$$\sigma_{||_{as}}(\Omega,\Delta) = \frac{-64\pi^4 \hbar c\{a''(-\Delta)+b''(-\Delta)\}}{N_v \lambda_\Omega \lambda_{\Omega+\Delta} n^2(\Omega+\Delta)\, n(\Omega)\, V} \exp(-h\Delta/(kT)) \tag{I.20}$$

Again analogous relations for the scattering cross sections into the single mode polarized perpendicular to the input polarization may be obtained by replacing $||$ with $\perp$ and $a''(-\Delta)+b''(-\Delta)$ with $\frac{1}{2}\, b''(-\Delta)$ in Equation (I.20).

Reproduced with permission of the copyright owner. Further reproduction prohibited without permission.

In using Equation (I.20) to evaluate Equations (I.14) and (I.15) it is to be noted that the only significant contributions to the integral come from the small frequency band near $\Delta = \Delta_o$ where the response functions are strongly peaked. It is also to be recognized that the factor $\exp(-\hbar\Delta/(kT))$ is slowly varying near Δ_o compared to $a''(-\Delta)$ and $b''(-\Delta)$. Hence we may approximate $\Omega \pm \Delta_o$ by $\Omega \pm \Delta_o$ and replace Δ with Δ_o in the exponential factor. The total cross section per unit solid angle for scattering into the modes polarized parallel to $\underline{E}_\Omega$ in the scattering plane perpendicular to $\underline{E}_\Omega$ is then written in the form

$$\frac{d\sigma_{T||s}}{d\Theta} = \frac{-32n(\Omega-\Delta)\pi^3\hbar\{\int_0^\infty (a''(-\Delta) + b''(-\Delta))d\Delta\}}{N_v\lambda^3_{\Omega-\Delta_o}\lambda_\Omega\, n(\Omega)}$$

$$\frac{d\sigma_{T||as}}{d\Theta} = \frac{-32n(\Omega+\Delta)\pi^3\hbar\{\int_0^\infty (a''(-\Delta) + b''(-\Delta))d\Delta\}\exp(-\frac{\hbar\Delta_o}{kT})}{N_v\lambda^3_{\Omega+\Delta_o}\lambda_\Omega\, n(\Omega)} \qquad \text{(I.21)}$$

Upon examining Table H.2 it is evident that all mechanisms which satisfy the condition $\hbar\Delta_o >> kT$ $(T \neq 0)$ exhibit response functions which may be approximated near the resonant frequency Δ_o by a Lorentzian lineshape of the form

$$a''(-\Delta) \simeq \frac{-\pi}{4}\delta\Delta_o\, L(\Delta)\, a''(\Delta_o)$$
$$b''(-\Delta) \simeq \frac{-\pi}{4}\delta\Delta_o\, L(\Delta)\, b''(\Delta_o) \qquad \text{(I.22)}$$

Reproduced with permission of the copyright owner. Further reproduction prohibited without permission.

where

$$L(\Delta) = \frac{2}{\pi} \frac{\delta\Delta_o/2}{(\Delta-\Delta_o)^2 + (\delta\Delta_o/2)^2} \tag{I.23}$$

is the Lorentzian lineshape normalized so that $\int_0^\infty L(\Delta)d\Delta = 1$ and we have assumed $a''(\Delta)$ and $b''(\Delta)$ to be odd functions of Δ (see Section 2.2).

Using Equations (I.22) and (I.23) to evaluate Equation (I.21) we obtain

$$\frac{d\sigma_{T||s}}{d\theta} = \frac{8n(\Omega-\Delta_o)\pi^4\hbar\{a''(\Delta_o) + b''(\Delta_o)\}\delta\Delta_o}{N_v\lambda^3_{\Omega-\Delta_o}\lambda_\Omega\, n(\Omega)} \tag{I.24}$$

$$\frac{d\sigma_{T||as}}{d\theta} = \frac{8n(\Omega+\Delta_o)\pi^4\hbar\{a''(\Delta_o) + b''(\Delta_o)\}\exp(-\hbar\Delta_o/(kT))\delta\Delta_o}{N_v\lambda^3_{\Omega+\Delta_o}\lambda_\Omega\, n(\Omega)} \tag{I.25}$$

which establishes the relationship between the nuclear response functions and the spontaneous scattering cross section for this "low temperature" case.

It is to be noted that the ratio of the Stokes and anti-Stokes cross sections given by Equations (I.24) and (I.25) is

$$\frac{d\sigma_{T||s}}{d\theta}\left(\frac{d\sigma_{T||as}}{d\theta}\right)^{-1} = \frac{n(\Omega-\Delta_o)}{n(\Omega+\Delta_o)}\frac{\lambda^3_{\Omega-\Delta_o}}{\lambda^2_{\Omega+\Delta_o}}\exp\left\{\frac{\hbar\Delta_o}{kT}\right\} \tag{I.26}$$

Recognizing that this relationship is for the "photon" scattering cross sections and invoking Equation (I.2) to obtain the ratio of scattered intensities, we find that

Reproduced with permission of the copyright owner. Further reproduction prohibited without permission.

$$\frac{dI_{T||s}}{d\Theta}\left(\frac{dI_{T||as}}{d\Theta}\right)^{-1} = \left(\frac{\lambda_{\Omega-\Delta_o}}{\lambda_{\Omega+\Delta}}\right)^4 \exp\left\{\frac{\hbar\Delta_o}{kT}\right\} \qquad \text{(I.27)}$$

where $\frac{dI_{T||s}}{d\Theta}$ and $\frac{dI_{T||as}}{d\Theta}$ are the intensities per unit solid angle in the Stokes and anti-Stokes modes respectively which are polarized parallel to the polarization of the incident wave. Again we emphasize that equivalent results apply to the modes which are polarized perpendicularly with respect to the input polarization.

Case 2. $kT >> \hbar\Delta$

In the second specific case which we will consider, the thermal energy is much greater than the mean Raman shift. This occurs in the case of librational scattering at room temperatures or when the scattering arises from reorientational fluctuations or intermolecular interactions (redistribution).

For librational scattering the lineshape is approximated by the same Lorentzian curve used in considering Case 1. Here however, the $kT >> \hbar\Delta$ limit is taken in evaluating the Bose-Einstein distribution so that it may be approximated by the factor $kT/(\hbar\Delta)$ for both Stokes and anti-Stokes cases. Assuming that the linewidth $\delta\Delta_o$ is again narrow compared to the Stokes shift Δ so that $\frac{\hbar\Delta}{kT} \simeq \frac{\hbar\Delta_o}{kT}$, it is easy to see that Equation (I.24) is modified to the form

$$\frac{d\sigma_{T||s}}{d\Theta} \simeq \frac{d\sigma_{T||as}}{d\Theta} \simeq \frac{8\pi^4\{a''(\Delta_o) + b''(\Delta_o)\}kT\ \delta\Delta_o}{N_v \lambda_\Omega^4 \Delta_o} \qquad \text{(I.28)}$$

Reproduced with permission of the copyright owner. Further reproduction prohibited without permission.

In considering the scattering due to reorientation and redistribution where the line is centered at $\Delta = 0$ we shall approximate the lineshape by the Lorentzian response functions which were derived for the case of reorientation as shown in Table H.2. Hence writing

$$-a''(-\Delta) = \frac{\pi\Delta}{2}\, a(0)\, L'(\Delta)$$

$$-b''(-\Delta) = \frac{\pi\Delta}{2}\, b(0)\, L'(\Delta) \qquad \text{(I.29)}$$

where the Lorentzian lineshape centered about $\Delta = 0$ is now given by

$$L'(\Delta) = \frac{2}{\pi}\, \frac{1/\tau}{\Delta^2 + (\frac{1}{\tau})^2} \qquad \text{(I.30)}$$

which again is normalized so that $\int_0^\infty L'(\Delta)d\Delta = 1$ and $\delta\Delta_o = \frac{2}{\tau}$.

Substitution of Equations (I.29) and (I.30) into Equations (I.16), (I.12), and (I.14) in succession then yields the result

$$\frac{d\sigma_{I||s}}{d\Theta} \simeq \frac{d\sigma_{||as}}{d\Theta} = \frac{16\pi^4\{a(0) + b(0)\}kT}{N_V \lambda_\Omega^4} \qquad \text{(I.31)}$$

In summary we see that Equations (I.12) through (I.15) provide a basis whereby the light scattering in any frequency band may be related to the nonlinear response functions $a(\Delta)$ and $b(\Delta)$. Two specific cases, the low and the high temperature limits, were considered in which the total light scattering cross sections integrated over the frequency band could be related to the nuclear response functions $a(\Delta)$ and $b(\Delta)$. Moreover, it was noted that the ratio of

Reproduced with permission of the copyright owner. Further reproduction prohibited without permission.

$2(a''(\Delta) + b''(\Delta))/b''(\Delta)$ is identical to the experimentally measurable depolarization ratio for light scattering $T = I_{||}/I_{\perp}$.

Reproduced with permission of the copyright owner. Further reproduction prohibited without permission.

APPENDIX J

Focusing Optics in the Ellipse Rotation Study

In Section (6.2) it was noted that one set of samples was cut so that the focusing lenses could be kept stationary as the samples were interchanged still maintaining collimation of the output beam with the focus of the lens system centered in the sample. This configuration is shown in Figure (J.1), where L is the length of the sample, n_2 its refractive index, f_1 and f_2 the focal lengths of the focusing and recollimating lenses respectively in the medium with index n_1, and ℓ_2 and ℓ_2 the respective spaces between the lenses and sample interfaces.

In order to calculate the value of ℓ_1 necessary to put the geometric focus at the center of the sample we use a ray matrix approach.[17,18] The input rays are specified by a two component vector $\underline{x}_1$ specifying the distance of a ray from the beam axis and the slope of the ray with respect to the axis. Thus at the input plane of the system

$$\underline{x}_1 = \begin{bmatrix} x_1 \\ x_1' \end{bmatrix} = \begin{bmatrix} x_1 \\ 0 \end{bmatrix} \tag{J.1}$$

The matrices for the focusing lens f_1, the space ℓ_1, the interface n_1 to n_2, and the space $L/2$ are given by

$$M_1 = \begin{bmatrix} 1 & 0 \\ -\frac{1}{f_1} & 1 \end{bmatrix} \tag{J.2}$$

Reproduced with permission of the copyright owner. Further reproduction prohibited without permission.

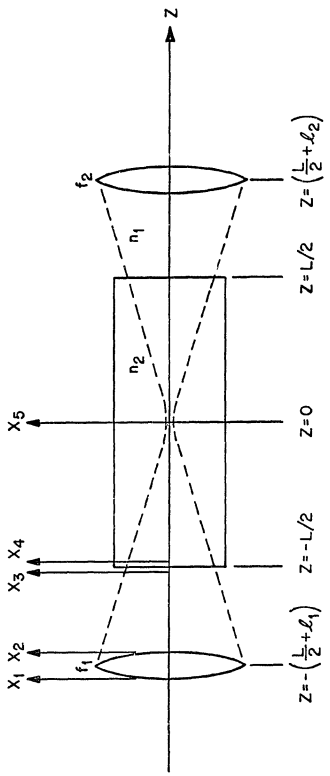

Figure J.1

Reproduced with permission of the copyright owner. Further reproduction prohibited without permission.

$$M_2 = \begin{bmatrix} 1 & \ell \\ 0 & 1 \end{bmatrix} \tag{J.3}$$

$$M_3 = \begin{bmatrix} 1 & 0 \\ 0 & \frac{n_1}{n_2} \end{bmatrix} \tag{J.4}$$

and

$$M_4 = \begin{bmatrix} 1 & L/2 \\ 0 & 1 \end{bmatrix} \tag{J.5}$$

respectively. Thus at the focus of the lens f_1 which is centered in the sample ($z = 0$)

$$\begin{bmatrix} x_5 \\ x_5' \end{bmatrix} = \begin{bmatrix} 0 \\ x_5' \end{bmatrix} = \underline{\underline{M_4}}\,\underline{\underline{M_3}}\,\underline{\underline{M_2}}\,\underline{\underline{M_1}} \begin{bmatrix} x_1 \\ 0 \end{bmatrix} \tag{J.6}$$

$$= \begin{bmatrix} 1 - \frac{\ell_1}{f_1} - \frac{Ln_1}{2n_2 f_1} & \ell_1 + \frac{Ln_1}{2n_2} \\ -\frac{n_1}{n_2 f_1} & \frac{n_1}{n_2} \end{bmatrix} \begin{bmatrix} x_1 \\ 0 \end{bmatrix}$$

The condition $x_5 = 0$ clearly requires that

$$\ell_1 = f_1 - \frac{Ln_1}{2n_2} \tag{J.7}$$

Reproduced with permission of the copyright owner. Further reproduction prohibited without permission.

which reduces to

$$\ell_1 = f_1 - \frac{L}{2n} \tag{J.8}$$

in the limit $n_1 = 1$ and $n_2 = n$.

Similarly symmetry tells us that

$$\ell_2 = f_2 - \frac{L}{2n} \tag{J.9}$$

Furthermore it is easy to see from the expression for the slopes at the focus that the spot sizes w at the input and output of the system obey the relationship,

$$\frac{w_{in}}{w_{out}} = \frac{f_1}{f_2} \tag{J.10}$$

From Equation (J.8) it is seen that the "effective focal length" of the focusing lens is

$$\ell_1 + \frac{L}{2} = f_1 + \frac{L}{2}\left(1 - \frac{1}{n}\right) \tag{J.11}$$

Thus the focus is kept at the center of each sample by requiring that L take on such a value that

$$\frac{L}{2}\left(1 - \frac{1}{n}\right) = \text{constant}. \tag{J.12}$$

Reproduced with permission of the copyright owner. Further reproduction prohibited without permission.

APPENDIX K

The Hyperpolarizability of CS_2

It was noted in Section 6.6 that the electronic parameter σ in liquid CS_2 is less than 1-1/2% of the nuclear parameter β so that the ellipse rotation parameter $\chi_3^{1221}(-\omega,\omega,\omega,-\omega)$ for CS_2 may be determined by a measurement of its Kerr constant.

The electronic portion of the Kerr constant is seen from Equation (3.21) and Table 5.1 to take the form

$$(B_o)_{elec} = \frac{2\pi}{n\lambda}\sigma \tag{K.1}$$

Experimentally, it is often convenient to specify the electronic parameter σ in terms of γ the "second hyperpolarizability per molecule".[19] This parameter may then be corrected for local field effects and multiplied by the number density of molecules in the liquid to yield the result (see Equation (7.13))

$$(B_o)_{elec} = \frac{2\pi}{n\lambda}\left\{\frac{n^2+2}{3}\right\}^4 \frac{N\gamma}{3} \tag{K.2}$$

Recent measurements of γ for CS_2 have been performed by Mayer[20] and Hauchecorne et al.[21] using two independent techniques (1) electric field induced second harmonic generation, and (2) three-wave mixing, applied to CS_2 vapor.

The second harmonic generation technique, although successful in finding γ for fifteen other molecules, found γ to be too small to detect in CS_2 ($\gamma < 10^{-37}$esu). The three-wave mixing studies using a ruby laser source determined values of $\gamma = 35\times10^{-37}$esu and 70×10^{-37} esu

Reproduced with permission of the copyright owner. Further reproduction prohibited without permission.

using Raman sources of hydrogen ($\Delta = 4150\ cm^{-1}$) and methane ($\Delta = 2914\ cm^{-1}$) respectively. Since the ratio of the susceptibility elements

$$\frac{\chi^{1111}(-(\omega+\Delta),\omega,\omega,-(\omega-\Delta))}{\chi^{1221}(-(\omega+\Delta),\omega,\omega,-(\omega-\Delta))} = \frac{9\sigma + 4\{a(\Delta) + b(\Delta)\}}{3\sigma + 2b(\Delta)} \qquad (K.3)$$

should be equal to three for a purely electronic contribution, the three-wave mixing signal should exhibit a power ratio of 9 between the two modes of polarization which are used to study three-wave mixing (i.e., Stokes beam polarized parallel to pump and Stokes beam polarized perpendicular to pump). This ratio was found to be 8.5 for the case of a hydrogen Raman cell and 19 for the case of the methane cell. Hence the value $\gamma = 34 \times 10^{-37}$ esu is likely to have been affected less by the nuclear contributions from neighboring Raman resonances in the TWM studies.

Using $\gamma = 35 \times 10^{-37}$ esu as an upper limit in Equation (K.2) with $N = 10^{22} cm^{-3}$ we find $(B_o)_{elec} \leq 3.6 \times 10^{-9}$ esu which is less than 1-1/2% of the total Kerr constant 253×10^{-9} esu for liquid CS_2 at 23°C and $\lambda = 6943\text{Å}$.

For the sake of completeness we should like to note that Bogaard et al.[22] using a temperature extrapolation of the d.c. Kerr constant of CS_2 vapor to infinite temperatures, where the effects of molecular reorientation should be small, have inferred that 11.3% of the Kerr constant of CS_2 arises from direct electronic distortion. In view of the large range of temperatures involved in the extrapolation and the fact that this is an attempt to determine a small electronic contribution in the background of a rather significant nuclear

Reproduced with permission of the copyright owner. Further reproduction prohibited without permission.

nonlinearity, we assess that this estimate is most probably erroneously high, and that the other measurements of γ yield results which are closer to the true value.

Reproduced with permission of the copyright owner. Further reproduction prohibited without permission.

REFERENCES FOR APPENDICES A-K

1. H. A. Lorentz, Theory of Electrons, Leipzig, 1909 (2nd edition, Dover Publications, New York, 1952).

2. N. Bloembergen, Nonlinear Optics (W. A. Benjamin Inc., New York, 1965), p. 5.

3. C. J. F. Bottcher, Theory of Electric Polarization (Elsevier Publishing Company, Amsterdam, 1952).

4. H. Goldstein, Classical Mechanics (Addison-Wesley Publ. Co. Inc., Reading, Mass. 1950(1965)), p. 109.

5. P. Debye, Polar Molecules (The Chemical Catalog Co., 1929; reprinted by Dover Publ. Inc.)

6. R. Y. Chiao and J. Godine, "Polarization Dependence of Stimulated Rayleigh-Wing Scattering and the Optical-Frequency Kerr Effect," Phys. Rev. 185, 430 (1969).

7. See, for example, P. D. Maker and R. W. Terhune, "Study of Optical Effects Due to an Induced Polarization Third Order in the Electric Field Strength," Phys. Rev. 137, A801 (1965).

8. N. Bloembergen, "The Stimulated Raman Effect," Am. J. Phys. 35, 989 (1967).

9. We note that one exception to this statement is the so-called "light by light scattering" or "stimulated four-photon interaction" (R. Y. Chiao, P. L. Kelley and E. Garmire, Phys. Rev. Lett. 17, 1158 (1966)); however, this process involves a Stokes-anti-Stokes coupling in a phase-matched direction, which has not been considered in this work.

10. Y. R. Shen and N. Bloembergen, "Theory of Stimulated Brillouin and Raman Scattering," Phys. Rev. 137, A1787 (1965).

Reproduced with permission of the copyright owner. Further reproduction prohibited without permission.

11. P. A. M. Dirac, The Principles of Quantum Mechanics (Oxford Univ. Press, Oxford, 1930; 4th ed. (1958)), Chap. 10.

12. W. Heitler, The Quantum Theory of Radiation, 2nd ed. (Oxford Univ. Press, Fair Lawn, New Jersey, 1944).

13. G. Mayer, "Experimental Features of First-Order Stimulated Scattering" in Proc. of the International School of Physics Enrico Fermi, Course XLII (Acad. Press, New York, 1969), ed. R. J. Glauber, p. 561.

14. F. Reif, Fundamentals of Statistical and Thermal Physics (McGraw-Hill Inc., New York, 1965), Chap. 9.

15. E. B. Wilson, J. C. Decius, and P. C. Cross, Molecular Vibrations (McGraw-Hill Inc., New York, 1955).

16. S. P. S. Porto, "Angular Dependence and Depolarization Ratio of the Raman Effect," J. Opt. Soc. Am. 56, 1585 (1966).

17. W. Brouwer, Matrix Methods in Optical System Design (W. A. Benjamin Inc., New York, 1964).

18. A. Yariv, Introduction to Optical Electronics (Holt, Rinehart, and Winston, New York, 1971).

19. A. D. Buckingham and B. J. Orr, "Molecular Hyperpolarizabilities," Quart. Rev. 21, 195 (1967).

20. G. Mayer, "Rayonnement de l'harmonique Pair d'une Onde Lumineuse Par Des Molecules Soumises a un Champ Electrique Statique," Compt. Rend. B267, 54 (1968).

21. G. Hauchecorne, P. Kerherve, and G. Mayer, "Mesure des Interactions Entre Ondes Lumineuses Dans Diverses Substances," Le Jour. de Physique 32, 47 (1971).

Reproduced with permission of the copyright owner. Further reproduction prohibited without permission.

22. M. P. Bogaard, A. D. Buckingham, and G. I. D. Ritchie, "The Temperature Dependence of Electric Birefringence in Gaseous Benzene and Carbon Disulphide," Mol. Phys. 18, 575 (1970).

Reproduced with permission of the copyright owner. Further reproduction prohibited without permission.

APPENDIX L

Reproduced with permission of the copyright owner. Further reproduction prohibited without permission.

INTENSITY-INDUCED CHANGES IN OPTICAL POLARIZATIONS IN GLASSES†

A. Owyoung,†† R.W. Hellwarth,††† and N. George

California Institute of Technology
Pasadena, California

ABSTRACT

Using a single mode ruby laser we have made the first measurements of intensity-induced changes of the optical polarization (ellipse rotation) in solids, viz. fused quartz and Schott BK-7 and SF-7 glasses for which we have obtained the nonlinear susceptibility values

$$c_{1221}(-\omega,\omega,\omega,-\omega) = 1.5,\ 2.3,\ \text{and}\ 9.9 \times 10^{-15}\ \text{esu}$$

respectively. These values are accurate to within 10% relative to the value for liquid CS_2 which we used for calibration and determined from other experiments to be 37.8×10^{-14} esu to within 2%. We also show theoretically that a comparison of these values with electric-field-induced birefringence (Kerr) data can determine uniquely the fractional contribution to both of purely electronic nonlinearities. Existing Kerr data are only accurate enough at present for us to conclude that the electronic nonlinearities might dominate our effect.

---

†Research supported in part by the Air Force Office of Scientific Research.

††Permanent Address: Sandia Laboratories, Albuquerque, New Mexico.

†††Present Address: Clarendon Laboratory, Oxford, England
Permanent Address: University of Southern California, Los Angeles, California.

Reproduced with permission of the copyright owner. Further reproduction prohibited without permission.

I. Introduction

A strong, elliptically polarized, optical beam induces an optical anisotropy in any normally isotropic medium through which it passes, and undergoes thereby a change in its state of polarization. Maker et al. first predicted and observed the intensity induced rotation of the polarization ellipse of a plane wave by monitoring the polarization of an elliptically-polarized ruby-laser giant pulse after it had traversed a liquid-filled absorption cell.[1] Here we report the first measurements of this intensity-induced ellipse rotation in solids, viz. fused quartz, BK-7 borosilicate crown glass and SF-7 dense flint glass. Being around 10% absolute accuracy, these constitute the most accurate measurements of any nonlinear coefficients for glasses to date.

As we show in Section II, both this effect of "ellipse rotation" and also the electric-field-induced birefringence (Kerr effect) depend on the (one) nonlinear electronic polarizability parameter, and also, but in different ways on another parameter that measures certain contributions of local nuclear redistribution to the effects. Hence these two experiments jointly offer a unique possibility of distinguishing between the two underlying physical mechanisms unambiguously in glasses and liquids. Of all other nonlinear optical effects observed in glasses only the purely electronic process of third harmonic generation (THG) depends on no other independent parameters than the two involved in these two effects. Wang and Baardsen have measured THG in borosilicate crown glass,[2] and their result is consistent with ours for BK-7 glass. The great difficulty in calibrating this effect led them to estimate their

Reproduced with permission of the copyright owner. Further reproduction prohibited without permission.

absolute accuracy to be a factor of three. So there is little significance in the comparison.

Maker and Terhune have observed three wave mixing (TWM) in fused quartz, BSC glass and in liquids and crystals.[3] They argued that, because no variation in the effect with frequency is observed in the glasses, it is probably purely electronic in origin. This interpretation of their data is not inconsistent with our results, but their experimental uncertainties were too large to confirm this conclusion by comparison with ours. The many other nonlinear optical effects that have been observed in glasses clearly involve index coefficients and physical mechanisms independent of those of interest here.

In Section III we describe our experimental results and the experimental means we have developed to overcome some of the difficulties that have arisen in the previous ellipse-rotation studies on liquids. When in the discussion of Section IV we use the theory of Section II to compare our experimental results with the Kerr data of Duguay and Hansen on fused quartz and BK-7 glass,[4,5] we find that the electronic contribution to either effect is not negligible, but the uncertainties in the Kerr data leave the possibility that the nuclear contribution may or may not be significant. Other evidence is discussed which suggests that the nuclear contribution cannot yet be ruled insignificant. Implications of our measurements to other nonlinear optical effects are also discussed in Section IV.

II. Relation Between Ellipse Rotation and Kerr Effects

In order to establish the desired relations between certain

Reproduced with permission of the copyright owner. Further reproduction prohibited without permission.

nonlinear susceptibility coefficients for isotropic media, we use the fact that the nonlinear polarization density $\vec{P}^{NL}(\vec{r},t)$, third order in the electric field, may be separated into two parts. First, there is an "electronic" part $\vec{P}_e(\vec{r},t)$ which results from a distortion of the electron orbits about the nuclei, considered fixed in a typical spatial configuration. This polarization responds so quickly in transparent media (within several electronic cycles) that we may consider the response to be instantaneous for the electromagnetic fields of interest. Therefore it may be expressed in the form,

$$\vec{P}_e(\vec{r},t) = \frac{1}{2}\sigma\,\vec{E}(\vec{r},t)\cdot\vec{E}(\vec{r},t)\vec{E}(\vec{r},t) \qquad (1)$$

for an isotropic material. This term alone would be responsible for third harmonic generation. The electronic nonlinear susceptibility coefficient σ exhibits dispersion which is small at the optical frequencies we employ and which we correct for when necessary. Evidently σ is independent of temperature at fixed density, but it varies with temperature at fixed pressure in a way not yet understood.

The remaining part of $\vec{P}^{NL}$ is a nuclear part $\vec{P}_n(\vec{r},t)$ which is due to the linear response of the electronic currents about nuclear arrangements whose statistical probabilities are altered slightly in order to lower the average field-crystal interaction energy. When (as here) the medium has no absorption near field frequencies and has negligible dispersion, the instantaneous fluctuation in this interaction energy density in a small volume (compared to a wavelength) about $\vec{r}$ may be written $-\vec{E}(\vec{r},t)\cdot\delta\vec{\varepsilon}(\vec{r},t)\cdot\vec{E}(\vec{r},t)/8\pi$,

Reproduced with permission of the copyright owner. Further reproduction prohibited without permission.

where $\overleftrightarrow{\delta\varepsilon}$ is the deviation from its average of the dielectric permittivity tensor appropriate to the nuclear placements in the neighborhood of $\vec{r}$ at time t. Since $\vec{P}_n(\vec{r},t)$ equals $\overleftrightarrow{\delta\varepsilon}\cdot\vec{E}(\vec{r},t)/4\pi$ averaged with a weighting function (i.e., density matrix) expanded to first order in the above interaction energy, it is easy to see that, for isotropic media, $\vec{P}_n$ must be of the form,

$$\vec{P}_n(\vec{r},t) = \vec{E}(\vec{r},t)\int a(t-s)E^2(\vec{r},s)ds + \int \vec{E}(r,t)\cdot\vec{E}(\vec{r},s)b(t-s)\vec{E}(\vec{r},s)ds \quad (2)$$

Here the scalars a(t) and b(t) are nuclear response functions for the "isotropic" and "anisotropic" parts of the nonlinear polarization respectively, formed from the appropriate two-time correlations of components of $\overleftrightarrow{\delta\varepsilon}$. It is often useful to think of these functions as weighted sums over normal modes (of the nuclear motions) of the mode coordinates' temporal response functions. The characteristic decay times in these response functions, and hence in a(t) and b(t), are several orders of magnitude longer than those for electronic nonlinearities. Also a and b are temperature-dependent at fixed density. However, no predictions of the temperature dependence for specific glasses is yet available, and so there is no known way of distinguishing nuclear and electronic contributions to nonlinear optical effects in glasses by observing their temperature variations.

Substituting into Equations (1) and (2) the specific forms of $\vec{E}(\vec{r},t)$ used in observing various nonlinear effects, we now proceed to solve Maxwell's equations to see what combinations of the infinitude of parameters contained in a(t) and b(t) describe the ellipse rotation and Kerr effects.

Reproduced with permission of the copyright owner. Further reproduction prohibited without permission.

Intensity Induced Rotation of the Polarization Ellipse

To analyze this effect, we assume that there is propagating in the medium a z-directed monochromatic plane wave of frequency ω composed of right and left circularly polarized waves having complex vector amplitudes $(\hat{x} \pm i\hat{y})E_{\pm}/\sqrt{2}$ and propagating with wave-vectors $\vec{k}_+$ and $\vec{k}_-$ respectively. Substituting such a field in Equations (1) and (2), one finds directly that Maxwell's equations are satisfied at the frequency ω if

$$\left(\frac{ck_{\pm}}{n\omega}\right)^2 = 1 + \pi[(\sigma + 2\alpha + \beta)E^2 + (\sigma + 2\beta)|E_{\mp}|^2]/n^2 \qquad (3)$$

where $E^2 \equiv |E_+|^2 + |E_-|^2$ is the time average of $2\vec{E} \cdot \vec{E}$, $\alpha \equiv \int a(s)ds$, $\beta \equiv \int b(s)ds$ and n is the (linear) refractive index at ω. We have neglected the terms which are proportional to the Fourier transforms of $a(t)$ and $b(t)$ at 2ω, because the nuclear response at this frequency is extremely small. According to Equation (3) the axes of the polarization ellipse rotate by an angle θ over a distance z so that a fraction

$$F(z) = (\sin 2\phi \sin \theta)^2 \qquad (4a)$$

of the field at z becomes orthogonally polarized to the field at $z = 0$; here $\tan \phi \equiv |E_+/E_-|$ and $\theta = (k_+ - k_-)z/2$. In our experiments $|k_+ - k_-| \ll n\omega/c$, whence

$$\theta = \pi\omega z E^2 (4nc)^{-1}(\sigma + 2\beta)\cos 2\phi. \qquad (4b)$$

Reproduced with permission of the copyright owner. Further reproduction prohibited without permission.

If focusing is weak enough so that no further self-focusing due to nonlinear effects occurs, then we expect geometrical optics to be valid. In this case the ellipse rotation angle may be computed for each ray by substituting $\int_{z_1}^{z_2} E^2(z)dz$ for $E^2 z$ in Equation (4b); here the integral is taken along the ray path. If this integral is calculated along an axial ray through the focus of an ideal gaussian beam, then

$$\int_{-\infty}^{\infty} E^2(z)dz = 8\pi\omega P/c^2 \tag{4c}$$

where P is the total power in the beam. We shall allow our nonlinear samples to completely encompass a focal region so as to take advantage of the independence of θ on beam geometry indicated here. We will ensure that self focusing and nonlinear absorption effects are negligible by confining measurements to low enough powers that the $\theta \propto E^2$ dependence of Equation (4b) is observed.

In terms of the "B" coefficient defined by Maker et al,[1] in their original description of ellipse rotation, and in terms of the appropriate commonly used "c-coefficients" defined by Maker and Terhune.[3]

$$\sigma + 2\beta = 4"B" = 24c_{1221}(-\omega,\omega,\omega,-\omega). \tag{5}$$

Kerr Effect

In an isotropic material a test beam $\vec{E}_\omega(\vec{r},t)$ of frequency ω will exhibit birefringence in the presence of a strong beam $\vec{E}_\nu(\vec{r},t)$ of frequency ν. This "electric-field-induced birefringence"

Reproduced with permission of the copyright owner. Further reproduction prohibited without permission.

is called the "ac Kerr effect" when ν is an optical frequency, and called the "dc Kerr effect" when ν is a radio frequency or lower. Both cases are described by a Kerr constant, B, defined by

$$B = \frac{\omega(\delta n_{\parallel} - \delta n_{\perp})}{2\pi c \langle E_{\nu}^2 \rangle_{av}} \tag{6}$$

where $\delta n_{\parallel} - \delta n_{\perp}$ is the difference between the induced changes in the refractive index parallel and perpendicular to the direction of $\vec{E}_{\nu}$ whose mean square value in time is $\langle E_{\nu}^2 \rangle_{av}$. Again using the forms of Equations (1) and (2) in Maxwell's equations, we come directly to values for the desired index changes (second order in E_{ν}) that yield

$$B = \omega(\sigma + \beta)/(nc) \tag{7}$$

provided that $b(t)$ has no appreciable Fourier component at 2ν and $|\omega - \nu|$, as is the case in the experimental works we will cite. In terms of the appropriate c-coefficients,

$$\sigma + \beta = 12[c_{1212}(-\omega,\omega,\nu,-\nu) + c_{1221}(-\omega,\omega,\nu,-\nu)].$$

From Equations (4) and (7) come the important consequence that (small angle) ellipse rotation measures $\sigma + 2\beta$ while the Kerr effect measures $\sigma + \beta$ and together the effects yield the electronic parameter σ and the nuclear parameter β separately.

III. Experiment

The first measurements by Maker et al.[1] of ellipse rotation

Reproduced with permission of the copyright owner. Further reproduction prohibited without permission.

coefficients, which (like subsequent measurements) were done in liquids, depended on an estimate of the beam profile for a weakly focused multi-mode beam. Wang,[6] and McWane and Sealer,[7] found by repeating the measurements with more carefully controlled unfocused (but multi-mode) beams, that the earlier estimates had yielded coefficients about an order of magnitude too small. In the present measurements on glasses we have attempted to avoid some of the earlier difficulties in several ways. First we have employed a single (transverse and longitudinal) mode beam, calibrated by measuring the ellipse rotation of CS_2, whose $\sigma + 2\beta$ value we are able to determine to within 2% from other experiments. We have also used strong enough focusing of the beam into the sample so as to ensure that the entire ellipse rotation takes place within the focal volume and to take advantage of the resulting independence of the ellipse rotation angle on sample and focal dimensions. This arrangement also allows the optical intensity at the entrance and exit air-glass interfaces to be much lower for a given ellipse rotation angle, thus eliminating the danger of a nondamaging, absorbing plasma forming at the entrance face. As a result we have obtained reproducible results, for all glasses studied, while using different focal length lenses and samples, and also after using both passive and active Q-spoiling techniques.

The experimental configuration is shown in Figure 1. The laser is a water cooled room temperature ruby laser Q-switched with a dye of cryptocyanine in acetone. Mode selection is performed by aperturing the 9/16 in. diam. x 4 in. ruby to give a 3mm output spot employing a sapphire etalon as the output reflector. The laser out-

Reproduced with permission of the copyright owner. Further reproduction prohibited without permission.

put is 0.05J in a 20ns pulse under a single mode operation. Power monitoring of the laser output is performed via a beam splitter which directs a portion of the beam to an ITT FW 114A S-20 biplanar photodiode. The rest of the beam is coupled through a Rochon prism (P1) to define its plane of polarization prior to its introduction into the fresnel rhomb (R1) which is oriented so as to produce an elliptically polarized input of desired eccentricity. The beam is then focused into the sample centrally by lens (L1) and then recollimated by lens (L2). A second Fresnel rhomb (R2) is oriented parallel to R1 so as to produce a linearly polarized output in the absence of ellipse rotation. This is followed by a Wollaston prism (P2) oriented to direct a maximum "transmitted" signal into D3 and a minimum "nulled" signal into D2 in the absence of ellipse rotation.

The laser power delivered to the sample is adjusted by moving the Schott high power neutral density filters from neutral density stack F1 to F2 thus ensuring a constant reference power level into the diodes in the absence of a nonlinearity. Any rotation of the polarization ellipse during propagation through the sample thus reveals itself as a relative increase in the "nulled" signal. Monitoring of the transmitted beam in D3 reveals any induced changes in the transmission path or changes in the spatial profile of the laser. A He-Ne laser operating at 6328Å and adjusted collinearly with the ruby laser beam was used continuously to ensure proper alignment of the system. The result of a typical run of the three glasses and liquid CS_2 is shown in Figure (2). The fraction F of orthogonal polarization is plotted versus input laser power P, and exhibits the P^2 dependence of Equation (4). Clearly this could not result if self focusing or

Reproduced with permission of the copyright owner. Further reproduction prohibited without permission.

absorptive nonlinear effects, which would alter the assumed beam shape in a power dependent way, were occuring to a significant degree.

In this study as in the Kerr effect measurements, liquid carbon disulphide (CS_2) was chosen as the standard to which measurements of ellipse rotation in fused quartz, and Schott BK-7 and SF-7 glasses were compared. The absolute value of the dc Kerr constant of CS_2 is the best known of any substance and has been determined in a recent very accurate measurement by Volkova et al., to be $3494 \pm 4 \times 10^{-10}$ esu at 546 nm and 23°C.[8] Using the variation of this "constant" with wavelength measured by McComb,[9] we obtain for it the value $253 \pm 5 \times 10^{-9}$ esu at 694 nm and 23°C. Mayer[10] and Hauchecorne et al.,[11] have found that σ is unobserable in CS_2 by a sensitive method (second harmonic generation in the presence of astatic field) that clearly would observe it directly. One can conclude from their data that $\sigma < 0.01\beta$ and so, from Equations (5) and (7) we conclude that for CS_2, $(\sigma + 2\beta)/24 = c_{1221}(-\omega,\omega,\omega,-\omega) = 37.8 \pm 0.7 \times 10^{-14}$ esu at 694 nm and 23°C.[12] Because the dielectric constant of CS_2 is equal to the square of the refractive index (at 6943A and 23°) to within less than 0.5%, we feel we can neglect dispersion corrections in inferring the ellipse rotation constant from the dc Kerr constant.

The results of interpreting our F vs P observations with Equation (4) are summarized in Table 1 along with ac Kerr, three-wave mixing data, and the linear refractive indices used in data reduction. The coefficients listed have been chosen so that they would all be equal to $c_{1221} = \sigma/24$ if nuclear motions and dispersion could be neglected. Fortunately for our purposes, CS_2 was also used to calibrate the ac Kerr effect observations. Although the three

Reproduced with permission of the copyright owner. Further reproduction prohibited without permission.

wave mixing effect depends in a different way (signified by δ) on $a(t)$ and $b(t)$, we have listed its measured values also, these being the most accurate of other existing related data.

IV. Discussion

It is evident from their definitions in Section II that both σ and β must be positive in order that the electronic and nuclear distortions lower the field-sample interaction energy. Therefore comparing our results with the Kerr data from Table I indicates that the electronic contribution to either effect is not negligible, but that the nuclear contribution may be. However, we hesitate to conjecture from these results that the relative nuclear contribution is in fact negligible, mainly for the following reason. As is the case for liquids, there is a rigorous connection between the Fourier transforms at frequency ω of the nuclear correlation functions $a(t)$ and $b(t)$ and the intensity of light scattered at a frequency shift $\Delta\omega$ from glasses.[15] This means, for one thing, that the nuclear contribution β to the ellipse rotation and Kerr effects could be found independently from the depolarized light scattering intensity, (just as for liquids[16]). Although the absolute intensity of the depolarized scattering from a glass has not yet been calibrated, it is known to be roughly as large as that from some liquids in which nuclear contributions to the Kerr effect are known to be important.[17]

The nuclear motions which cause electrostriction and which appear in the isotropic $a(t)$ term of Equation (2) are well known to be important to self-focusing in glasses. It is instructive to estimate for comparison the electronic contribution to the commonly

Reproduced with permission of the copyright owner. Further reproduction prohibited without permission.

used nonlinear index n_2 for linearly polarized light, assuming that all of our ellipse rotation results were electronic. From equation (3) one has immediately that $n_2 = \pi(3\sigma/2 + 2\beta + 2\alpha)/n$ in general and $n_2 = 3\pi\sigma/(2n)$ for purely electronic effects. With our results in Table I this would give $n_2 = 1.2$, 1.7, and 6.9 x 10^{-13}esu respectively for fused quartz, BK-7 and SF-7 glasses. These values alone imply critical powers for the electronics self-focusing of a Gaussian beam in an infinite medium from around 0.25 to 1.5 MW, close to what is expected from transient electrostriction and to what is commonly observed.

If the nonlinear medium were not isotropic then the relations we derived in Section II and all of the foregoing discussion and interpretation which derived from them would not apply. The strain birefringence that can be observed in some glass samples indicates that anisotropic regions may exist within glass samples. We have determined that such inhomogeneities did not contribute to our results (to within our stated errors) from the following observations. First, the strain birefringence was too small to be observable in our samples which produced extinction of $\sim 10^{-3}$ between crossed polarizers. More important, our results were reproducible (within the stated errors) when the samples were rotated about the beam axis and when different samples of the same glass were employed.

In summary, we have demonstrated here that intensity-induced index changes for a monochromatic beam can be seen and measured in glasses, and with an absolute accuracy (~ 10%) that makes quantitative interpretation useful. We have shown that comparison of these effects with the electric-field-induced birefringence

Reproduced with permission of the copyright owner. Further reproduction prohibited without permission.

(Kerr) effect in the same glass can yield a unique determination of the relative contributions of electronic and nuclear mechanisms to these effects, and that existing Kerr data indicate that electronic mechanisms must be important in the glasses which we have studied.

Reproduced with permission of the copyright owner. Further reproduction prohibited without permission.

FOOTNOTES

1. P.D. Maker, R.W. Terhune and C.M. Savage, Phys. Rev. Lett., 12, 507-509, (1964).

2. C.C. Wang and E.L. Baardsen, Phys. Rev., 185, 1079, (1969). Phys. Rev., B1, 2827, (1970).

3. P.D. Maker and R.W. Terhune, Phys. Rev., 137, A801, (1965).

4. M.A. Duguay and J.W. Hansen, Spring Meeting of the Optical Soc. of America, Phil., Pa., Apr. 7-10, 1970. See Physics Abstracts 73, Abstract No. 72308, (1970).

5. M.A. Duguay and J.W. Hansen, Symposium on Damage in Laser Materials, Boulder, Colorado, June 24-25 1970, NBS Special Publ. 341, pp. 45-50.

6. C.C. Wang, Phys. Rev. 152, 149 (1966).

7. P.D. McWane and D.A. Sealer, Appl. Phys. Letters, 8, 278, (1966).

8. Y.A. Volkova, V.A. Zamkoff, L.V. Nalbandoff, Zhurnal Optica i Spectroscopia XXX, 556, (1971).

9. Landolt - Bornstein Zahlenwerte und Functionen, Vol. 2, pt. 8, Table 285813 (Springer Verlag, Berlin, 1962).

10. G. Mayer, Compt Rend., 267, 54, (1968).

11. G. Hauchecorne, F. Kerherve and G. Mayer, Le Journal de Physique, 32, 47, (1971).

12. Note that in contradiction to reference 11, M.P. Bogaard, A.D. Buckingham, and G.L.D. Ritchie, Mol. Phys. 18, 575, (1970) have inferred that 10% of the Kerr constant of CS_2 vapor is electronic at room temperature by the less direct method of extrapolating eight vapor measurements between 2 and 91°C to infinite temperature. If this result could be taken to mean (as standard

Reproduced with permission of the copyright owner. Further reproduction prohibited without permission.

theory would indicate) that 10% of the Kerr constant of the liquid CS_2 were also electronic, then we would replace the values in the first column of Table I by 1.43, 2.2, 9.4, and 360 respectively from top to bottom. This alteration would not change appreciably any of our other conclusions.

13. F.J. McClung, Hughes Res. Lab., Report No. 306.
14. J.P. Jesson and H.W. Thompson, Proc. Roy. Soc. (London), A268, 68 (1962).
15. R.W. Hellwarth, (to be published).
16. R.W. Hellwarth, J. Chem. Phys. 52, 2128 (1970).
17. S.P.S. Porto, (private communication).

Reproduced with permission of the copyright owner. Further reproduction prohibited without permission.

Reproduced with permission of the copyright owner. Further reproduction prohibited without permission.

Material	$\frac{(\sigma + 2\beta)}{24}$	$\frac{(\sigma + \beta)}{24}$	$\frac{(\sigma + \delta)}{24}$	$n_{6943\text{Å}}$
	from ER[a]	From ac Kerr[b]	from TWM	
fused quartz	1.5(1.5)	1.7(9)	2.0(4)[c] 1.75[d]	1.455
BK-7	2.3(2)	2.6(9)	3.8(8)[c]	1.513
SF-7	9.9(10)	-	-	1.631
LaSF-7	-	13.3(40)	-	1.91
CS_2	378(7)	189(4)	-	1.62

(a) The uncertainties in the last digit relative to CS_2 are given in the parentheses. The absolute uncertainty in the value for CS_2 is given.

(b) The data are taken from refs. (4) and (5) with the uncertainty in the last digit relative to CS_2 given in parentheses. The absolute uncertainty for errors in the CS_2 value are quoted as obtained from the literature cited in the text.

(c) The data are taken from ref. (3) and normalized to the value for the resonant Raman cross section for benzene at 992 cm^{-1} obtained in the two independent studies of refs. (13) and (14); $c_{1111}(-\omega-\Delta,\omega,\omega,\Delta-\omega) = 35 \pm 7 \times 10^{-14}$esu. The uncertainties in the last digit relative to this value are quoted in parentheses.

(d) This value was given in ref. (11) where the authors also discussed at length the difficulties in calibrating the value and assigning limits of error to it.

TABLE I

Results of ellipse rotation (ER) measurements on glasses tabulated with ac Kerr and three wave mixing (TWM) data for comparison (all in units 10^{15} esu).

ACKNOWLEDGMENT

One of us (RWH) would like to thank the National Science Foundation for its support and the Clarendon Laboratory, Oxford, for its hospitality during part of this work.

Reproduced with permission of the copyright owner. Further reproduction prohibited without permission.

FIGURE CAPTIONS

Figure 1. Schematic diagram of the experimental arrangement used to observe ellipse rotation. BS = beam splitter, P-1 = Rochon Prism, P-2 = Wollaston Prism, F-1 and F-2 = Schott neutral density stacks totaling N.D. = 4.0, F-3, F-4 and F-5 6943Å spike filters, D-1, D-2 and D-3 = ITT FW 114A biplanar photodiodes, R-1 and R-2 = fresnel rhombs, L-1 and L-2 = lenses (10-15 cm f.l.).

Figure 2. Composite graph of F vs P for fused quartz, BK-7 and SF-7 glass, and CS_2. Unit abscissa corresponds to an absolute power P = 0.6kW and the ordinate 10 corresponds to an angular ellipse rotation $\theta \simeq 2°$, both of which are cross sectional averages of uncertain precision. (From Equation (4) it is noted that for each ray $F \propto \theta^2$ for small θ).

Reproduced with permission of the copyright owner. Further reproduction prohibited without permission.

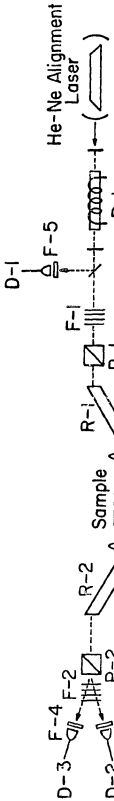

Figure 1

Reproduced with permission of the copyright owner. Further reproduction prohibited without permission.

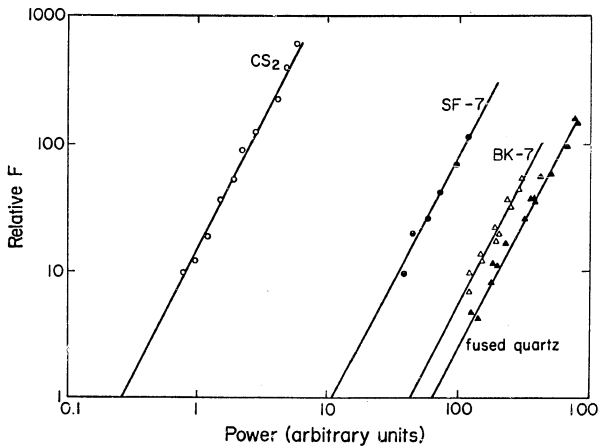

Figure 2

Reproduced with permission of the copyright owner. Further reproduction prohibited without permission.

APPENDIX M

Reproduced with permission of the copyright owner. Further reproduction prohibited without permission.

ORIGIN OF THE NONLINEAR REFRACTIVE INDEX OF LIQUID CCl_4[†]

R. W. Hellwarth,[*] Adelbert Owyoung,[**] and Nicholas George

California Institute of Technology

Pasadena, California 91109

(Received 26 July 1971)

We report here the first determination for a simple liquid (specifically liquid CCl_4) of the fraction of its Kerr effect that arises from the (nearly instantaneous) nonlinear response of its electronic currents, and hence would exist even if the nuclei were frozen in position. To do this, we have remeasured the power dependence of the rotation of the polarization ellipse of a monochromatic beam in CCl_4 with greatly improved accuracy (± 10% absolute) using a single Gaussian mode ruby (giant pulse) laser. We then compare the results of this ellipse rotation measurement with existing Kerr data, and, using a general relation between the relative electronic contributions to both effects which we demonstrate, we show that (54 ± 16) percent of the Kerr effect in CCl_4 arises from nonlinear electronic response. The method should be useful for any isotropic material.

[†]Research supported in part by the Air Force Office of Scientific Research and Clarendon Laboratory, Oxford, England.

[*]Present Address: Clarendon Laboratory, Oxford, England, and Permanent Address: University of Southern California, Los Angeles, California, 90007, U.S.A.

[**]Permanent Address: Sandia Laboratories, Albuquerque, N.M., 87115.

Reproduced with permission of the copyright owner. Further reproduction prohibited without permission.

I. INTRODUCTION

The second-order nonlinear electric susceptibility tensor $\chi^{(2)}$ of a material manifests itself in a variety of commonly observed effects, such as electric-field-induced birefringence (Kerr effect). The physical mechanisms which can contribute to this nonlinear susceptibility at frequencies well below any electronic absorption frequency are of two distinct types, and contribute additively to $\chi^{(2)}$. An "electronic" contribution arises from a nonlinear distortion of the electron orbits around the nuclei, considered to be fixed in an average or typical arrangement.[1] This contribution would be observable, in principle, within a few electronic cycles ($\sim 10^{-16}$s) after sudden application of a strong electric field, and is independent of temperature at constant density. The second, or "nuclear", contribution arises from an electric-field-induced change in the motions of nuclei; in the presence of these changed motions the electronic currents respond linearly to the impressed electric fields.[2] This nuclear contribution could be observed after the sudden impression of a field only following a time lapse of the order of the time ($\sim 10^{-12}$sec) required for a thermal nucleus to move a typical internuclear distance or execute a vibrational cycle. These nuclear contributions are generally temperature-dependent at constant density.

Owing mainly to the fact that observed temperature dependences of the Kerr effect (at constant pressure) are generally too large to be consistent with the former electronic mechanism, it has usually been assumed that the latter nuclear contributions

Reproduced with permission of the copyright owner. Further reproduction prohibited without permission.

dominate in liquids.[2] However recent measurements of this temperature dependence in various simple liquids (composed of electronically saturated, non-associating, electrically isotropic and neutral atoms or molecules) have yielded dependencies sometimes small enough to be consistent with electronic mechanisms being important.[3] This is especially evident in the case of the commonest and most widely studied of simple liquids: carbon tetrachloride (CCl_4).[3] In this liquid, measured light scattering intensities are more consistent with its Kerr constant being partly electronic than not.[4] Furthermore, recent measurements of the purely electronic nonlinearity in CCl_4 gas,[5-7] when extrapolated to liquid density by unreliable theory, also suggest that the two classes of mechanisms may contribute comparable amounts to the Kerr effect in CCl_4. Since so much of the interpretation of various data on CCl_4 depends on the relative importance of these mechanisms, we have undertaken a more direct measurement of the electronic fraction of the room temperature Kerr constant of liquid CCl_4 using a novel technique (discussed in Section II) which we have employed previously to answer similar questions about nonlinear optical effects in glasses.[8]

We find this fraction to be $(54 \pm 16)\%$ by comparing our measurements (described in Section III) of the power-dependent rotation of the polarization ellipse of a monochromatic beam in CCl_4 with previous measurements of its Kerr effect, all in the light of a general relation between the two effects derived in Section II. Our value for the ellipse rotation is roughly 50% higher than that measured previously by Wang[9] and over five times

Reproduced with permission of the copyright owner. Further reproduction prohibited without permission.

that reported by Maker et al.,[10] in their original prediction and first measurements of this effect. Unlike in these earlier investigations, we have been able to employ new techniques to obtain a single Gaussian mode laser beam, a fact which we believe is mainly responsible for the discrepancies.

In our concluding Section IV, we discuss various alternative methods of separating electronic from nuclear contributions to the nonlinear polarization (third order in the electric field), including the extrapolation to liquid densities of recent hyperpolarizability measurements on vapors and absolute measurements of light scattering intensities. We argue that our technique of comparing Kerr and ellipse-rotation data offers the simplest and most accurate method presently available for distinguishing these mechanisms in isotropic media.

II. RELATION BETWEEN ELLIPSE-ROTATION AND KERR EFFECTS

We outline here how the two classes of mechanisms determine the ellipse-rotation and Kerr effects in such a way as to allow their unique separation by measuring the two effects. More details of this and related relations are given elsewhere.[8,11]

We start from the fact that the nonlinear polarization density $\vec{P}^{NL}(\vec{r},t)$, third order in the electric field, may be separated into two parts. First, there is an electronic part $\vec{P}_e(\vec{r},t)$ which results from a distortion of the electron orbits about the nuclei, considered fixed in a typical spatial configuration. This polarization responds so quickly in transparent media (within several electronic cycles) that we may approximate it by the instantaneous

Reproduced with permission of the copyright owner. Further reproduction prohibited without permission.

form

$$\vec{P}_e(\vec{r},t) = \frac{1}{2}\sigma\vec{E}(\vec{r},t) \cdot \vec{E}(\vec{r},t)\vec{E}(\vec{r},t) \qquad (1)$$

for any isotropic material. The electronic nonlinear susceptibility coefficient σ exhibits a small dispersion at the optical frequencies employed which we correct for when necessary. Evidently σ is independent of temperature at fixed density (although it varies with temperature at fixed pressure in a way not well understood).

The remaining part of $\vec{P}^{NL}$ is a nuclear part $\vec{P}_n(\vec{r},t)$ which is due to the linear response of the electronic currents about nuclear arrangements whose statistical probabilities are altered slightly in order to lower the average field-crystal interaction energy. When (as here) the medium is nonpolar, has no absorption near field frequencies and has little dispersion, the instantaneous fluctuation in this interaction energy density in a volume about $\vec{r}$ which is small compared to a wavelength may be written $-(1/8\pi)\vec{E}(\vec{r},t)\cdot\delta\overleftrightarrow{\varepsilon}(\vec{r},t)\cdot\vec{E}(\vec{r},t)$, where $\delta\overleftrightarrow{\varepsilon}$ is the deviation from its average of the dielectric permittivity tensor appropriate to the nuclear placements in the neighborhood of $\vec{r}$ at time t. Since $\vec{P}_n(\vec{r},t)$ equals $\delta\overleftrightarrow{\varepsilon}\cdot\vec{E}(\vec{r},t)/4\pi$ averaged with a weighting function (i.e.,density matrix) expanded to first order in the above interaction energy, it must be proportional to the electric field at the same time (t) times a convolution of the square of the electric field at earlier times. In an isotropic medium, this means that the nuclear contribution to the nonlinear polarization

Reproduced with permission of the copyright owner. Further reproduction prohibited without permission.

must have the form

$$\vec{P}_n(\vec{r},t)=\vec{E}(\vec{r},t)\int a(t-s)E^2(\vec{r},s)\,ds+\int \vec{E}(\vec{r},t)\cdot\vec{E}(\vec{r},s)\,b(t-s)\vec{E}(\vec{r},s)\,ds \qquad (2)$$

Here $a(t)$ and $b(t)$ are nuclear response functions for the "isotropic" and "anisotropic" parts of the nonlinear polarization respectively, formed from the appropriate two-time correlations of components of $\delta\overleftrightarrow{\epsilon}$. The characteristic decay times in these response functions are several orders of magnitude longer than those for electronic nonlinearities. Also a and b are temperature-dependent, both at fixed density and fixed pressure, but in a way too poorly understood to yet be useful for the purpose of distinguishing nuclear and electronic contributions to nonlinear optical effects in liquids by observing their temperature variations.

Substituting into Equations (1) and (2) the specific forms of $\vec{E}(\vec{r},t)$ used in observing various nonlinear effects, we now proceed to solve Maxwell's equations to see what combinations of the infinitude of parameters contained in $a(t)$ and $b(t)$ describe the ellipse rotation and Kerr effects.

Intensity - Induced Rotation of the Polarization Ellipse

To analyse this effect, we assume that there is propagating in the medium a z-directed monochromatic plane wave of frequency ω composed of right and left circularly polarized components having complex vector amplitudes $(\hat{x} \pm i\hat{y})E_{\pm}/\sqrt{2}$. The two wavevectors $\vec{k}_{\pm}$ corresponding to these components are found by substituting the field into Equations (1) and (2), transforming these expressions into the

Reproduced with permission of the copyright owner. Further reproduction prohibited without permission.

frequency domain, and substituting the resultant expression for $\vec{P}^{NL}(\omega)$ into Maxwell's equations i.e., the wave equation in the frequency domain. Since the Fourier transforms of the nuclear response functions $a(t)$ and $b(t)$ are negligibly small at optical frequencies in $E^2(t)$, we find that at frequency ω,

$$(ck_{\pm}/n\omega)^2 = 1 + \pi[(\sigma + 2\alpha + \beta)E^2 + (\sigma + 2\beta)|E_{\mp}|^2]/n^2 \qquad (3)$$

where $E^2 \equiv |E_+|^2 + |E_-|^2$ is the time average of $2\vec{E} \cdot \vec{E}$, $\alpha \equiv \int a(s)ds$, $\beta \equiv \int b(s)ds$ and n is the (linear) refractive index at ω. According to Equation (3) the axes of the polarization ellipse rotate by θ over a distance z so that a fraction

$$F(z) = (\sin 2\phi \ \sin\theta)^2 \qquad (4a)$$

of the field at z becomes orthogonally polarized to the field at $z = 0$; $\tan \phi \equiv |E_+/E_-|$ and $\theta = (k_+ - k_-)z/2$. In our experiments $|k_+ - k_-| \ll n\omega/c$, whence

$$\theta = \pi\omega z E^2 (4nc)^{-1}(\sigma + 2\beta)\cos 2\phi. \qquad (4b)$$

If the beam is weakly focused, and $\theta \ll 1$ so that no further self-focusing due to nonlinear effects occurs, then we expect geometrical optics to be valid. In this case the ellipse rotation angle may be computed for each ray by substituting $\int_{z_1}^{z_2} E^2(z)dz$ for zE^2 in Equation (4b); here the integral is taken along the ray path. If this integral is calculated along an axial ray through the focus

Reproduced with permission of the copyright owner. Further reproduction prohibited without permission.

of an ideal Gaussian beam, we have[12]

$$\int_{-\infty}^{\infty} E^2(z)dz = 8\pi\omega P/c^2 \qquad (5)$$

where P is the total power in the beam. In our experiments we take advantage of this independence of θ on beam dimensions when the liquid sample completely surrounds the focal region, measuring θ by measuring the orthogonally polarized fraction F of the emerging beam.

In terms of the "B" coefficient defined by Maker et al.[10], in their original description of ellipse rotation, and in terms of the appropriate commonly used "c-coefficients" defined by Maker and Terhune,[13] we see from Equation (3) that

$$\sigma + 2\beta = 4 \text{ "B"} = 24c_{1221}(-\omega,\omega,\omega,-\omega) . \qquad (6)$$

Kerr Effect

In an isotropic material a test beam $\vec{E}_\omega(\vec{r},t)$ of frequency ω will exhibit birefringence in the presence of a strong beam $\vec{E}_\nu(\vec{r},t)$ of frequency ν. This "electric-field-induced birefringence" is called the "a.c. Kerr effect" when ν is an optical frequency, and called the "d.c. Kerr effect" when ν is a radio frequency or lower. Both cases are usually described by a Kerr constant B (not the "B" above) defined by

$$B = \frac{\omega(\delta_\parallel - \delta n_\perp)}{2\pi c\langle E_\nu^2\rangle_{av}} \qquad (7)$$

Reproduced with permission of the copyright owner. Further reproduction prohibited without permission.

where $\delta n_{\parallel} - \delta n_{\perp}$ is the difference between the induced changes in the refractive index parallel and perpendicular to the direction of $\vec{E}_{\nu}$ whose mean square value in time is $\langle E_{\nu}^2 \rangle_{av}$.

Again $\delta n_{\parallel}$ and $\delta n_{\perp}$ may be calculated by substituting the two monochromatic plane waves into Equations (1) and (2) in the frequency domain and using $\vec{P}^{NL}(\omega)$ in Maxwell's equations. Substituting the resulting refractive index changes (second order in E) into Equation (7) we find that

$$B = \omega(\sigma + \beta)/(nc) \tag{8}$$

Here it is assumed that $b(t)$ has no appreciable Fourier component a 2ν and $|\omega - \nu|$. In terms of the appropriate c coefficients,

$$\sigma+\beta = 12[c_{1212}(-\omega,\omega,\nu,-\nu)+c_{1221}(-\omega,\omega,\nu,-\nu)]. \tag{9}$$

Now one can see the important consequence that (small angle) ellipse rotation measures $\sigma + 2\beta$, while the Kerr effect measures $\sigma + \beta$ and together the effects yield the electronic parameter σ and the nuclear parameter β separately.

III. EXPERIMENT

In the present ellipse-rotation experiments on CCl_4 we have attempted to avoid the difficulties encountered in earlier such measurements in several ways. First, we have employed a single (transverse and longitudinal) mode beam, calibrated by measuring the ellipse rotation of CS_2, whose $\sigma + 2\beta$ value we are able to determine to within 2% from other experiments. (Fortunately, the Kerr constant of

Reproduced with permission of the copyright owner. Further reproduction prohibited without permission.

CCl_4 is also known most accurately in terms of that of CS_2.) We have also used stronger focusing into the sample so as to ensure that the ellipse rotation takes place entirely within the focal volume, thus taking advantage of the resulting independence of the ellipse rotation angle of sample and focal dimensions. This arrangement also allows the optical intensity at the entrance and exit air-glass interfaces to be much lower for a given ellipse rotation angle, thus eliminating the danger of a nondamaging, absorbing plasma forming at the entrance face. As a result we observe a value of F/P^2 reproducible to within ten percent, while using different focal length lenses, and samples, and also after changing the ruby laser beam diameter and employing both active and passive Q-spoiling techniques.

The experimental configuration is shown in Figure 1. The laser is a water cooled room temperature ruby laser Q-switched with a dye of cryptocyanine in acetone. Mode selection is performed by aperturing the 9/16" diam. x 4" ruby to give a 3 mm output spot employing a sapphire etalon as the output reflector. The laser output is 0.05J in a 20 ns pulse under single mode operation. Power monitoring of the laser output is performed via a beam splitter which directs a portion of the beam to an ITT FW 114A S-20 biplanar photodiode. The rest of the beam is coupled through a Rochon prism (P1) to define its plane of polarization prior to its introduction into the fresnel rhomb (R1) which is oriented so as to produce an elliptically polarized input of desired eccentricity. The beam is then focused into the sample centrally by lens (L1) and then recollimated by lens (L2). A second Fresnel rhomb (R2) is oriented parallel to R1 so as to produce a linearly polarized output in the absence of ellipse

Reproduced with permission of the copyright owner. Further reproduction prohibited without permission.

rotation. This is followed by a Wollaston prism (P2) oriented to direct a maximum "transmitted" signal into D3 and a minimum "nulled" signal into D2 in the absence of ellipse rotation.

The laser power delivered to the sample is adjusted by moving the Schott high power neutral-density filters from neutral-density stack F1 to F2 thus ensuring a constant reference power level into the diodes in the absence of a nonlinearity. Any rotation of the polarization ellipse during propagation through the sample thus reveals itself as a relative increase in the "nulled" signal. Monitoring of the transmitted beam in D3 reveals any induced changes in the transmission path or changes in the spatial profile of the laser. A He-Ne laser operating at 6328Å and adjusted collinearly with the ruby laser beam was used continuously to ensure proper alignment of the system.

Figure (2) shows the result of a typical run on the liquids CCl_4 and CS_2. From this and similar other data we conclude that at 6943Å and 23°C,

$$\frac{(\sigma + 2\beta)/n \text{ of } CS_2}{(\sigma + 2\beta)/n \text{ of } CCl_4} = 56 \pm 6. \qquad (10)$$

Using Equation (8) we find that a previous direct measurement of the ratio of the Kerr constants of CS_2 and CCl_4 gives[3]

$$\frac{(\sigma + \beta)/n \text{ of } CS_2}{(\sigma + \beta)/n \text{ of } CCl_4} = 40.8 \pm 0.8. \qquad (11)$$

at 6943Å and 23°C, (This measurement, which was performed at 6328Å,

Reproduced with permission of the copyright owner. Further reproduction prohibited without permission.

actually gave 41.6 for this ratio, and we have applied a small dispersion correction obtained from the wavelength variation data given in the Landolt-Bornstein tables[14].)

Mayer,[5] and Hauchecorne, et al.,[6] have found σ to be unobservable in CS_2 by a sensitive method (second harmonic generation in the presence of an electric field) with which they are able to observe the electronic hyperpolarizability in fifteen other molecules (including CCl_4). From their data we conclude that $\sigma < 0.01\ \beta$ for CS_2,[15] and so Equations (10) and (11) combine to give for the electronic fraction $\sigma/(\sigma + \beta)$ of the Kerr constant of CCl_4 (at 6943Å and 23°C)

$$\sigma/(\sigma + \beta) = 0.54 \pm 0.16. \qquad (12)$$

We can derive from Equations (10) and (11) absolute values for σ and β of CCl_4 with the aid of the recent very accurate determination of the Kerr constant of CS_2 by Volkova, et al.,[16] who found it to be $3494 \pm 4 \times 10^{-10}$ esu at 546 nm and 23°C. Using the less accurate data of McComb to estimate the wavelength variation of this "constant", we deduce that it is $253 \pm 5 \times 10^{-9}$ esu at 6943Å and 23°C.[14] Using refractive index values 1.62 and 1.46 for CS_2 and CCl_4 respectively, the previously mentioned measurements imply that

$$\sigma + \beta = 100 \pm 4 \times 10^{-15} \text{ esu} \qquad (13)$$

for CCl_4 at 6943Å and 23°C. (This value is well within the range of values deduced from the literature, and a little more accurate.)

Reproduced with permission of the copyright owner. Further reproduction prohibited without permission.

IV. DISCUSSION

Maker et al.[10], and Wang[9] have also measured the ellipse rotation constant for both liquids CS_2 and CCl_4 but used multimode beams. Their results give 32 and 34 respectively for the ratio of Equation (10) instead of 56 as we have found. (Wang's absolute value of β for CS_2 however agrees well with our value.) However Wang believed his relative values for various liquids to be accurate only to roughly ± 25% and so the discrepancy is not surprising especially in view of the fact that CCl_4, having a relatively weak ellipse rotation, was extremely susceptible to errors from self-focusing and other spurious effects.

One of us has derived a relation between the constant β and the total of the depolarized light scattering intensity for a classical liquid.[4] Although it was derived on the basis of a microscopic approximation (the linear dipole approximation), we have recently shown it to be a somewhat more general theorem than that derivation implies, and probably reliable to within a percent or so.[11] With the six (pre-laser) measurements of the absolute depolarized light scattering intensity from liquid CCl_4 and the existing Kerr data the theorem predicted that $\beta/(\sigma + \beta)$ was between 0.36 and 0.60 for CCl_4,[4] in almost perfect agreement with Equation (12). However a laser measurement of the scattering intensity was about 50 per cent greater than previous values.[4] There were also pre-laser experimentors who disagreed with the scattering values for other liquids given by the sources of the CCl_4 data.[4] Therefore, no definite conclusions could be drawn at the time. Our present results

Reproduced with permission of the copyright owner. Further reproduction prohibited without permission.

now lead us to believe that the standard pre-laser literature-values for both the depolarized scattering and Kerr constants of liquid CCl_4 are correct within their limits of error. Furthermore, the strengthening of the basis for the scattering - Kerr - effect relation now leads us to prefer the "high" values for the light scattering from CS_2 (and also from benzene) that are quoted many places in the literature in competition with a large number of experimentors who prefer "low" values (about 40% lower).[11]

Attempts to distinguish electronic and nuclear contributions to the Kerr constant of CCl_4 (and other symmetric - molecule liquids) by studying its temperature dependence have proved inconclusive, mainly because one has no accurate way to calculate the dependence in such simple liquids.

One might hope that picosecond laser pulses could be produced short enough to "freeze out" nuclear motions and see only σ. From the frequency width of the depolarized scattering spectrum of liquid CCl_4, one can see that the nuclear response time of the main central component is a good deal shorter than the shortest of present laser pulses (~ one psc). But even if this central component could be frozen out, the Raman lines which produce a nuclear contribution in around 10^{-13}sec would still compete with the electronic mechanism, and thus picosecond pulse methods give little promise of distinguishing the electronic effect unambiguously.

Two methods have been used recently to measure the electronic hyperpolarizability of CCl_4 molecules in the vapor phase. Mayer,[5] and Hauchecorne, et al.,[6] have measured the second harmonic produced by a ruby laser beam in the presence of a static electric field. Bogaard,

Reproduced with permission of the copyright owner. Further reproduction prohibited without permission.

at al., have measured the Kerr constant of CCl_4 vapor.[7] If we use these data in the standard theory of the electronic Kerr effect in liquids, with local field corrections,[1,2] we predict a value of σ for liquid CCl_4 that is just below the lower limit of Equation (12) from the second harmonic measurements and a value just above the upper limit of Equation (12) from the Kerr measurements. Considering that the standard theory of the Kerr effect for liquids errs commonly by a factor of two or more in predicting the nuclear contribution from vapor data, it is difficult to say more than that, though inconsistent with each other, neither of the above hyperpolarizabilities may be said presently to be inconsistent with our results.

Aside from third harmonic generation, which has proven to be extremely difficult to calibrate in dense media, we know of no methods other than those which we have just discussed for distinguishing the electronic from nuclear mechanisms in the third order nonlinear polarization of liquids. Now that the techniques for producing a single Gaussian mode laser pulse have been developed, it would seem fairly evident from the foregoing discussion of these other methods that the comparison of Kerr and ellipse-rotation constants is the simplest and most accurate method presently available for comparing the electronic and nuclear contributions to these effects in isotropic media.

Reproduced with permission of the copyright owner. Further reproduction prohibited without permission.

ACKNOWLEDGMENT

One of us (RWH) would like to thank the Clarendon Laboratory, Oxford, for hospitality extended, and the National Science Foundation for support, during part of this work.

Reproduced with permission of the copyright owner. Further reproduction prohibited without permission.

FOOTNOTES

1. W. Voight, Ann der Physik 4, 197 (1901).

2. T.H. Havelock, Proc. Roy. Soc. A80, 28 (1907 ibid A84, 492 (1911); P. Langevin, Le Radium 7, 249 (1910); P. Debye, Marx's Handbuch der Radiologie VI (Akademische Verlagsgesellschaft, Leipzig, 1925) Chap. V; A.D. Buckingham and R.E. Raab, J. Chem. Soc. 2, 2341 (1957); S. Kielich, Acta Phys. Polonica 30, 683 (1966); and others.

3. N. George, R.W. Hellwarth, and C.R. Cooke, Electron Technol. (Poland) 2, 229 (1969).

4. R.W. Hellwarth, J. Chem. Phys. 52, 2128 (1970).

5. G. Mayer, Comptes Rendus. B.267, 54 (1968).

6. G. Hauchecorne, F. Kerheve, G. Mayer, Le Journal de Physique 32, 47 (1971).

7. M.P. Bogaard and A.D. Buckingham (private communication) have measured the Kerr constant of CCl_4 vapor, and deduced a value for the molecular hyperpolarizability γ of $9.96 \pm 0.32 \times 10^{-36}$ esu.

8. A. Owyoung, R.W. Hellwarth, and N. George, Phys. Rev. (to be published).

9. C.C. Wang, Phys. Rev. 152, 149 (1966).

10. P.D. Maker, R.W. Terhune, and C.M. Savage, Phys. Rev. Letters 12, 507 (1964).

11. R.W. Hellwarth (to be published).

12. H. Kogelnik, Appl. Opt. 4, 1562, (1965).

13. P.D. Maker and R.W. Terhune, Phys, Rev. 137A, 801 (1965).

14. K.H. Hellwege and A.M. Hellwege, Landolt-Bornstein Zahlenwerte und Funktionen II/8 (Springer-Verlag, Berlin, 1962) pp. 849-860.

Reproduced with permission of the copyright owner. Further reproduction prohibited without permission.

15. M.P. Bogaard, A.D. Buckingham, and G.L.D. Ritchie, Molecular Physics 18, 575 (1970) have deduced a value for the molecular hyperpolarizability by extrapolating Kerr measurements on CS_2 vapor to infinite temperature. Their value, with standard but unreliable theory, predicts that about a tenth the Kerr constant of liquid CS_2 is electronic. However, the temperature extrapolation from data whose origin is primarily not electronic would seem to be much less direct. If this extrapolation were correct however, we would have to alter the values in Equations (12) to 0.61 ± 0.16, 556 (1971).

16. Y.A. Volkova, V.A. Zamkoff, L.V. Nalbandoff, Zhurnal Optika i Spectroscopia XXX, 556 (1971).

Reproduced with permission of the copyright owner. Further reproduction prohibited without permission.

FIGURE CAPTIONS

Figure 1. Schematic diagram of the experimental arrangement used to observe ellipse rotation. BS = beam splitter, P-1, = Rochon Prism, P-2 = Wollaston Prism, F-1 and F-2 = Schott neutral density stacks totaling N.D. = 4.0, F-3, F-4 and F-5 6943Å spike filters, D-1, D-2, and D-3 = ITT FW 114A biplanar photodiodes, R-1 and R-2 = fresnel rhombs, L-1 and L-2 = lenses (10–15 cm f.l.).

Figure 2. Typical graph of F vs optical power P. Unit abscissa corresponds approximately to an absolute P = 0.6kW and the ordinate 10 corresponds to an angular ellipse rotation of $\theta \simeq 2^{\circ}$, both of which are cross sectional averages of uncertain precision. (From Eq. (4) it is to be noted that for each ray $F \propto \theta^2$ for small θ).

Reproduced with permission of the copyright owner. Further reproduction prohibited without permission.

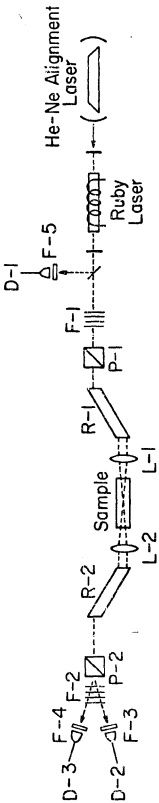

Figure 1

Reproduced with permission of the copyright owner. Further reproduction prohibited without permission.

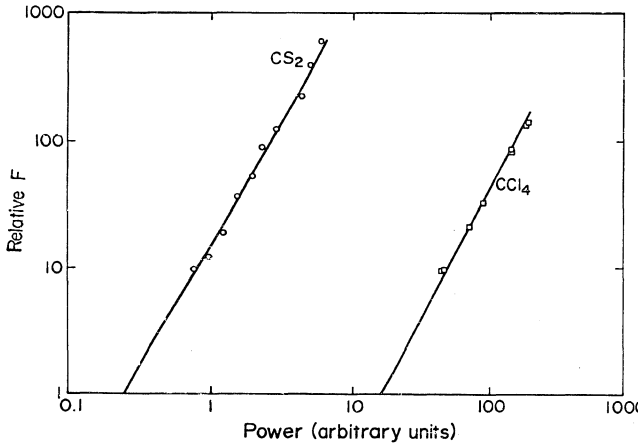

Figure 2

Reproduced with permission of the copyright owner. Further reproduction prohibited without permission.